CHEMBIOCHEM

Supporting Information

Predicted Incorporation of Non-native Substrates by a Polyketide Synthase Yields Bioactive Natural Product Derivatives

Kenny Bravo-Rodriguez,[a] Ahmed F. Ismail-Ali,[b] Stephan Klopries,[b] Susanna Kushnir,[b] Shehab Ismail,[c, d] Eyad K. Fansa,[c] Alfred Wittinghofer,[c] Frank Schulz,*[b] and Elsa Sanchez-Garcia*[a]

cbic_201402206_sm_miscellaneous_information.pdf

Supplementary Information

I Computational Section

I.1 Methods

Generation of the monAT5 model: The homology model of the AT5 domain of the monensin PKS (monAT5) was generated based on the amino acid sequence of AT5 and with the X-Ray structures of the $AT3_{DEBS}$ (PDB ID: 2QO3)[1] and $AT5_{DEBS}$ domains (PDB ID: 2HG4)[2] of DEBS and of malonyl-CoA: acyl carrier protein transacylase (MAT) as templates. $AT3_{DEBS}$ and $AT5_{DEBS}$ were used due to their high sequence homology with monAT5. On the other hand, the active site of monAT5 is more similar to the active site of MAT than to the active sites of $AT3_{DEBS}$ or $AT5_{DEBS}$. Thus, MAT was also considered when building the monAT5 model. This is important, since we found that homology models of monAT5 that were created based only on $AT3_{DEBS}$ and $AT5_{DEBS}$ were not consistent with experimental information. The program Modeller v. 9.10 was used in all cases.[3] Two of the resulting homology models (model 2 and model 3) were used for the simulations. Four substrates were considered, malonyl-CoA (*MCoA*), methylmalonyl-CoA (*MMCoA*), ethylmalonyl-CoA (*EtMCoA*) and propargylmalonyl-SNAC (*propargyl-MSNAC*). All substrates have the *(2S)*-configuration around the chiral carbon atom of the malonyl region. Our previously published model of $AT6_{DEBS}$ with methylmalonyl-CoA ($AT6_{DEBS}$ – *MMCoA*) was used as template for the initial placement of the substrates in the active site.[4] The protonation states of titrable residues were assigned using PropKa[5] and corroborated by visual inspection.

Molecular dynamics simulations (MD): The program NAMD2.9[6] was used for all MD simulations with the CHARMM22 force field[7] for the protein and the TIP3P model[8] for water. Parameters for the substrates were generated using Swissparam[9] and previously tested by us.[4] In all simulations the distance between the protein and the wall of the periodic cell was 15 Å. The PME method was used for the treatment of the electrostatics interactions.[10]

The interactions between the active site and each substrate were simulated two times for each model of monAT5, starting from different orientations of the substrates in the active site. The molecular dynamics simulations are named MD2 (protein model 2) and MD3 (protein model 3) for the first orientation of the ligands inside the active site and MD2A and MD3A for the second orientation. The systems were solvated and neutralized using VMD.[11] NVT MD simulations were performed with all protein atoms and ligand fixed followed by NPT simulations with only the backbone atoms of the protein fixed. Subsequently, 100 ns NPT production dynamics without any restrictions were performed at 300 K with a time step of 2 fs. Thus we modeled the interaction of AT5 with each substrate for a total of 400 ns.

Free energy calculations: Relative free energy differences (ΔΔG) were calculated to assess the preference of the active site toward the different lateral chains of the substrates. The alchemical transformations of *MMCoA* in *EtMCoA*, and propargylmalonyl-CoA (*propargyl-MCoA*) were computed using Free Energy Perturbation theory.[12] Since the direct transformation of *MMCoA* into *propargyl-MSNAC* would involve the annihilation and creation of too many atoms we decided to estimate the *MMCoA* → *propargyl-MSNAC* ΔΔG value through the *MMCoA* → *PCoA* transformation. The alchemical transformation was achieved in each case using 50 windows for the parameter (λ) connecting the initial and final states. Both the forward and backward transformation were calculated. The free energy calculations were analyzed using the parseFEP plugin of VMD.[13] The Bennet acceptance ratio was used to calculate the error in the ΔΔG values.[14] Soft-core potentials were employed to avoid instabilities and improve accuracy and convergence of the simulation for small values of λ. No restrictions in the substrates or the protein were imposed. For each window 50000 MD equilibration steps were taken preceding 150000 MD steps to collect the data and perform the ensemble averages.

Quantum Mechanics/Molecular Mechanics calculations (QM/MM): QM/MM (BP86-D2/SVP//CHARMM22)[15] optimizations were also used to study the interaction between *propargyl-MSNAC* and the active site. Snapshots taken at the beginning and end of the simulations (model2 of monAT5) were optimized and compared for an additional assessment of the evolution of key contacts between the substrate and residues in the active site. The QM region was defined as the entire substrate. All residues within a distance of 30 Å to the substrate were allowed to freely move during the optimizations. The HDLC optimizer was used.[16] QM calculations were handled with Turbomole5.10 while DL_POLY was used for the MM calculations.[17] All QM/MM optimizations were performed with the Chemshell3.5 code.[18]

I.2 Extended discussion of results

monAT5 without substrate: The MD simulations of the protein without any ligand in the active site show that, in aqueous media, the overall initial structure of the homology model is conserved. Residues 267 to 339 form the most flexible region of the protein. These residues build four antiparallel β-sheets and two α helices, which are located at the upper part of the active site. Along the MD simulations these residues tend to move away from the rest of the protein as shown by the distance between the α carbon atoms (CA) of the R323 – L417 and S329 – Q149 pairs. The initial values for these distances in Model2 and Model3 are 14.10, 13.93 Å and 8.81, 8.82 Å respectively. The average distances along the MD simulations are 16.42 ± 0.85, 16.84 ± 1.79 Å and 11.52 ± 0.93, 11.21 ± 1.09 Å. This movement makes the

active site more open and exposed to the ligand. There is no hydrogen bond formed between S232 and the nearby histidine residues (H231 and H334). H334 formed in both MD simulations a contact with the backbone oxygen of N384 with average distances of 2.09 ± 0.33 and 2.21 ± 0.33 Å.

monAT5 with natural substrates: The natural substrates of monAT5 are *MMCoA* and *EtMCoA*. The MD simulations performed with these substrates show a structured active site able to accommodate the ligands. We take as reference the monAT5 – *MMCoA* MD of model2 to discuss the interactions between the protein and the ligand, which is latter compared to the remaining MD simulations with *MMCoA* and *EtMCoA*.

The main interaction between *MMCoA* and the active site is the salt bridge formed between the carboxylate group of *MMCoA* and R257, which is located in the bottom of the active site. This interaction prevents the ligand from wandering inside the active site. As can be seen in Table S1 the carboxylate group interacts almost symmetrically with R257. The distances $R257_{H}$ – O and $R257_{H1}$ – O1 are 1.66 ± 0.08 and 1.72 ± 0.13 Å. Q233 is found near the carboxylate (distance between the amide proton HE and O1 of 1.96 ± 0.39 Å). H334 is also close to the carboxylate but does not establish conserved interactions with it. Along the MD simulation, H334 interacts alternatively with the carboxylate group and with the backbone oxygen of N384. The average distances are 3.14 ± 0.73 and 2.97 ± 1.13 Å. The thioester and the amide groups of *MMCoA* further contribute to the positioning of the ligand in the active site. The simultaneous interactions of the thioester and the first amide groups with the backbone of Q149 help the substrate to adopt a conformation where S232 is close to the thioester with $Q149_{OB}$ – H1 and $Q149_{HN}$ – O2 distances of 2.80 ± 0.81 and 2.13 ± 0.31 Å, respectively. The other amide group in *MMCoA* is placed close to the backbone of V414. The distance $V414_{OB}$ – H2 is 2.22 ± 0.71 Å. The phosphate group interacts with R323 and R325. Along the MD simulation S232 remains close to the carbon atom of the thioester group as shown by the distances $S232_{OG}$ – C and $S232_{CA}$ – C (average values of 3.55 ± 0.27 and 5.47 ± 0.26 Å, respectively, Table S1). In the rest of the MD simulations of all models and substrates, S232 either interacts with H231 or with the carboxylate group of the ligand, but never with H334.

The other MD simulations with *MMCoA* as ligand show a similar behavior to MD2, except MD2A. There, the value of the distances $S232_{OG}$ – C and $S232_{CA}$ – C (4.50 ± 0.66 and 6.55 ± 0.61 Å) places the substrate further from S232 with respect to the other three models. However, if the MD simulation is prolonged for another 40 ns *MMCoA* suffers a conformational change that drives the thioester group closer to S232 (Figure S1).

EtMCoA establishes a similar network of interactions with the active site. In all cases the ethyl group points towards V331 in the loop over the carboxylate group of the substrate. For *EtMCoA* the MD simulations MD3 and MD3A result in the ligand being placed far from S232 especially in MD3 (see distances $S232_{OG}$ – C and $S232_{CA}$ – C in Tables S3 and S4). However, the interaction with R257 remains stable along the entire MDs, meaning that *EtMCoA* remains trapped in the interior of the active site and it is not rejected toward the solvent. In MD3 and MD3A, *EtMCoA* is close to V331, S329 and M270, in the upper part of the active site. The fact that *EtMCoA* moves away from S231 and H231 is related to an initial unfavorable positioning of the side chains of Q149 and Q233 which results in the loss of the interactions $Q149_{OB}$ – H1, $Q149_{HN}$ – O2 and $Q233_{HE}$ – O1. This allows the ligands to adopt conformations placing them away from S232. The larger size of the aliphatic substituent in *EtMCoA* also contributes to the stronger interaction between the ligand and the non-polar amino acids M270 and V331.

monAT5 with non-native substrates: In MD2, MD2A and MD3 the distances between R257 and the carboxylate group of *MCoA* take average values larger than 2.20 Å (Figure 2B and Tables S1, S2 and S3). Only in MD3A the carboxylate group remains close to R257 with values for the distances $R257_{H}$ – O and $R257_{H1}$ – O1 of 1.71 ± 0.14 and 1.72 ± 0.15 Å, respectively. However, in MD3A the values of the distances $S232_{OG}$ – C and $S232_{CA}$ – C (4.59 ± 0.77 and 6.11 ± 0.64 Å) show that the substrate is far from S232. The lack of secondary interactions between *MCoA* and the active site in the four MDs can be seen in Tables S1, S2, S3 and S4 that show that only in MD2A Q149 interacts with the ligand and toward the end of MD3A Q233 is found close to the ligand.

MD2 and MD3A of *propargyl-MSNAC* show an unfavorable positioning of the ligand in the active site. Important interactions are lost after a short time, like the interaction with Q149 and the interaction with Q233. Even more important, the distances to R257 are quite large and unsymmetrical. In the case of MD3A the distances $R257_{H}$ – O and $R257_{H1}$ – O1 take values of 1.89 ± 0.45 and 3.21 ± 0.65 Å. Results for MD2A and MD3 evidence a completely different picture. MD3 shows the substrate correctly placed in the active site with slightly large values of the distance $S232_{OG}$ – C (4.11 ± 0.26 Å). For MD2A, the values of all relevant distances are almost identical to those of *EtMCoA* Model2 (Table S2). Like the ethyl group of *EtMCoA*, the triple bond of *propargyl-MSNAC* is then pointing toward V331 (Figure 2C).

Free Energy Perturbation Calculations: The relative free energy differences associated with the alchemical transformations of the substrates were calculated. In all cases the

underlying probability distribution of the free energy values along the transformation have a very good overlapping for the forward and backward transformation and narrow peaks (Figures S2, S3). A small hysteresis is obtained for the transformation of *MMCoA* in *EtMCoA* and *propargyl-MCoA* (Figures S4 and S5).

QM/MM calculations: Snapshots from MD2 and MD3 of *propargyl-MSNAC* were submitted to QM/MM optimizations (Table S5). Snapshots 6, 7, 8, 9 and 10 correspond to an unfavorable orientation of the ligand inside the active site while the remaining snapshots correspond to favorable orientations. The interaction distances are in very good agreement with the MD values.

I.3 Tables

Table S1. Values of selected distances (Å) for the five MD simulations performed with Model 2.

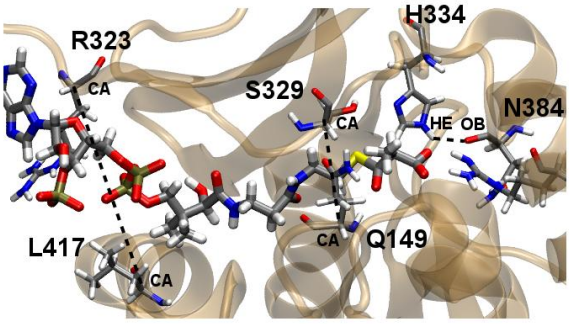

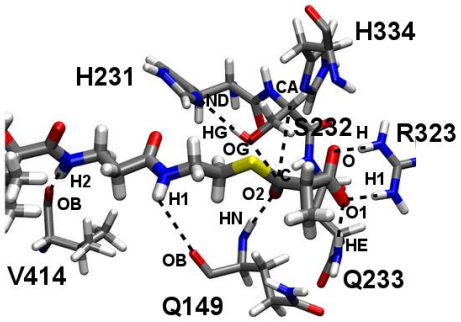

Distance	monAT5	monAT5 & *MCoA*	monAT5 & *MMCoA*	monAT5 & *EtMCoA*	monAT5 & *propargyl-MSNAC*
			Model 2		
			Protein – Protein Distances		
S232HG – H231ND	-	-	2.40 ± 0.73	-	-
H334HE – N384OB	2.09 ± 0.33	-	2.97 ± 1.13	-	2.72 ± 0.87
R323CA – L417CA	16.42 ± 0.85	14.30 ± 0.76	14.26 ± 0.99	11.75 ± 1.58	14.74 ± 1.76
S329CA – Q149CA	11.52 ± 0.93	8.97 ± 0.64	9.04 ± 0.69	9.23 ± 0.74	9.70 ± 1.08
			Protein – Substrate Distances		
Q149OB – H1	-	-	2.80 ± 0.81	-	-
Q149HN – O2	-	-	2.13 ± 0.31	-	-
S232OG – C	-	3.84 ± 0.49	3.55 ± 0.27	3.69 ± 0.30	4.80 ± 0.89
S232CA – C	-	5.55 ± 0.38	5.47 ± 0.26	5.80 ± 0.44	6.81 ± 1.04
Q233HE – O1	-	-	1.96 ± 0.39	1.98 ± 0.32	-
R257H – O	-	2.92 ± 0.54	1.66 ± 0.08	1.68 ± 0.09	2.32 ± 0.75
R257H – O1	-	3.08 ± 0.67	1.72 ± 0.13	1.71 ± 0.12	1.71 ± 0.13
H334HE – O	-	-	3.14 ± 0.73	2.66 ± 1.20	-
V414OB – H2	-	-	2.22 ± 0.71	-	-

Table S2. Values of selected distances (Å) for the five MD simulations performed with Model 2A.

Distance	monAT5	monAT5 & *MCoA*	monAT5 & *MMCoA*	monAT5 & *EtMCoA*	monAT5 & *propargyl-MSNAC*
Model 2A					
Protein – Protein Distances					
S232HG – H231ND	-	-	-	-	-
H334HE – N384OB	-	-	3.56 ± 0.81	3.57 ± 0.89	3.36 ± 0.53
R323CA – L417CA	-	16.32 ± 0.92	14.42 ± 0.56	14.00 ± 0.72	14.03 ± 1.09
S329CA – Q149CA	-	9.24 ± 0.55	10.33 ± 1.25	8.53 ± 0.64	8.61 ± 0.51
Protein – Substrate Distances					
Q149OB – H1	-	2.21 ± 0.56	-	2.02 ± 0.36	1.94 ± 0.26
Q149HN – O2	-	-	-	2.16 ± 0.41	2.10 ± 0.23
S232OG – C	-	3.80 ± 0.31	4.50 ± 0.66	3.70 ± 0.34	3.59 ± 0.30
S232CA – C	-	5.39 ± 0.24	6.55 ± 0.61	5.41 ± 0.30	5.42 ± 0.26
Q233HE – O1	-	-	-	1.90 ± 0.29	1.89 ± 0.20
R257H – O	-	2.29 ± 0.69	1.72 ± 0.18	1.69 ± 0.17	1.68 ± 0.09
R257H – O1	-	2.89 ± 0.98	1.74 ± 0.20	1.69 ± 0.10	1.68 ± 0.10
H334HE – O	-	-	2.42 ± 0.84	2.79 ± 0.88	2.82 ± 0.86
V414OB – H2	-	-	2.07 ± 0.40	-	-

Table S3. Values of selected distances (Å) for the five MD simulations performed with Model 3.

Distance	monAT5	monAT5 & *MCoA*	monAT5 & *MMCoA*	monAT5 & *EtMCoA*	monAT5 & *propargyl-MSNAC*
Model 3					
Protein – Protein Distances					
S232HG – H231ND	-	-	-	2.73 ± 1.23	2.05 ± 0.17
H334HE – N384OB	2.21 ± 0.33	2.49 ± 0.70	2.96 ± 1.08	-	-
R323CA – L417CA	16.84 ± 1.79	13.71 ± 1.06	15.39 ± 0.89	15.00 ± 0.96	13.46 ± 1.10
S329CA – Q149CA	11.21 ± 1.09	9.89 ± 1.27	8.65 ± 1.05	10.52 ± 0.94	8.33 ± 0.57
Protein – Substrate Distances					
Q149OB – H1	-	-	-	2.23 ± 0.58	-
Q149HN – O2	-	-	-	-	2.04 ± 0.25
S232OG – C	-	4.23 ± 0.55	3.86 ± 0.35	4.37 ± 0.68	4.11 ± 0.26
S232CA – C	-	6.13 ± 0.55	5.54 ± 0.29	6.24 ± 0.61	5.25 ± 0.23
Q233HE – O1	-	-	3.09 ± 1.92	-	-
R257H – O	-	1.82 ± 0.34	1.68 ± 0.09	1.69 ± 0.09	1.68 ± 0.14
R257H – O1	-	2.49 ± 1.00	1.70 ± 0.12	1.71 ± 0.14	1.70 ± 0.10
H334HE – O	-	-	-	-	-
V414OB – H2	-	-	-	-	-

Table S4. Values of selected distances (Å) for the five MD simulations performed with Model 3A.

Distance	monAT5	monAT5 & *MCoA*	monAT5 & *MMCoA*	monAT5 & *EtMCoA*	monAT5 & *propargyl-MSNAC*
Model 3A					
Protein – Protein Distances					
S232HG – H231ND	-	2.41 ± 0.90	2.31 ± 0.79	-	-
H334HE – N384OB	-	3.25 ± 1.15	3.87 ± 0.80	2.53 ± 0.58	2.22 ± 0.51
R323CA – L417CA	-	15.41 ± 1.07	14.67 ± 0.49	16.65 ± 1.02	16.88 ± 1.55
S329CA – Q149CA	-	10.64 ± 1.39	10.96 ± 1.13	11.16 ± 0.79	10.75 ± 1.35
Protein – Substrate Distances					
Q149OB – H1	-	-	1.95 ± 0.24	-	-
Q149HN – O2	-	-	2.48 ± 0.45	-	-
S232OG – C	-	4.59 ± 0.77	3.61 ± 0.28	4.22 ± 0.39	5.42 ± 0.46
S232CA – C	-	6.11 ± 0.64	5.24 ± 0.24	5.20 ± 0.28	7.55 ± 0.69
Q233HE – O1	-	2.97 ± 1.81	2.85 ± 1.83	-	-
R257H – O	-	1.71 ± 0.14	1.69 ± 0.10	1.76 ± 0.21	1.89 ± 0.45
R257H – O1	-	1.72 ± 0.15	1.72 ± 0.10	2.02 ± 0.69	3.21 ± 0.65
H334HE – O	-	-	-	-	-
V414OB – H2	-	-	-	-	-

Table S5. Values of selected distances (Å) and QM energies (a.u) for the optimized snapshots from MD2 and MD3 of monAT5 **–** *propargyl-MSNAC*.

Distance / Energy	Snapshot				
	1	2	3	4	5
	-1141.898	-1141.907	-1141.909	-1141.892	-1141.887
Protein – Protein Distances					
S232HG – H231ND	2.06	2.18	2.16	2.17	2.11
H334HE – N384OB	4.32	4.35	4.42	4.18	4.25
R323CA – L417CA	12.99	13.83	13.11	13.25	13.30
S329CA – Q149CA	9.56	9.17	9.48	9.06	9.48
Protein – Substrate Distances					
Q149OB – H1	2.02	1.97	1.95	1.95	1.89
Q149HN – O2	1.98	2.03	1.93	1.97	1.94
S232OG – C	3.84	3.78	3.72	3.70	3.72
S232CA – C	5.79	5.81	5.76	5.67	5.71
Q233HE – O1	1.84	1.86	1.85	1.81	1.82
R257H – O	1.66	1.66	1.66	1.66	1.66
R257H – O1	1.66	1.64	1.66	1.64	1.64
H334HE – O	1.72	1.74	1.74	1.75	1.73
V414OB – H2	-	-	-	-	-

Table S5. (Continuation)

Distance / Energy	Snapshot				
	6	7	8	9	10
	-1141.908	-1141.887	-1141.896	-1141.901	-1141.907
Protein – Protein Distances					
S232HG – H231ND	5.46	5.48	5.37	5.32	4.99
H334HE – N384OB	2.03	1.91	2.17	1.84	1.86
R323CA – L417CA	16.13	15.71	15.56	15.64	15.90
S329CA – Q149CA	10.06	9.81	9.76	9.67	9.45
Protein – Substrate Distances					
Q149OB – H1	5.99	6.36	6.21	5.39	3.93
Q149HN – O2	5.94	3.99	6.02	6.30	5.09
S232OG – C	5.87	5.71	5.80	5.85	5.63
S232CA – C	8.08	7.84	8.08	7.97	7.89
Q233HE – O1	7.97	7.99	8.31	8.22	8.29
R257H – O	3.25	3.14	3.22	2.88	3.46
R257H – O1	1.68	1.68	1.68	1.66	1.76
H334HE – O	4.18	4.10	4.08	4.22	4.36
V414OB – H2	-	-	-	-	-

Table S5. (Continuation)

Distance / Energy	Snapshot				
	11	12	13	14	15
	-1141.907	-1141.919	-1141.897	-1141.894	-1141.894
Protein – Protein Distances					
S232HG – H231ND	1.90	1.89	1.91	1.91	1.91
H334HE – N384OB	4.54	4.59	4.62	4.57	5.01
R323CA – L417CA	13.19	13.34	13.68	14.18	14.51
S329CA – Q149CA	8.37	8.21	8.24	8.33	8.47
Protein – Substrate Distances					
Q149OB – H1	1.75	1.78	1.70	1.76	1.80
Q149HN – O2	1.88	1.86	1.88	1.89	1.90
S232OG – C	4.44	4.51	4.52	4.43	4.22
S232CA – C	5.57	5.52	5.59	5.45	5.34
Q233HE – O1	1.85	1.84	1.87	1.85	1.89
R257H – O	1.74	1.73	1.73	1.72	1.69
R257H – O1	1.66	1.64	1.64	1.65	1.64
H334HE – O	1.89	1.84	1.91	1.88	3.13
V414OB – H2	-	-	-	-	-

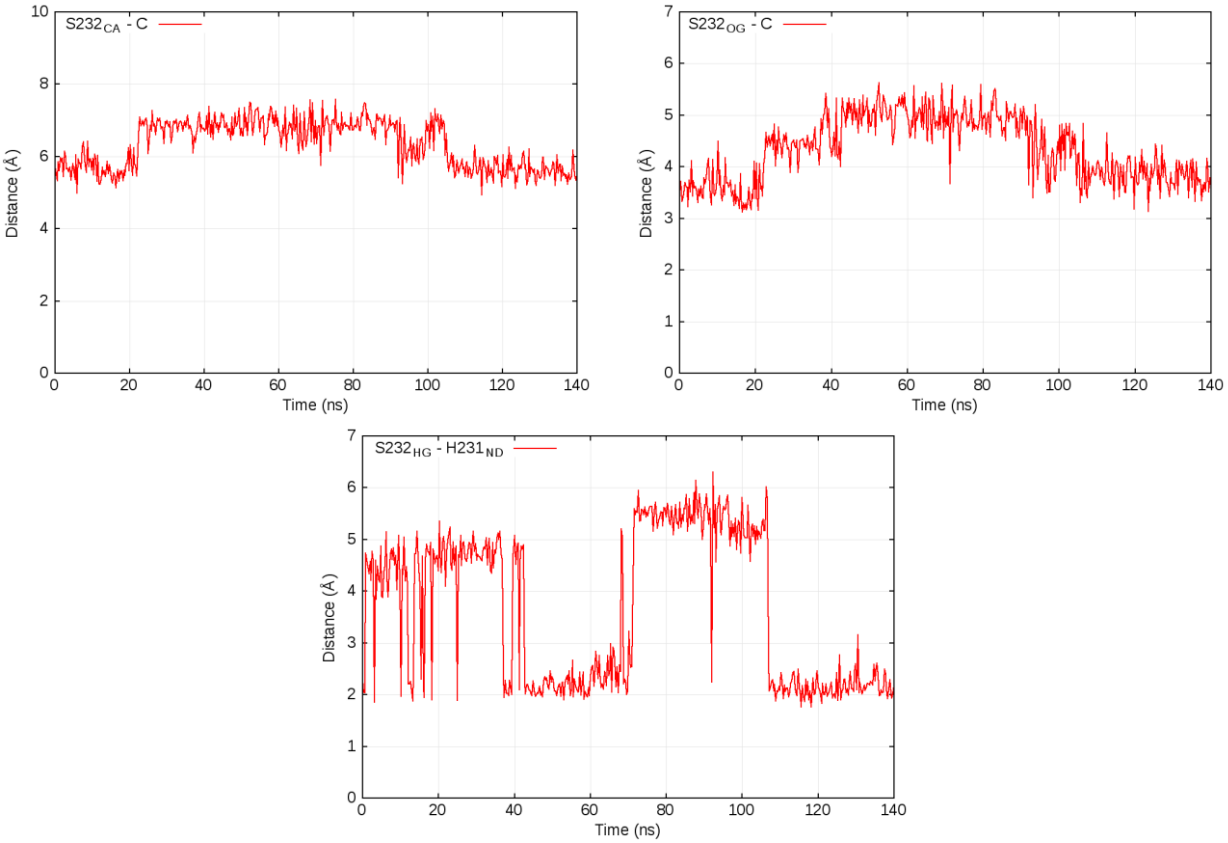

SI Figure 1: If MD2A is prolonged for additional 40 ns, *MMCoA* is accommodated in the active site and the distances $S232_{CA}$ – C (upper left), $S232_{OG}$ – C (upper right) and $S232_{HG}$ – $H231_{ND}$ (bottom) take the regular values of a prereactive complex.

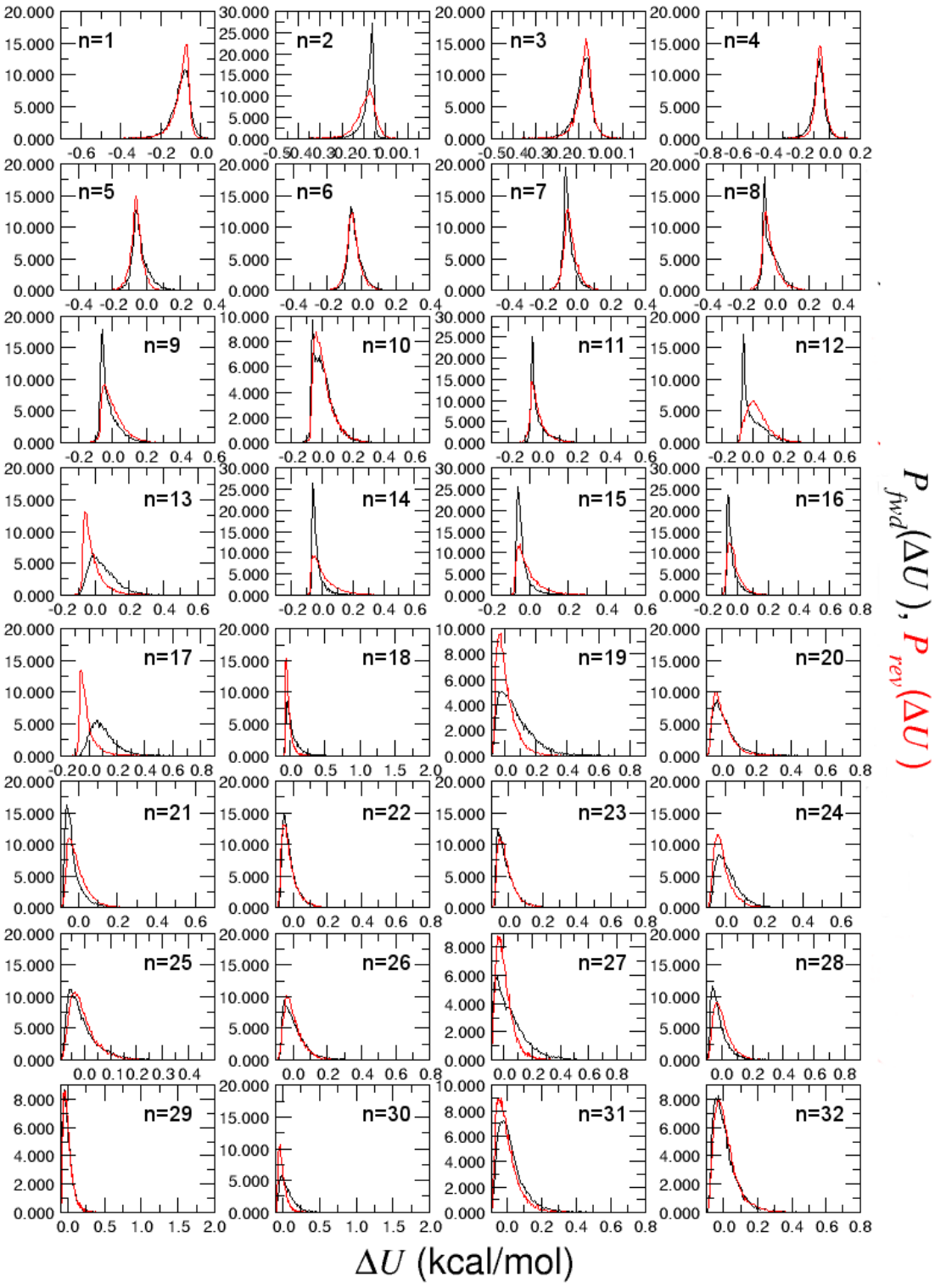

SI Figure 2: Probability distribution for the backward and forward transformation *MMCoA → EtMCoA.*

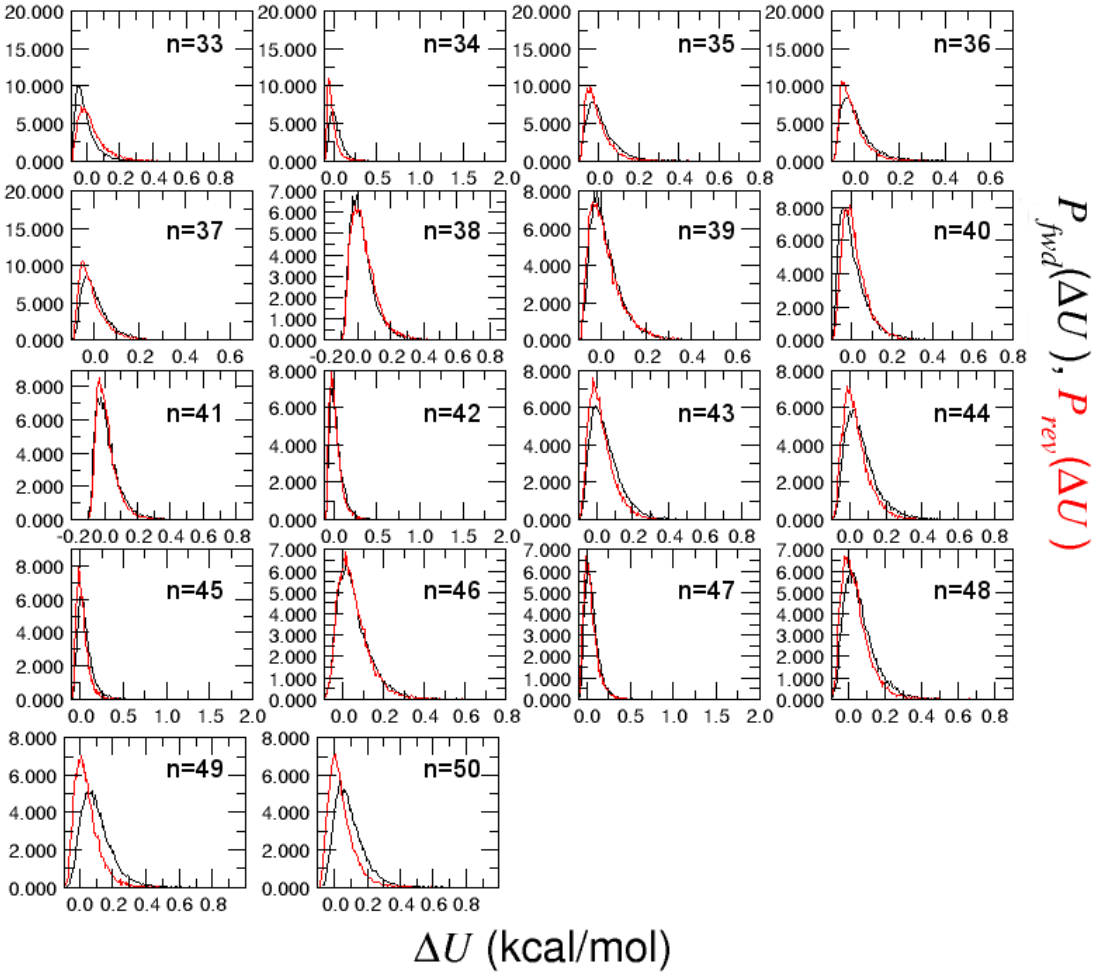

SI Figure 2 (Continuation)

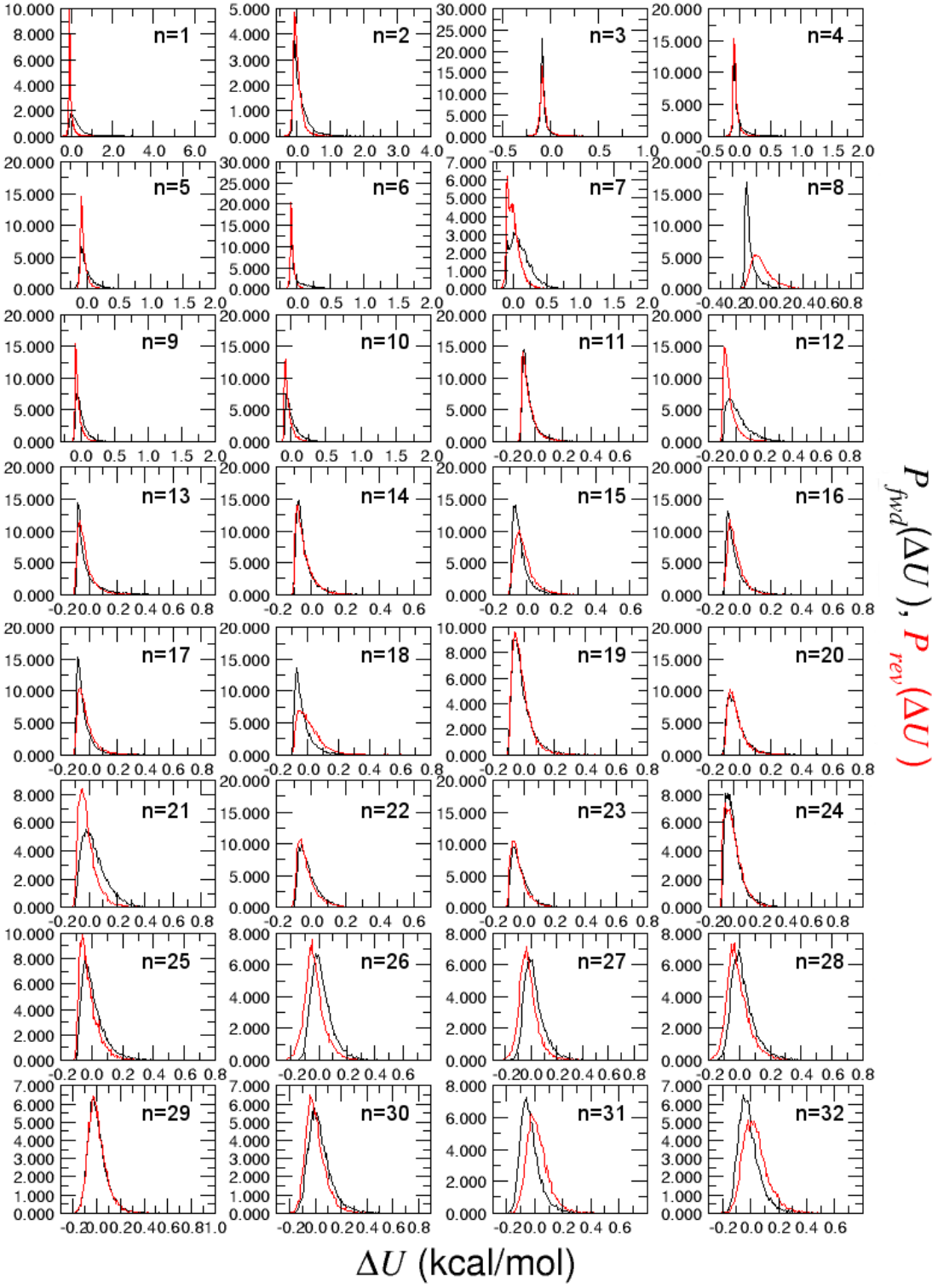

SI Figure 3: Probability distribution for the backward and forward transformation *MMCoA → propargyl-MCoA*.

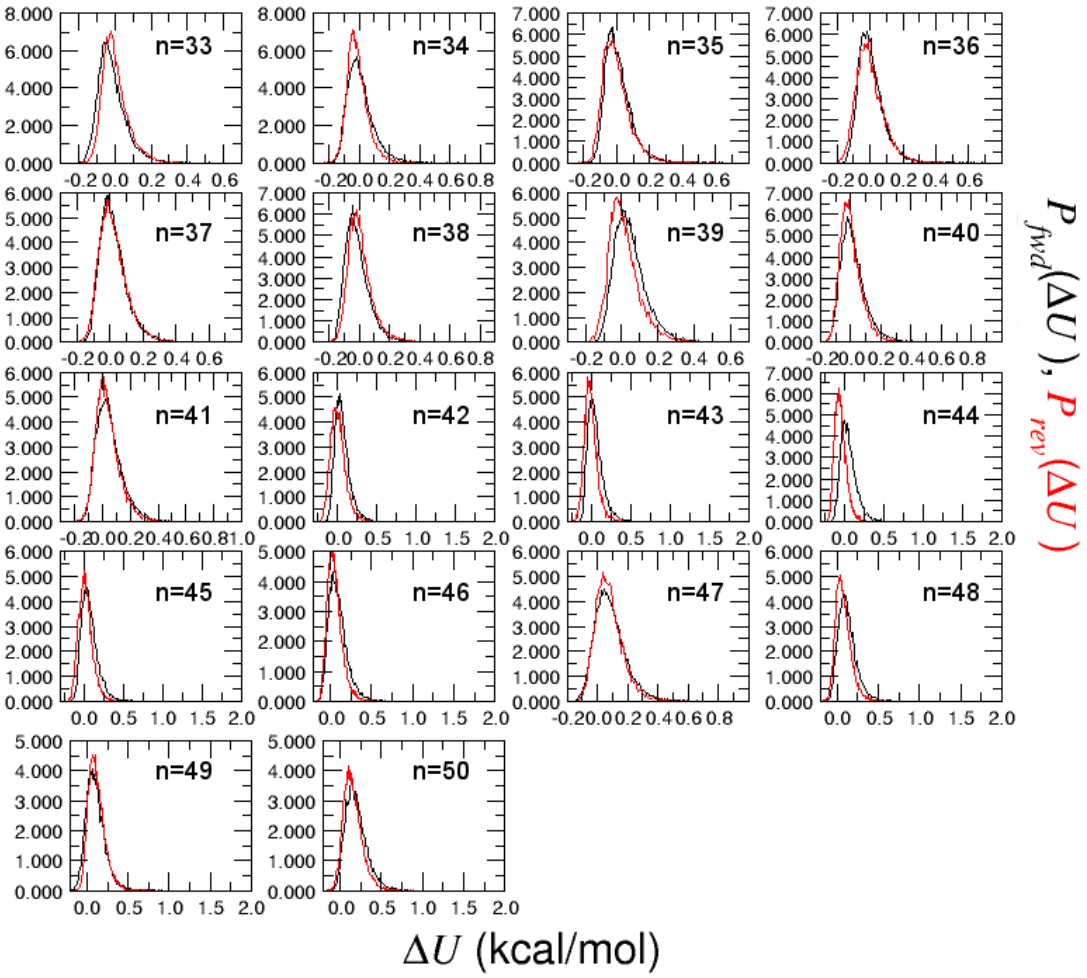

SI Figure 3 (Continuation)

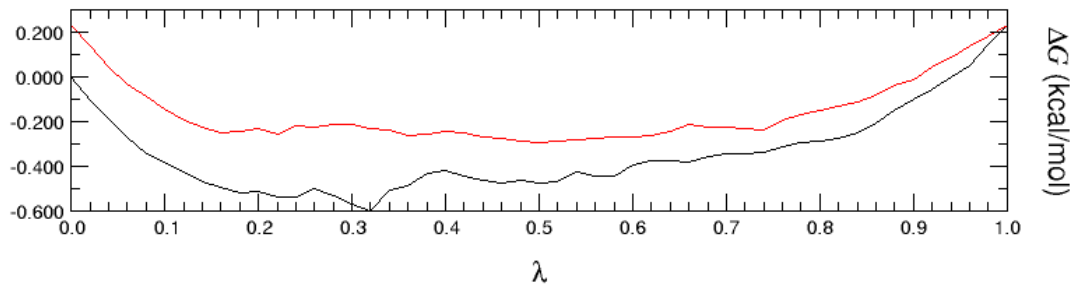

SI Figure 4: Change in the free energy of the system for the forward and backward transformation *MMCoA → EtMCoA*.

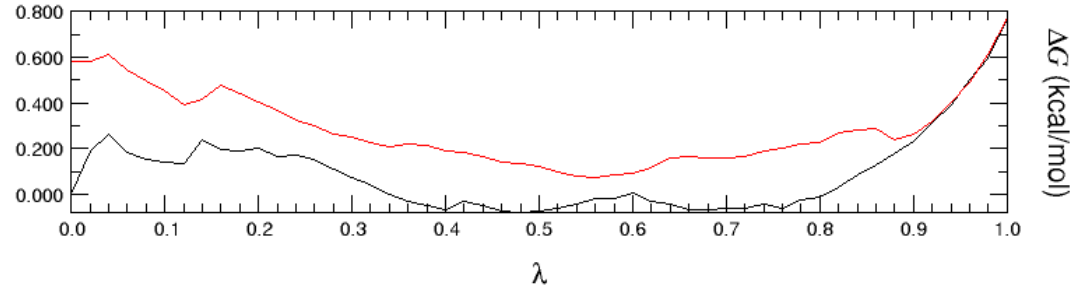

SI Figure 5: Change in the free energy of the system for the forward and backward transformation *MMCoA → propargyl-MCoA*.

II Feeding experiments

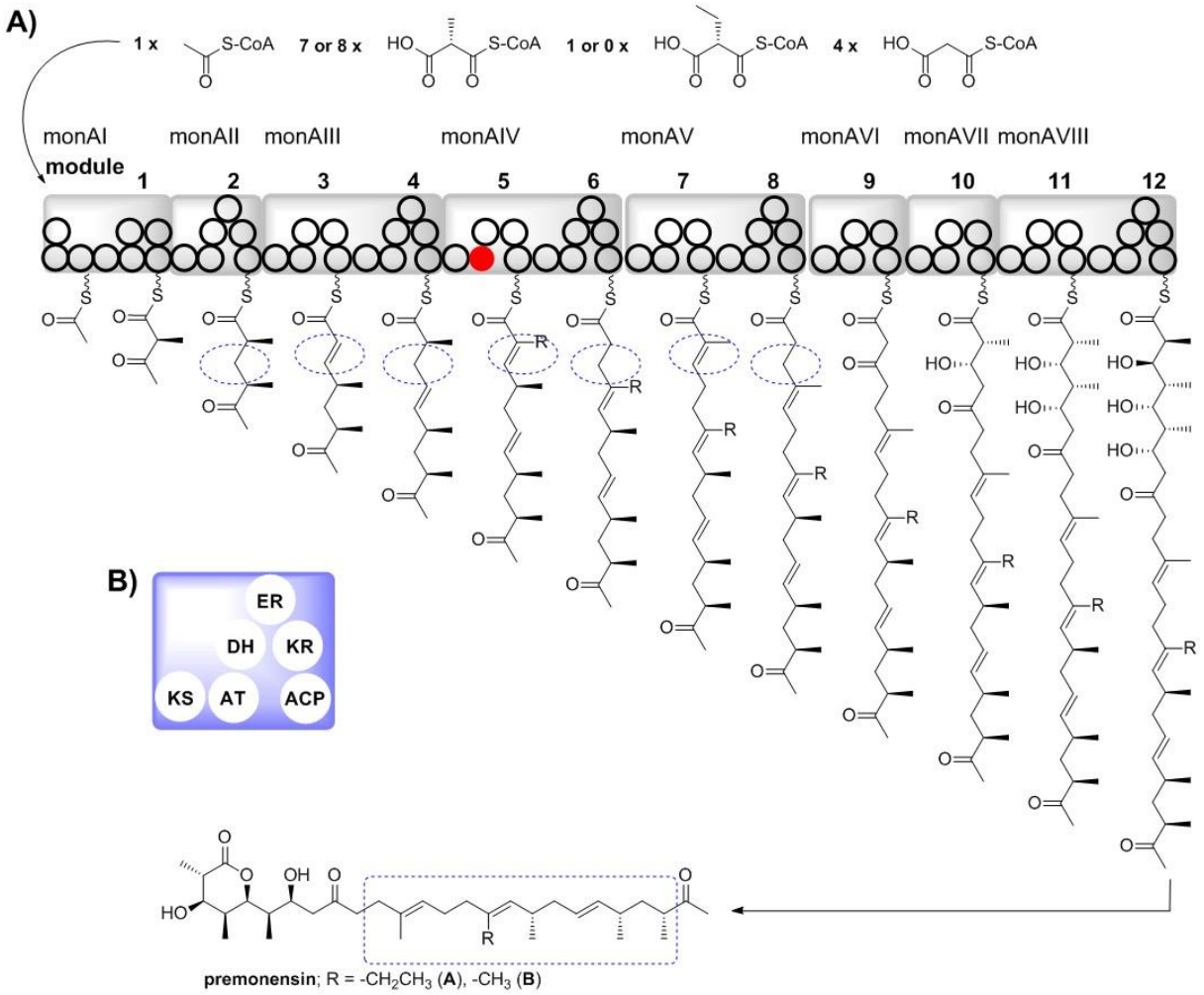

SI Figure 6: Organization of the Monensin PKS (monPKS), with blocked post-PKS processing leading to the shunt products premonensin A and B. monAI to monAVIII denote the multidomain enzymes in the monensin PKS, single modules are enumerated in Arabic numbers. For clarity, the individual catalytic domains are simplified as circles. **A:** Overview over PKS machinery. The Acyltransferase domain in module 5 is highlighted in red. **B:** Zoom into a single module with a complete reductive loop (such as modules 2, 4, 6, and 8). All modules are organized in the same way, yet in many cases with an incomplete set of the reductive domains (KR, DH, ER), whereas all modules contain the essential set of domains required for chain extension (KS, AT, ACP). KS: Ketosynthase, AT: Acyltransferase, ACP: Acyl Carrier Protein, KR: Ketoreductase, DH: Dehydratase, ER: Enoylreductase.

S. cinnamonensis A495 (BHΔCIBIBII) was initially grown for 48 hours in 3 mL tryptic soy broth (Difco Laboratories, Detroit, USA) at 30°C/180 rpm in an orbital shaker with 5 cm deflection for use as inoculum. 15 mL SM16 medium (MOPS20.90 g/L, L-proline10 g/L, glucose 20g/L, NaCl 0.5 g/L, $K_2HPO_4$2.10 g/L, EDTA0.25 g/L, $MgSO_4$×7 H_2O 0.49 g/L,

$CaCl_2$×2 H_2O 0.029 g/L, supplemented with 10 mM, 20 mM or 30 mM of the respective malonyl-SNAC derivative) were inoculated with 5% pre-culture. SM16 cultures were grown for 5 days at 30°C/180 rpm for optimal production levels. On days 4 and 5, SM16 cultures were supplemented with 20 g/L XAD16 resin (Sigma). *S. cinnamonensis* A495 was cultivated without any malonyl-SNAC derivative supplementation to serve as a control for the fermentation.

II.1 Analysis of fermentation products

For characterization via HPLC-ESI-MS, cell paste and XAD resin from the fermentation cultures were extracted with 2 volumes of ethyl acetate overnight at 19°C. The solvent phase was evaporated and the residue was re-dissolved in 0.5 mL methanol. 3µl were used for analysis.

LC-ESI-MS for routine analysis were measured using an Agilent 1100 series binary pump together with a C18 (EP 150/2 NUCLEODUR C18 ISIS, 3µm. Macherey-Nagel) column coupled to a Finnigan LTQ linear ion trap (Thermo Electron Corporation, Dreieich, Germany). A flow rate of 250 µl/min was used with a linear gradient starting with 60% solvent A / 40% solvent B for one minute and increasing to 0% solvent A / 100% solvent B in 11 min. After the column was washed with 0% solvent A / 100% solvent B for 4 min and re-equilibrated to starting conditions for additional 4 min (solvent A: water containing 0.1% formic acid, solvent B: acetonitrile containing 0.1% formic acid).

For the determination of accurate mass-to-charge ratios the bacterial extracts were analyzed by HPLC coupled to high resolution mass spectrometry. The separations were carried out on an Accela HPLC-System (consisting of a pump, autosampler, column oven and a PDA detector) coupled online to an Orbitrap mass spectrometer equipped with a LTQ XL linear ion trap (Thermo Electron Corporation, Dreieich, Germany) using the standard electrospray ionization source. All solvents were LC-MS grade (Chromasolv, Sigma-Aldrich, Munich, Germany). 2 µl of each sample were injected (T = 10 °C) onto a Hypersil GOLD column (1.9 µm particle size, 50 mm length, 1 mm ID, 30 °C column temperature, Thermo Electron

Corporation, Dreieich, Germany) using a flow rate of 250 µl/min and a linear gradient starting with 95 % solvent A / 5 % solvent B for one minute and increasing to 10 % solvent A / 90 % solvent B in 8.5 min. Afterwards the column was washed with 10 % solvent A / 90 % solvent B for 5 min and re-equilibrated to starting conditions for additional 5 min (solvent A: water containing 0.1 % formic acid, solvent B: acetonitrile containing 0.1 % formic acid). For mass spectrometric detection the electrospray ionization was carried out in positive ionization mode using a source voltage of 3.8 kV. The capillary voltage was set to 41 V, the capillary temperature to 275 °C, and the tube lens voltage to 140 V. Spectra were acquired in full scan centroid mode with a mass-to-charge range from 100 to 2000. The resolution in the Orbitrap was set to 60,000, the FTMS full AGC target to 500,000 and for internal calibration a lock mass of 391.2843 (diisooctyl phthalate) was used.

II.2 LC-MS-ESI Chromatograms of crude extractions from *S. cinnamonensis* A495 feeding experiments

Allyl-premonensin (4a)

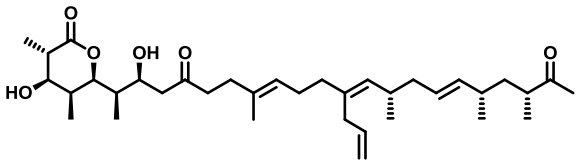

Exact Mass: 586,4233

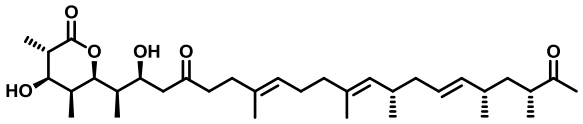

Premonensin B (2a)

Exact Mass: 560,4077

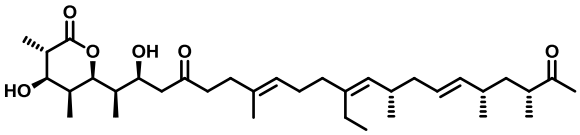

Premonensin A (3a)

Exact Mass: 574,4233

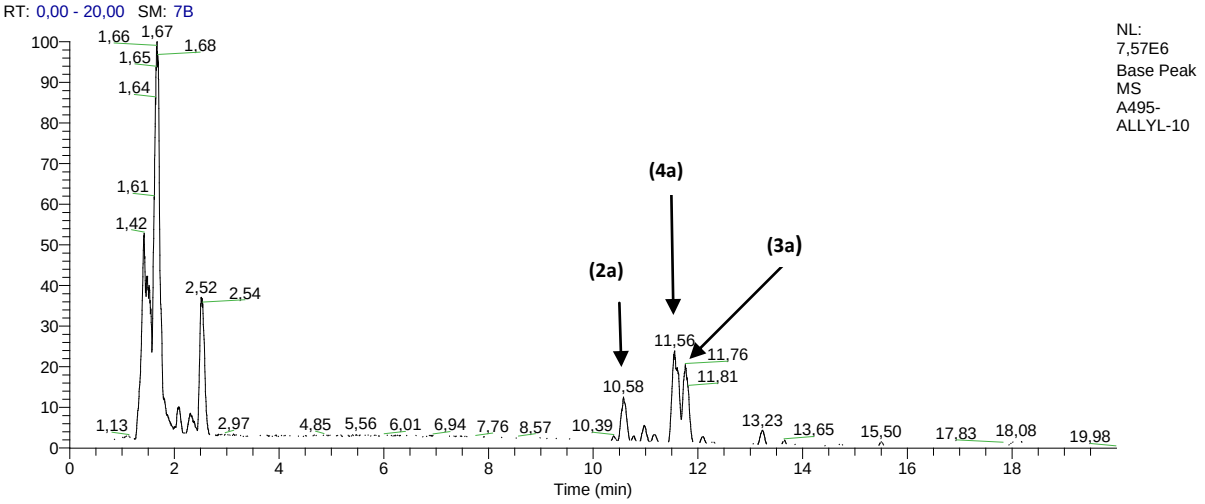

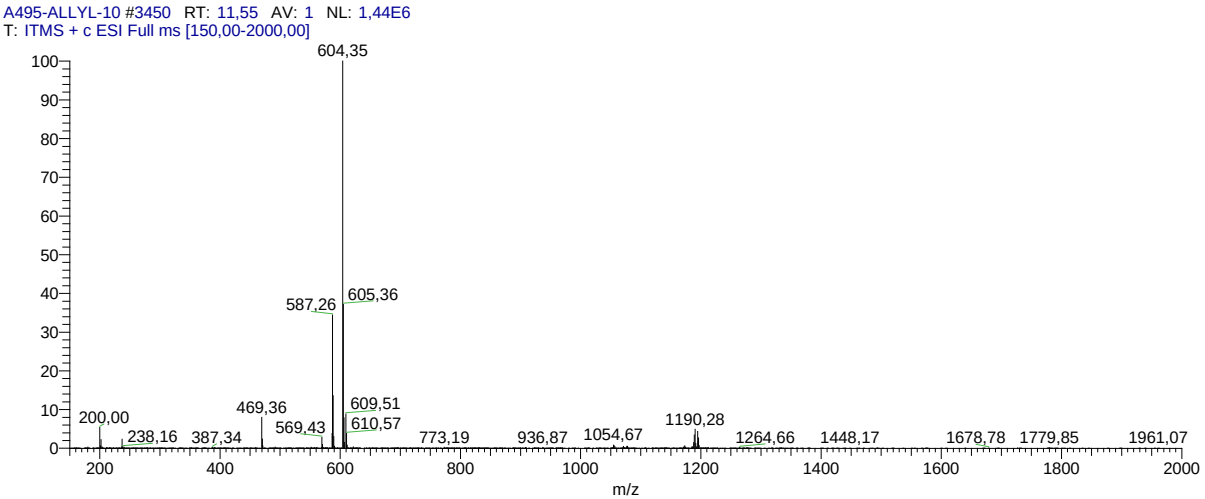

Propargyl-premonensin (5a)

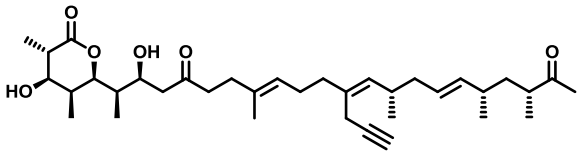

Exact Mass: 584,4077

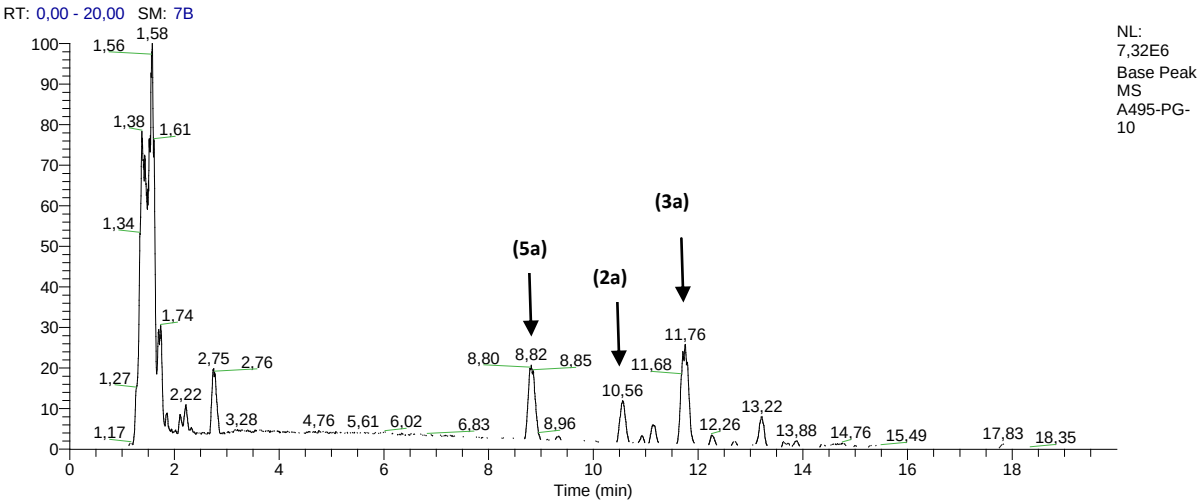

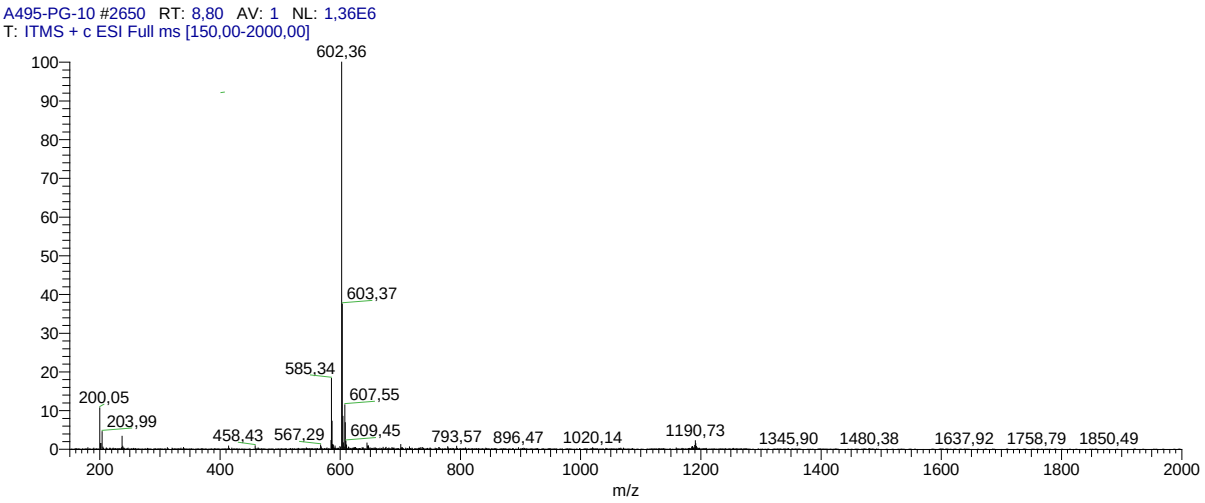

Propyl-premonensin (6a)

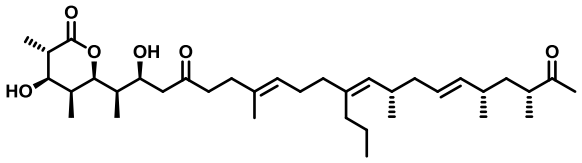

Exact Mass: 588,4390

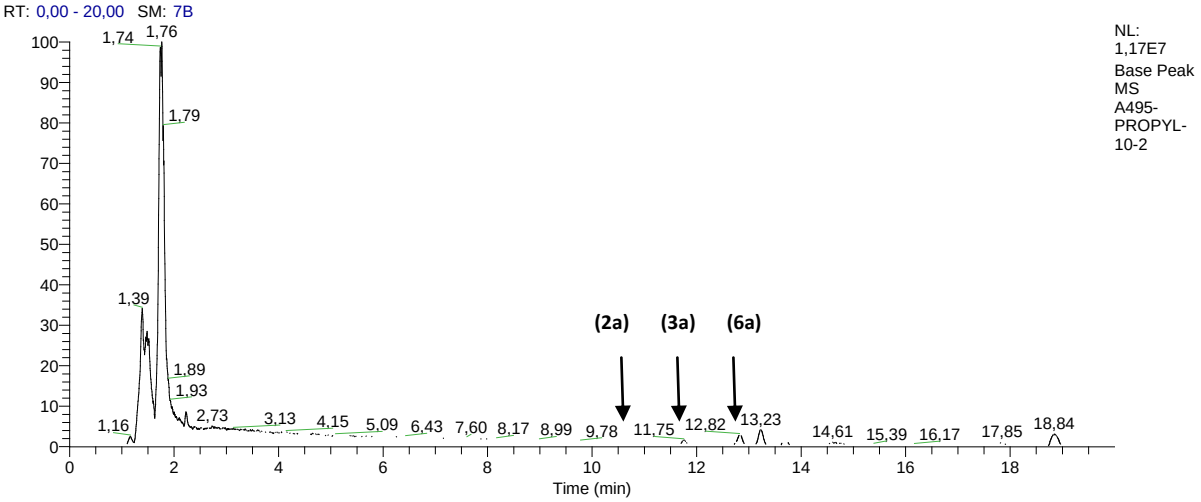

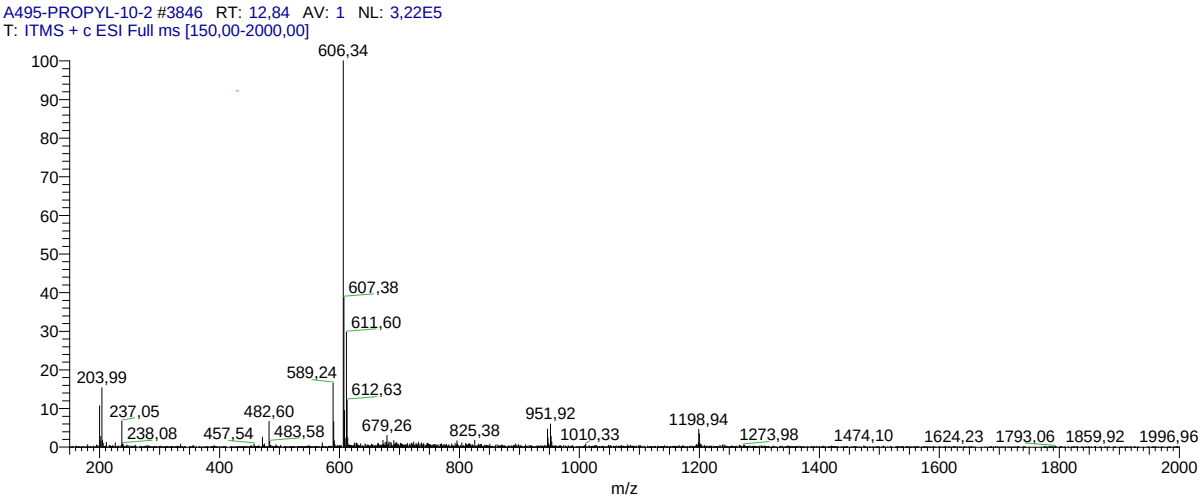

Butyl-premonensin (7a)

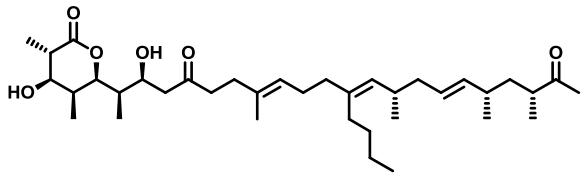

Exact Mass: 602,4546

10mM

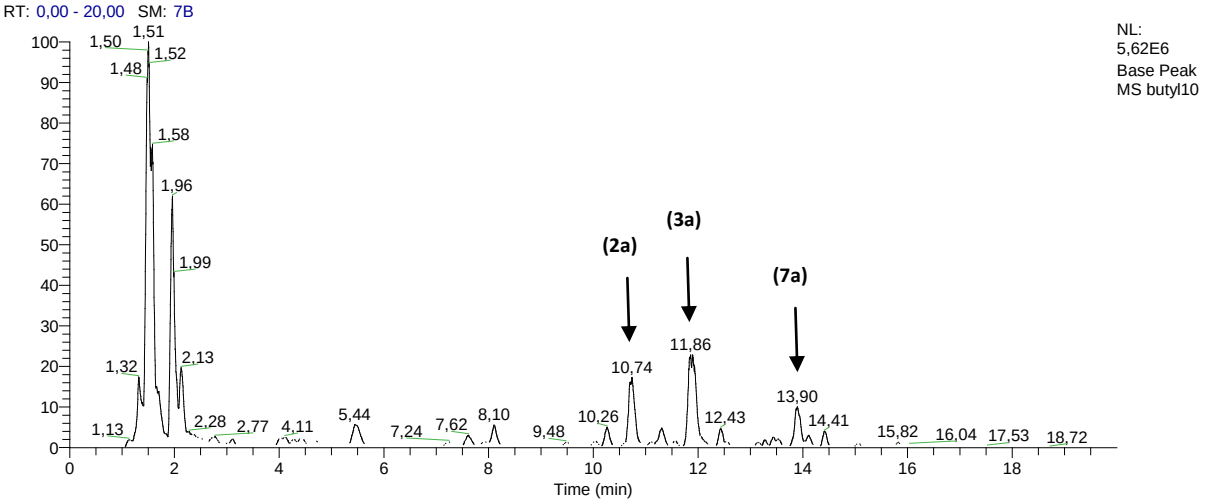

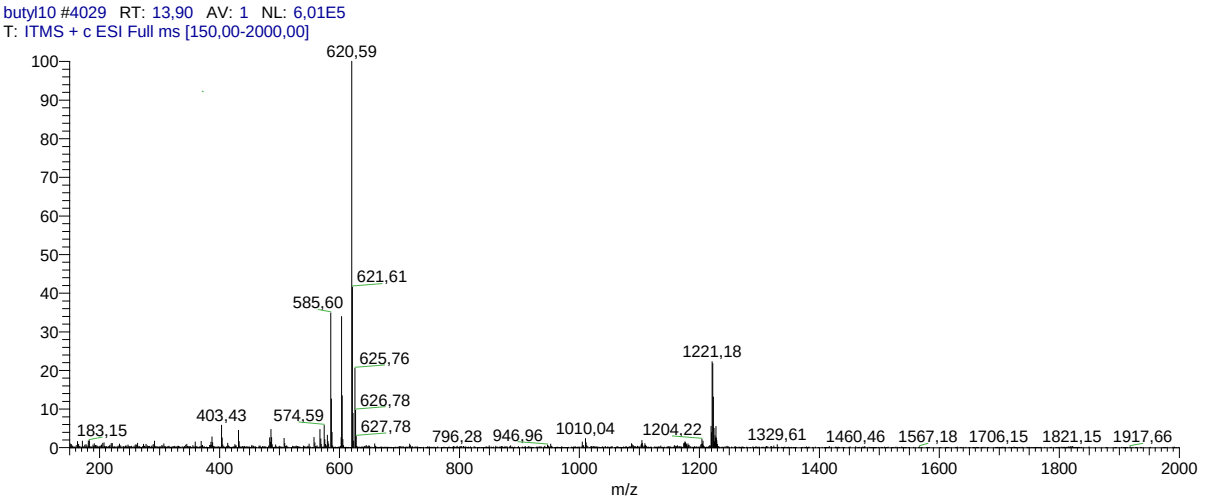

20 mM

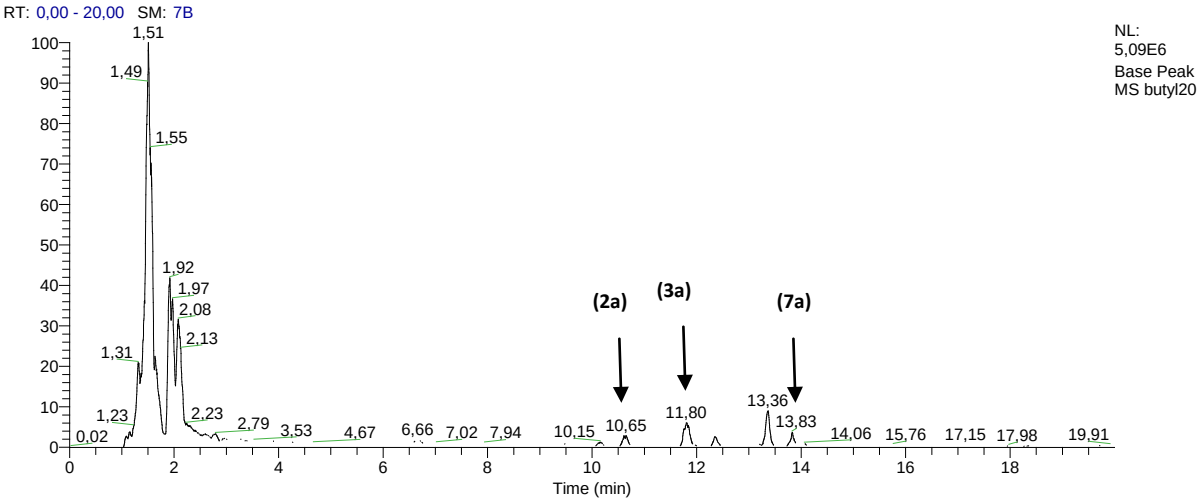
RT: 0,00 - 20,00 SM: 7B
NL:
5,09E6
Base Peak
MS butyl20
(2a)
(3a)
(7a)
Time (min)

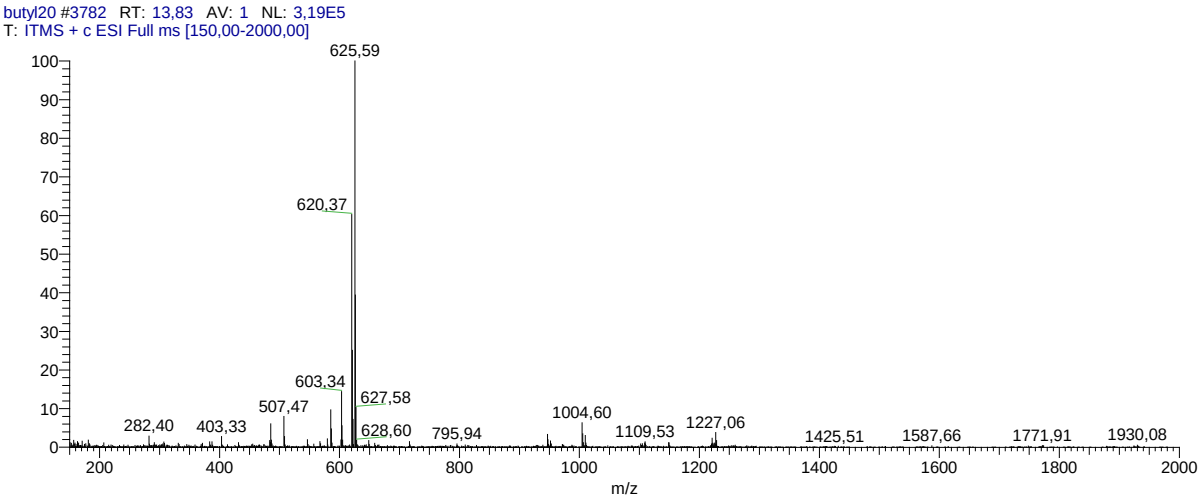
butyl20 #3782 RT: 13,83 AV: 1 NL: 3,19E5
T: ITMS + c ESI Full ms [150,00-2000,00]
m/z

30mM

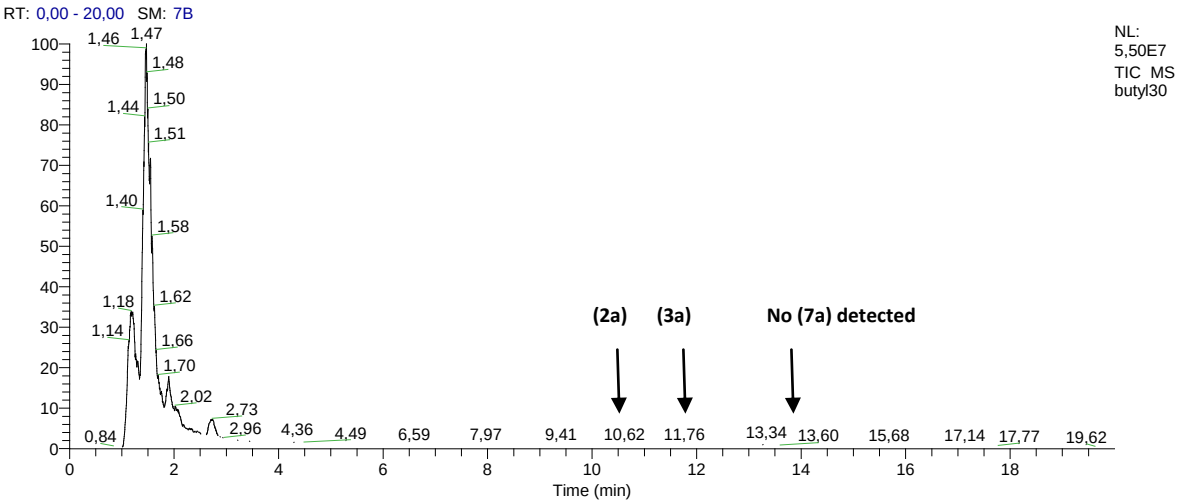
RT: 0,00 - 20,00 SM: 7B
NL:
5,50E7
TIC MS
butyl30
(2a)
(3a)
No (7a) detected
Time (min)

Allyl-ER2^0 (4b)

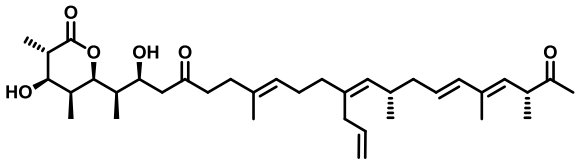

Exact Mass: 584,4077

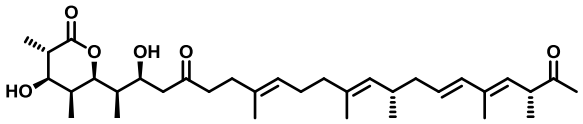

ER2^0 B (2b)

Exact Mass: 558,3920

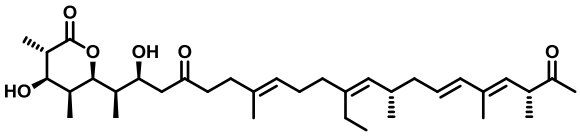

ER2^0 A (3b)

Exact Mass: 572,4077

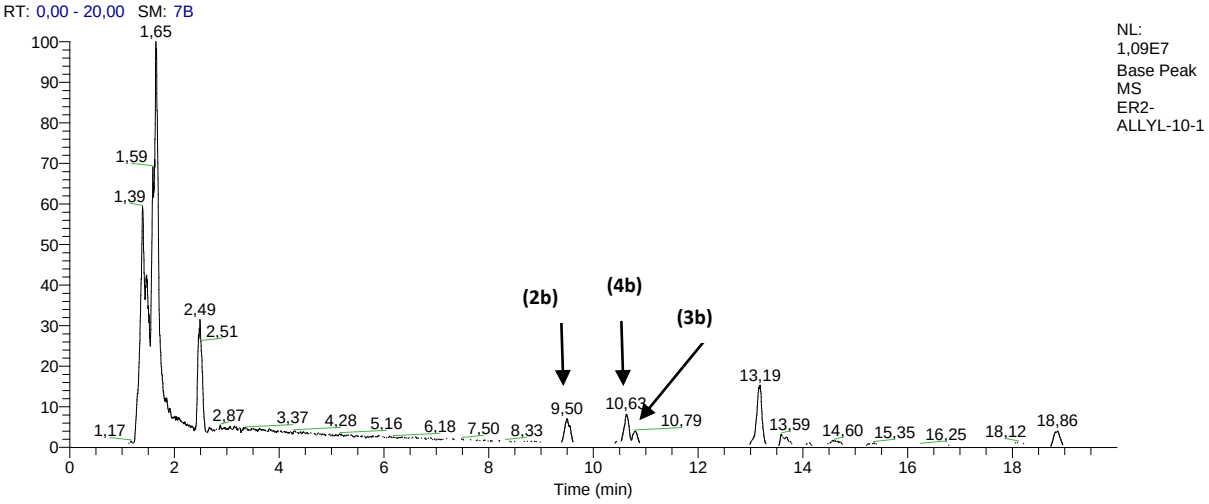

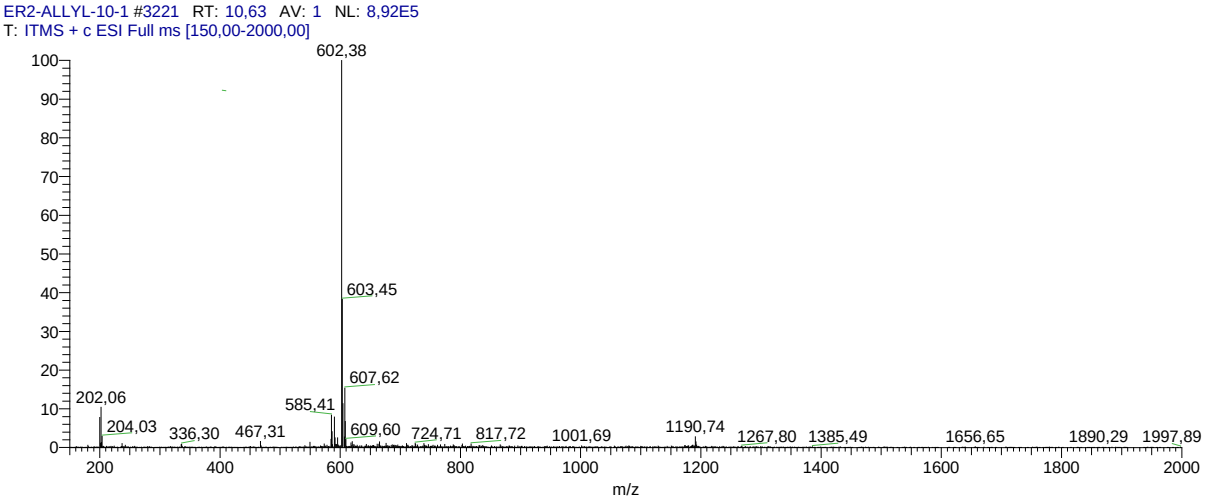

Propyl-ER2^0 (6b)

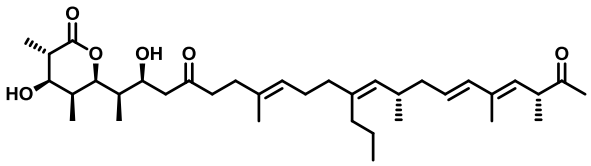

Exact Mass: 586,4233

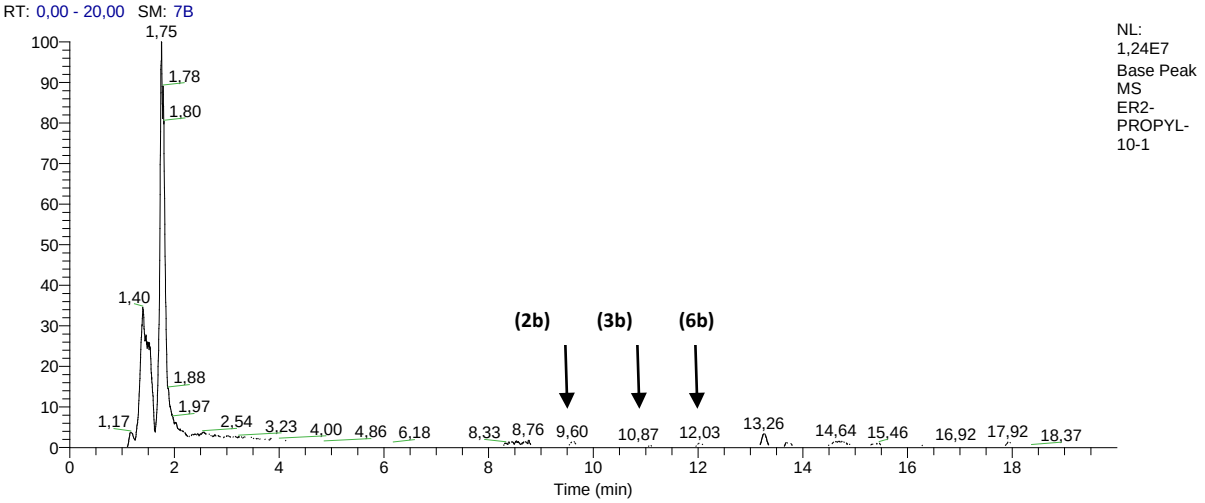

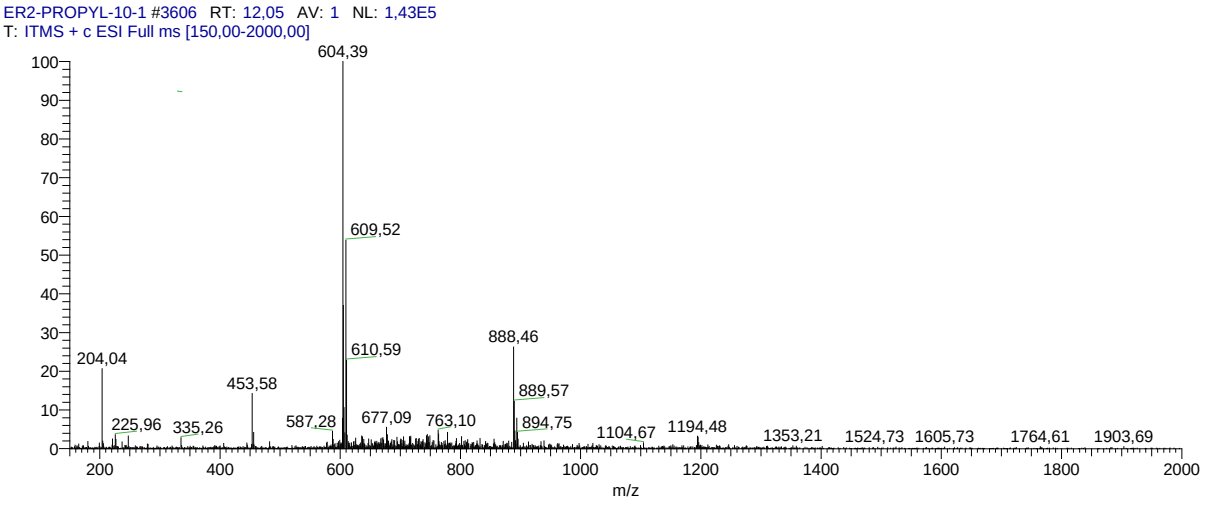

Propargyl-ER2^0 (not detected)

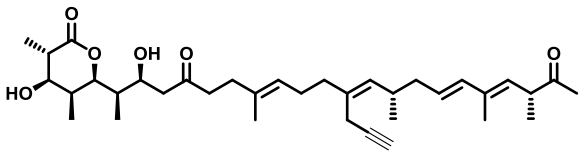

Exact Mass: 582,39

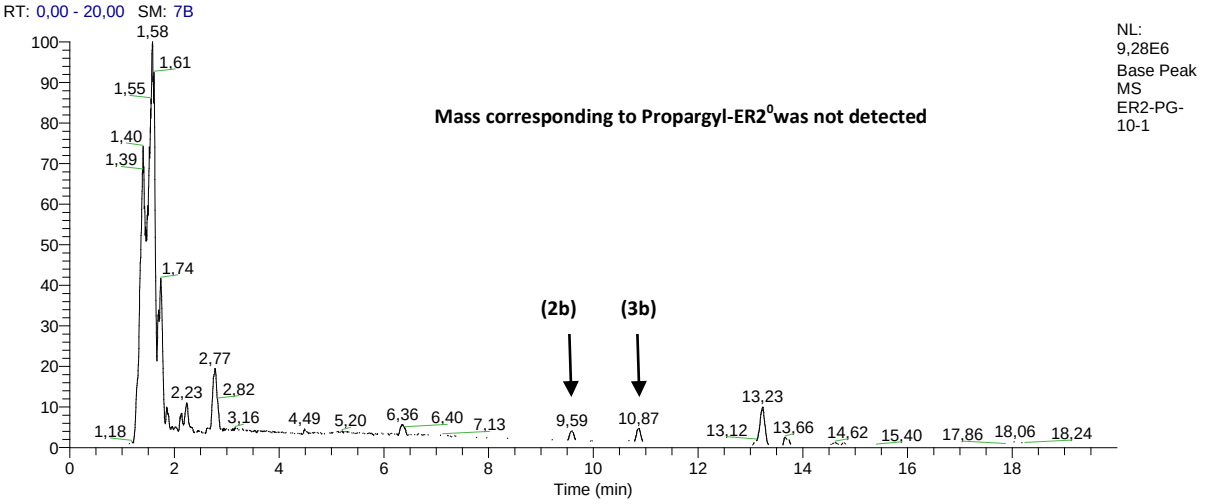

II.3 High-Resolution MS-results

Allyl-premonensin (4a)

$C_{36}H_{58}O_6$: $[M+NH_4]^+$theor.: 604.4572, exp.: 604.4575, diff.: 0.58 ppm

Propargyl-Premonensin (5a)

$C_{36}H_{56}O_6$: $[M+NH_4]^+$theor.: 602.4415, exp.: 602.4411, diff: -0.70 ppm

$[M+H]^+$theor.: 585,4150, exp.: 585.4143, diff: -1.09 ppm

$[M+Na]^+$theor.: 607.3969, exp.: 607.3965, diff: -0.75 ppm

Propyl-premonensin (6a)

$C_{36}H_{60}O_6$: $[M+NH_4]^+$theor.: 606.4728, exp.: 606.4724, diff.: -0.63 ppm

Butyl-Premonensin (7a)

$C_{37}H_{62}O_6$: $[M+NH_4]^+$theor.: 620.4885, exp.: 620,4875, diff: -1,50 ppm

$[M+H]^+$theor.: 603.4619, exp.: 603.4614, diff: -0.92 ppm

$[M+Na]^+$theor.: 625.4439, exp.: 625.4431, diff: -1.16 ppm

Allyl-ER2^0 (4b)

$C_{36}H_{56}O_6$: $[M+NH_4]^+$theor.: 602.4415 exp.: 602.4412, diff: -0.50 ppm

$[M+H]^+$theor.: 585.4150, exp.: 585.4150, diff: -0.65 ppm

$[M+Na]^+$theor.: 607.3969, exp.: 607.3967, diff: -0.42 ppm

Propyl-ER2^0 (6b)

$C_{36}H_{58}O_6$: $[M+NH_4]^+$ theor.: 604.4572, exp.: 604.4572, diff.: -0.04 ppm

II.4 Extraction and purification of Propargyl-premonensin (5a)

Cell paste and XAD-16 resin obtained from a culture volume of 1.8 L fermentation supplemented with 10 mM 2-propargylmalonyl-SNAC was extracted 4 times at room temperature for 1 hour with an equal volume of ethyl acetate, followed by an additional overnight extraction. The combined extracts were concentrated *in vacuo*at 35°C to yield a crude extract. The extract was then fractionated by flash chromatography on silica gel (0.035-0.070 nm, Acros Organics) using a gradient of cyclohexane and EtOAc (80-20 to 30-70). This first purification separated the premonensin analogs from co-eluted media components and metabolites.

Further purification using preparative LC-MS was performed on an Agilent 1100 series with two preparative pumps coupled to a LC/MSD VL system (Agilent Technologies) equipped with a C18 (VP 250/16 NUCLEODUR C18 ISIS, 5µm. Macherey-Nagel) column, using a CH_3CN/H_2O gradient as mobile phase at a flow rate of 15 mL/min. From the same fermentation batch, premonensin A (**PreA**) and B (**PreB**) were purified using a modified protocol from Kushnir *et al*.[19]

	Propargyl-Premonensin	Premonensin	
Fermentation volume	1.8 L	1.8 L	
Compound	**5a**	**2a**	**3a**
Isolated amount (mg)	1,0	9,8	3,2

II.5 NMR-analysis of propargyl-premonensin and premonensin A

Propargyl-premonensin

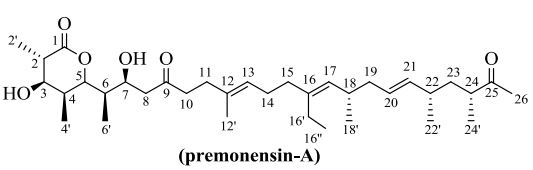
(premonensin-A)

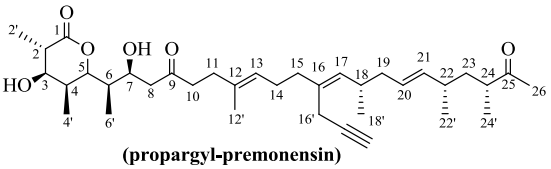
(propargyl-premonensin)

	premonensin-A (CDCl$_3$, 500 MHz)			propargyl-premonensin (CDCl$_3$, 600 MHz)		
Protons	σ(ppm)	multiplicity	*J* (Hz)	σ(ppm)	multiplicity	*J* (Hz)
H-2	2.47	m	-	2.39-2.51	m	-
H-2'	1.41	d	7.5	1.40-1.42	d	7.1
H-3	3.85	dd	4.0; 10.0	3.84-3.86	dd	4.2; 10.2
H-4	2.44	m	-	2.39-2.51	m	-
H-4'	0.96	d	7.0	0.96-0.97	d	6.0
H-5	4.22	dd	2.0; 9.5	4.19-4.23	m	-
H-6	1.75	m	-	1.74-1.77	m	-
H-6'	1.10	d	7.0	1.10-1.11	d	6.6
H-7	4.20	dt	2.0; 9.5	4.19-4.23	m	-
H-8a	2.67	dd	10.0; 18.0	2.65-2.70	dd	12.0; 6.0
H-8b	2.53	m	-	2.53	m	-
H-10	2.55	m	-	2.54-2.57	m	-
H-11	2.26	t	7.5	2.25-2.28	t	7.6
H-12'	1.61	s	-	1.62	s	-
H-13	5.12	t	7.5	5.13-5.14	m	-
H-14	2.05	m	-	1.94-1.97	m	-
H-15	1.96	m	-	1.94-1.97	m	-
H-16'	2.05	m	-	2.91-2.92	m	-
H-16''	0.94	t	8.0	-	-	-
H-16'''	-	-	-	2.17	s	-
H-17	4.85	d	10.0	5.00-5.02	d	9.5
H-18	2.36	m	-	2.39-2.51	m	-
H-18'	0.91	d	7.0	0.93-0.94	d	6.6
H-19	1.92	m	-	1.94-1.97	m	-
H-20	5.33	dt	7.0 ; 15.0	5.30-5.36	m	-
H-21	5.15	dd	8.5; 15.0	5.16-5.19	m	-
H-22	2.10	m	-	2.10-2.13	m	-
H-22'	0.97	d	7.0	0.97-0.98	d	6.0
H-23a	1.60	m	-	1.59-160	m	-
H-23b	1.22	m	-	1.20-1.24	m	-
H-24	2.50	m	-	2.54-2.57	m	-
H-24'	1.03	d	6.5	1.03-1.04	d	6.8
H-26	2.11	s	-	2.11	s	-

^{13}C NMR:

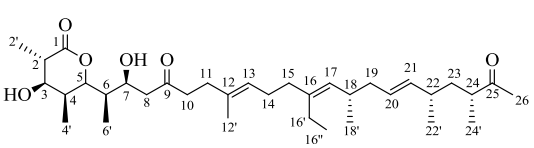

(premonensin-A)

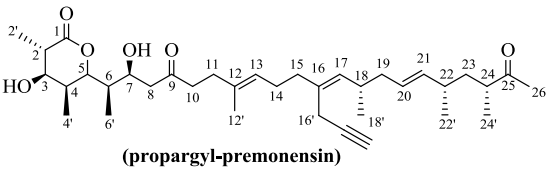

(propargyl-premonensin)

Carbons	premonensin-A ($CDCl_3$, 100 MHz)	propargyl-premonensin ($CDCl_3$, 100 MHz)
C-1	173.6	173.9
C-2	40.1	40.1
C-2'	14.6	14.7
C-3	74.1	74.2
C-4	35.3	35.4
C-4'	4.9	5.0
C-5	81.4	81.5
C-6	38.7	38.8
C-6'	10.0	10.0
C-7	66.2	66.4
C-8	46.6	46.6
C-9	212.2	212.3
C-10	42.3	42.4
C-11	33.4	33.5
C-12	132.9	133.1
C-12'	16.2	16.3
C-13	125.4	125.1
C-14	26.9	26.8
C-15	36.5	36.7
C-16	138.9	133.6
C-16'	23.4	20.1
C-16''	13.6	68.5
C-16'''	-	82.6
C-17	130.6	131.1
C-18	32.6	33.0
C-18'	21.2	20.8
C-19	40.8	40.5
C-20	128.2	127.9
C-21	136.2	136.8
C-22	35.2	35.3
C-22'	21.7	21.8
C-23	40.0	40.0
C-24	45.3	45.4
C-24'	16.1	16.1
C-25	213.1	213.3
C-26	28.1	28.2

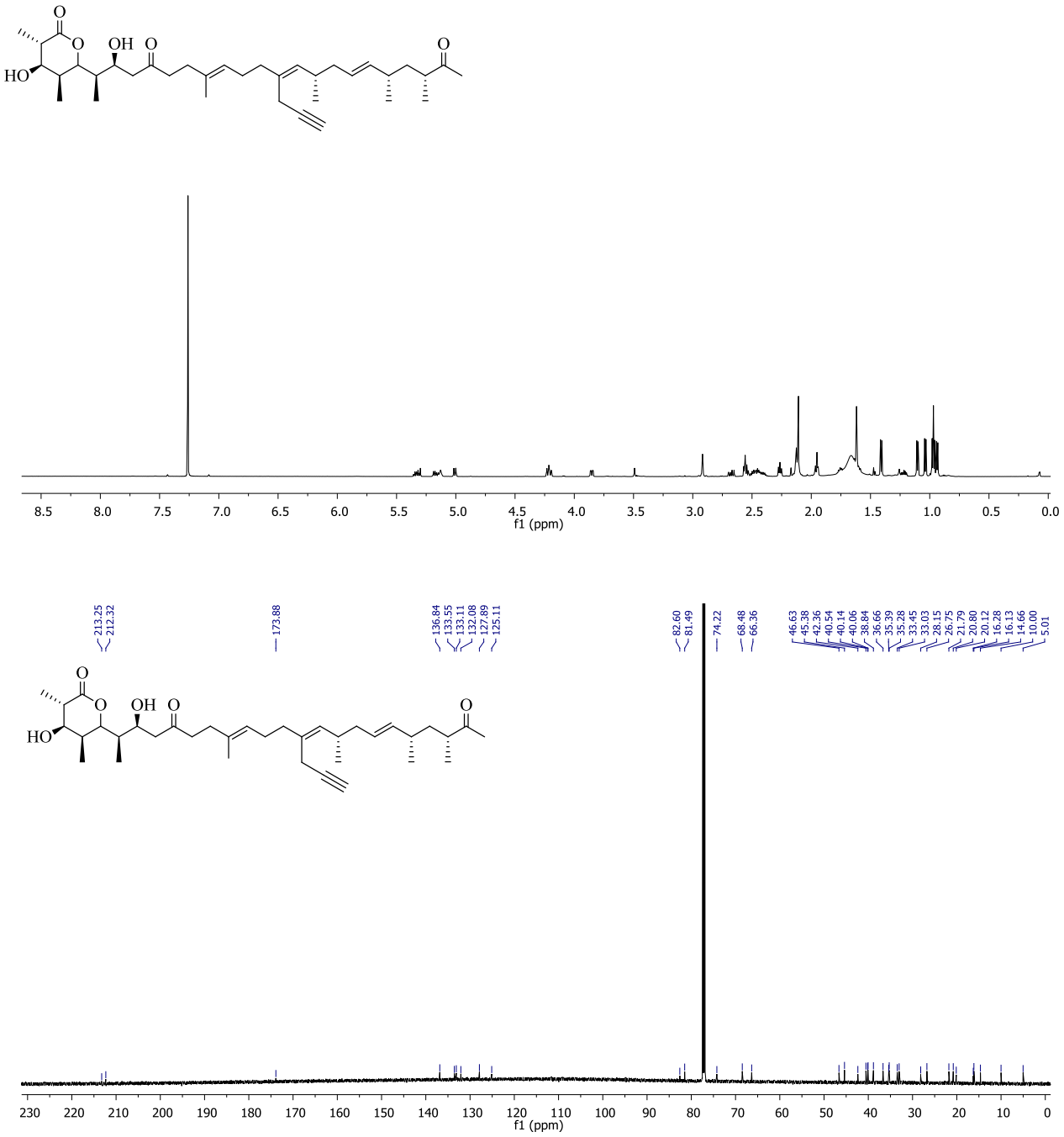

SI Figure 7: ^{1}H-NMR- and ^{13}C-NMR-spectra of propargyl-premonensin (**5a**) in $CDCl_3$-d_1.

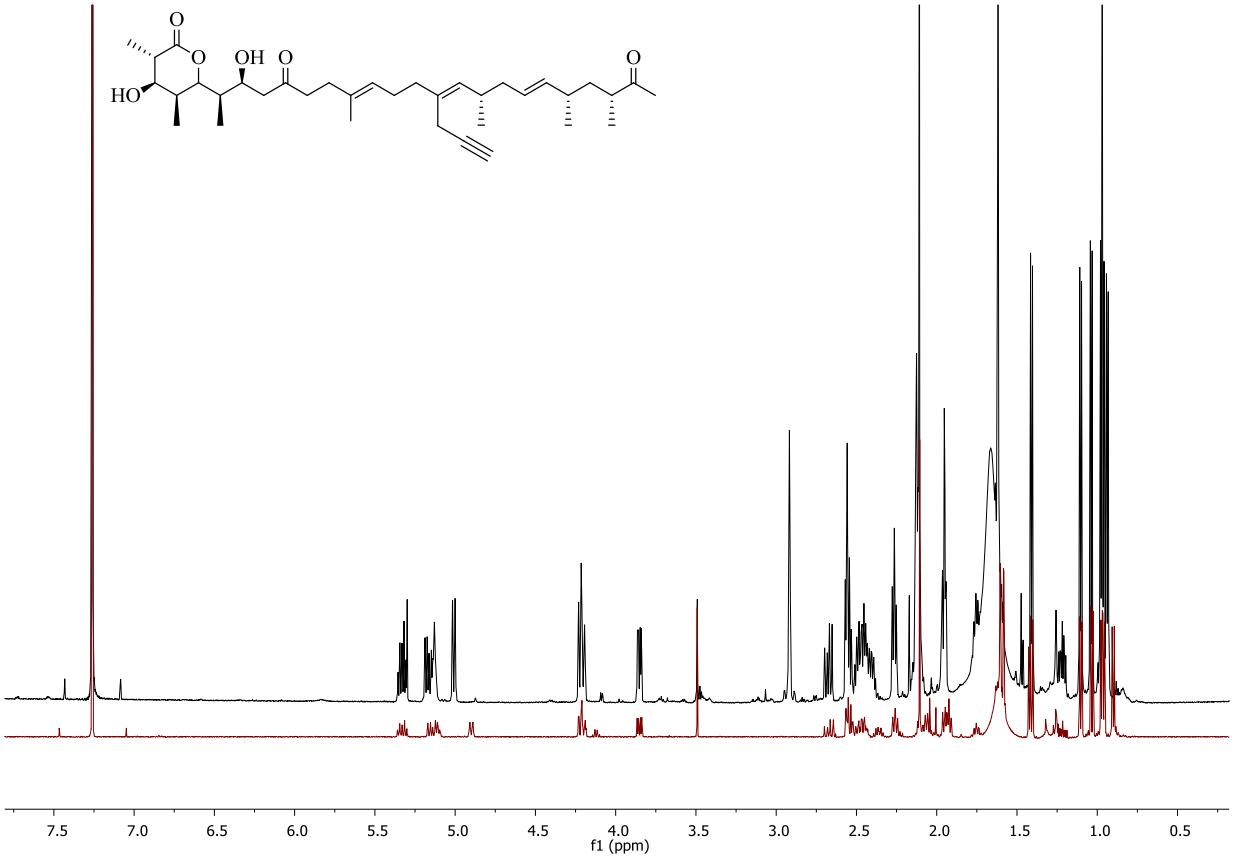

SI Figure 8: Overlay of ^{1}H-NMR-spectra of propargyl-premonensin (black) and premonensin (red) in $CDCl_3$-d_1.

Premonensin A

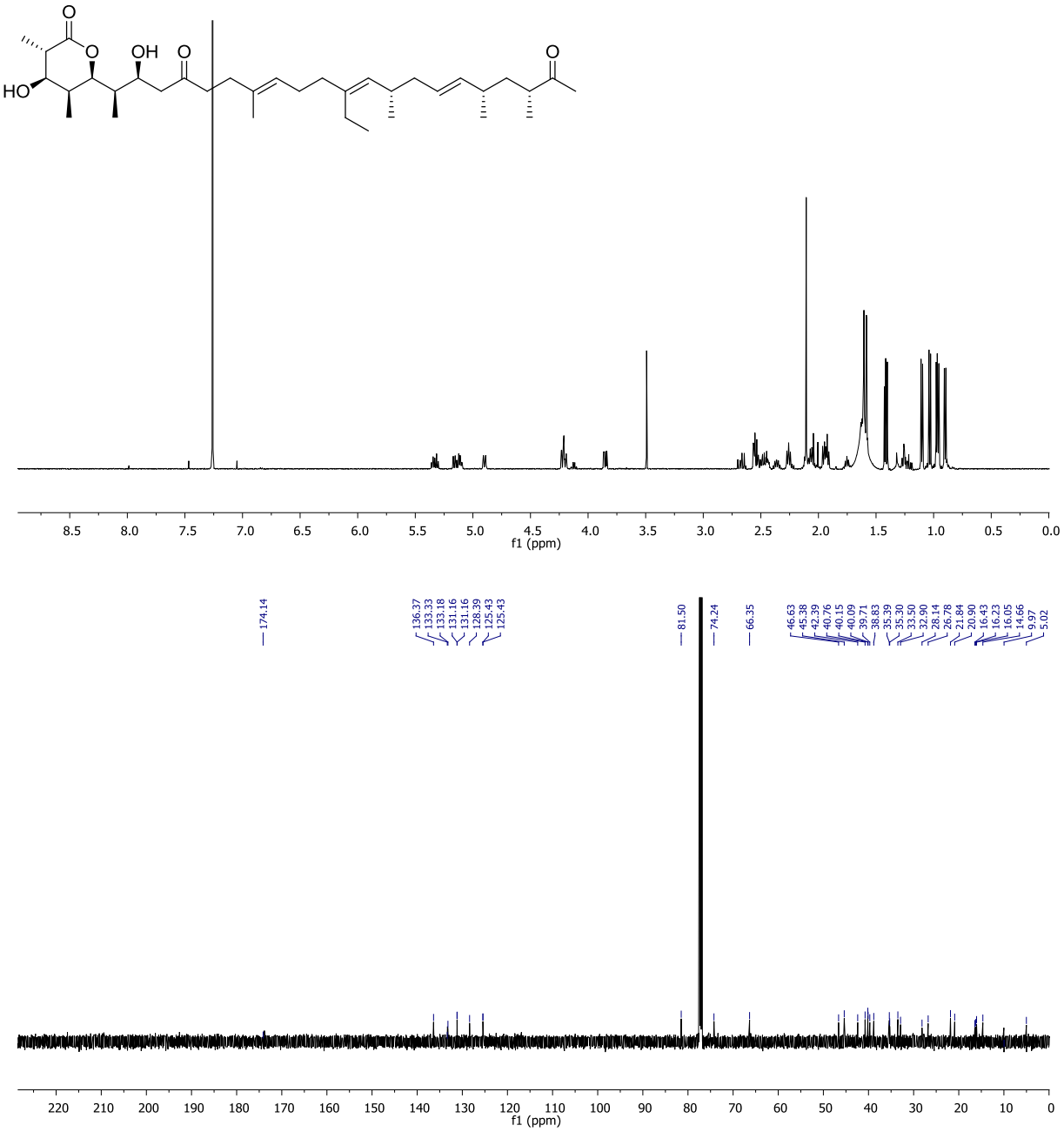

SI Figure 9: ^{1}HNMR- and ^{13}C-spectra of premonensin A (**3a**) in $CDCl_3$-d_1.

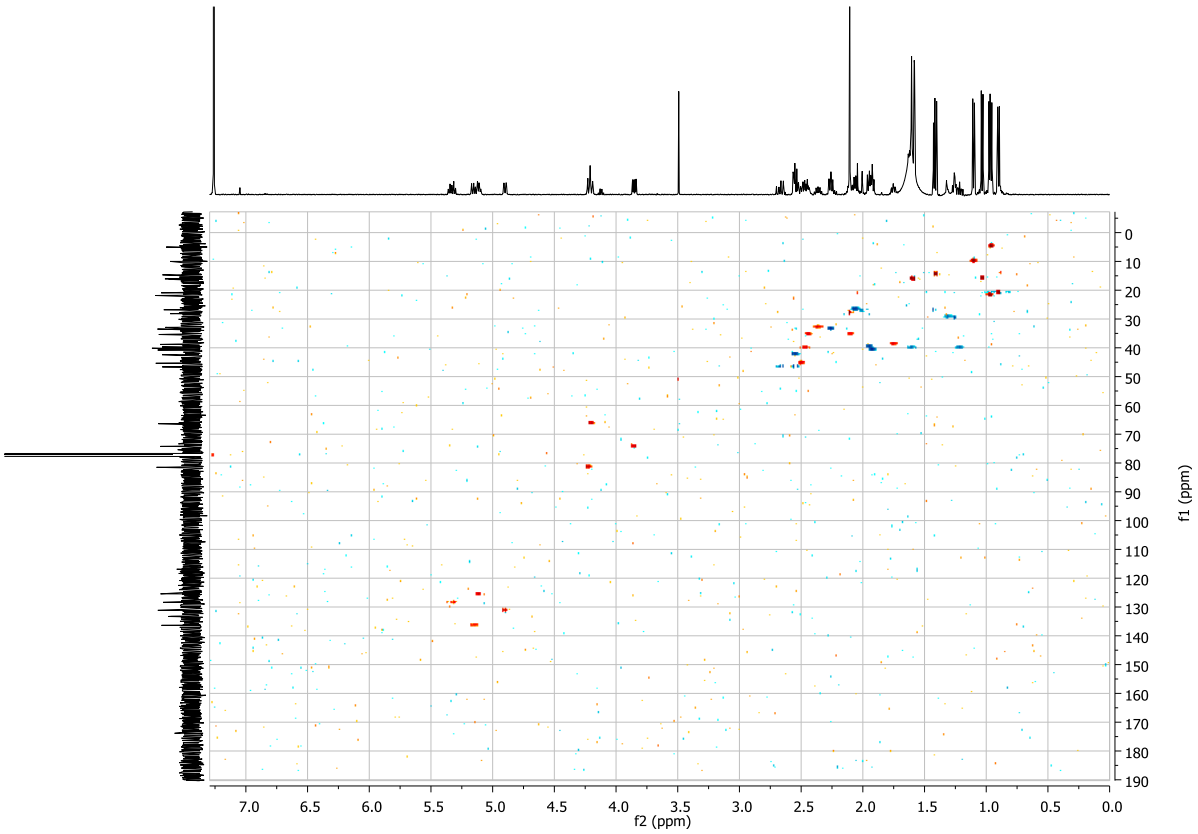

SI Figure 10: gHSQC-spectra of premonensin A (**3a**) in $CDCl_3$-d_1.

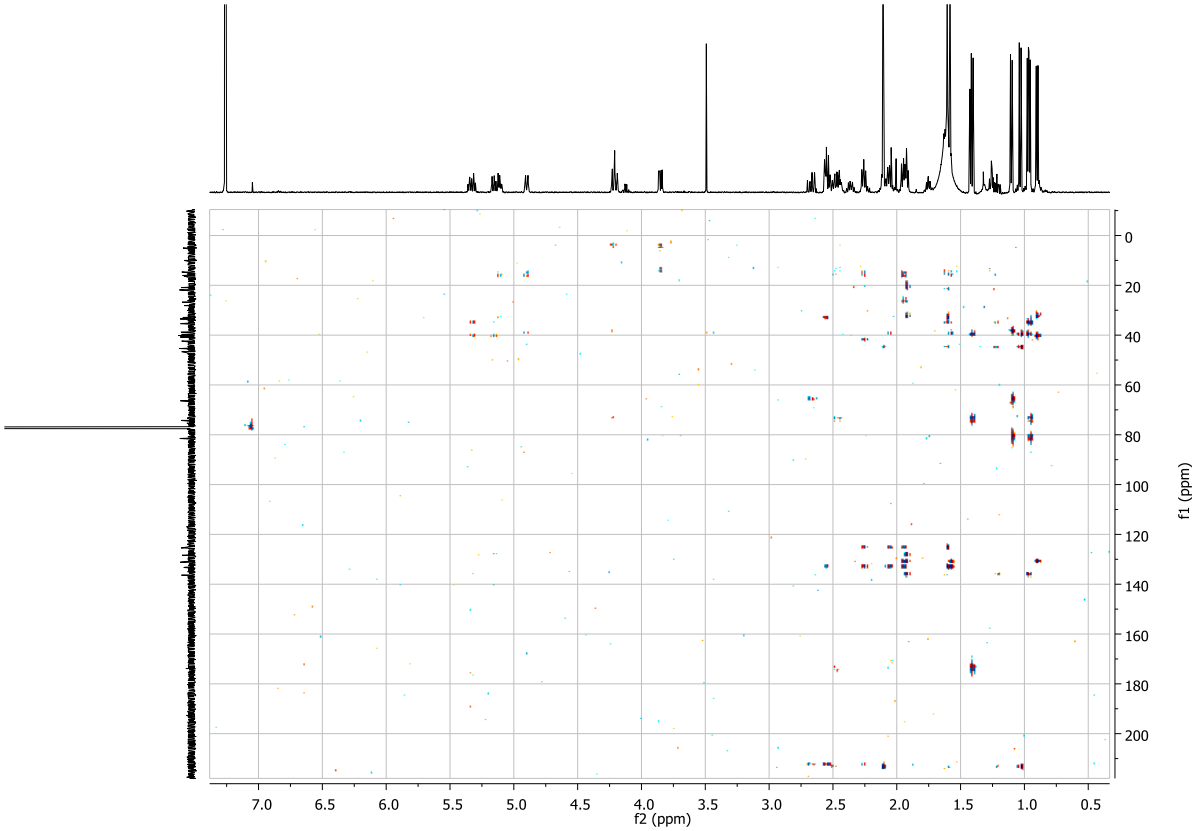

SI Figure 11: gHMBC-spectra of premonensin A (**3a**) in $CDCl_3$-d_1.

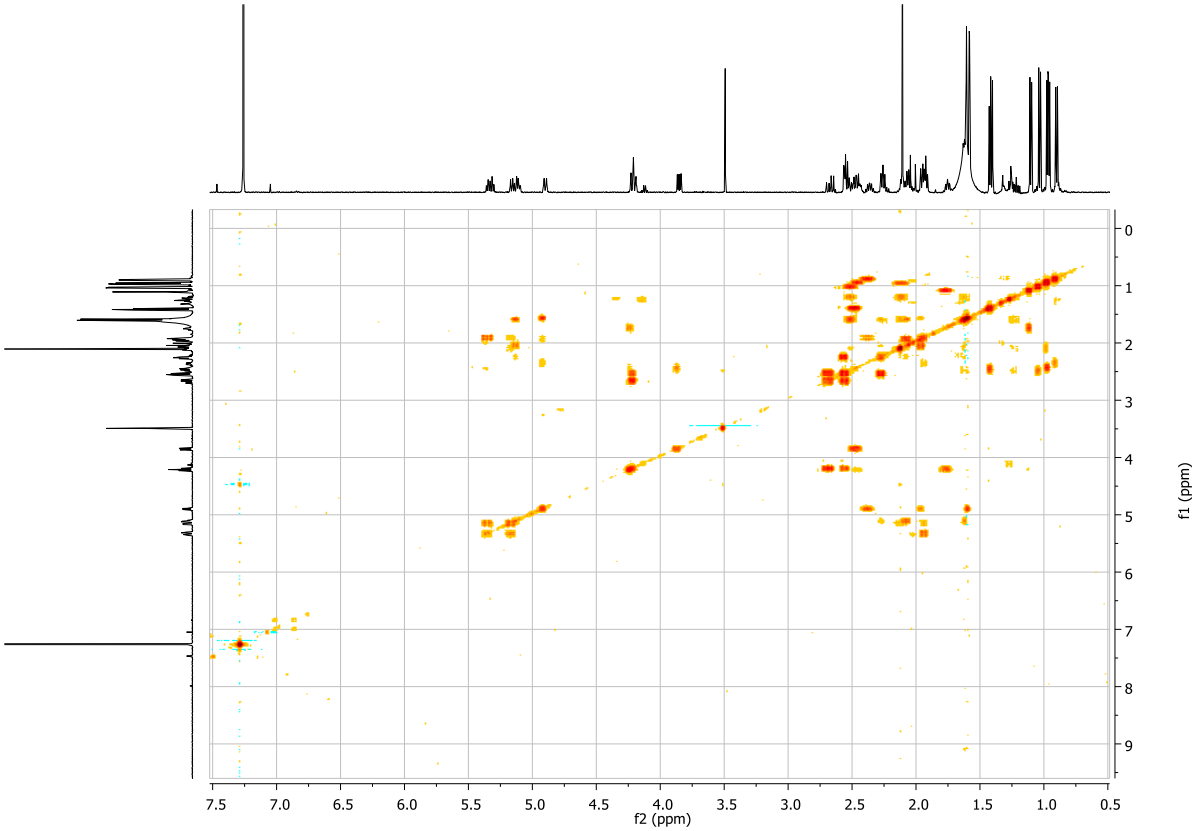

SI Figure 12: gCOSY-spectra of premonensin A (**3a**) in $CDCl_3$-d_1.

III Biological Profiling of premonensin and its Derivatives

III.1 Protein purification

E. coli RosettaTM2 was used for expression of PDEδ. Cells were grown in TB medium supplied with ampicillin and chloramphenicol at 25°C. Protein expression was induced by addition of 100 µM IPTG at 18°C overnight and the resulting protein was purified by nickel affinity chromatography followed by size exclusion chromatography.[20]

III.2 Fluorescence polarization

Fluorescence polarization measurements were carried out at 20°C in a buffer containing 30 mM Tris-HCl (pH 7.5), 150 mM NaCl and 3 mM DTT. Data were recorded using a Fluoromax-4 spectrophotometer (JobinYvon, Munich, Germany). For fluorescein-labeled RheB peptide, excitation and emission wavelengths of 495 nm and 520 nm, respectively, were used. Data analysis was performed with the Grafit 5.0 program (Erithracus Software).[20] 10 mM stock solutions of premonensin B (**2a**) and propargyl-premonensin (**5a**) were prepared in 20% v/v MQ water and 80% v/v DMSO supplemented with 16.8 mg/ml CAVASOL W7 HP Pharma and 5 µL methanol. Equivalent concentrations of MQ water and DMSO supplemented with methanol and 16.8 mg/mL CAVASOL W7 HP Pharma served as negative control.

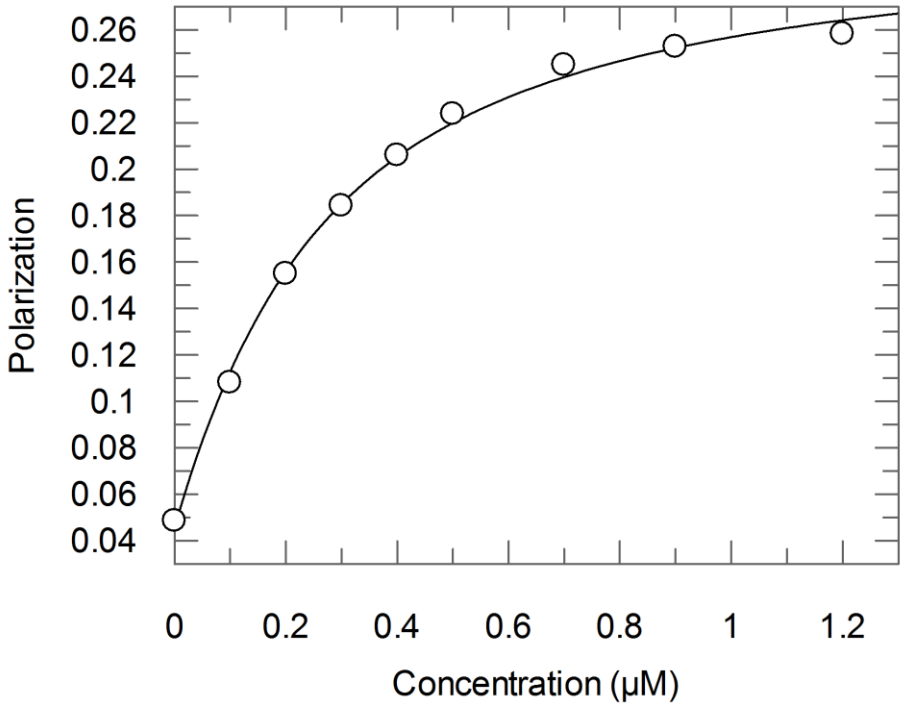

Parameter	Value	Std. Error
Kd	0.2142	0.0215
Fluorescence offset	0.0458	0.0040
Fluorescence maximum	0.3060	0.0068

SI Figure 13: A solution of fluorescently labeled Rheb peptide at a concentration of 0,1 µM was titrated against increasing concentrations of PDEδ

IV Synthesis of building blocks

IV.1 General information

Unless otherwise stated, materials for chemical synthesis were obtained from commercial suppliers (Sigma-Aldrich, Alfa Aesar, Fluka, Acros) in the highest purity available and used without further purification. Dry solvents were purchased from Sigma-Aldrich, stored over molecular sieves and used as supplied. Solvents used for extraction and chromatography were purchased from Thermo Fisher Scientific. Flash chromatography was carried out using Acros silica gel 60 (35–70 µm mesh). Thin-layer chromatography (TLC) was performed on aluminium-backed, precoated silica gel (60 F245) from Merck with cyclohexane/EtOAc or DCM/MeOH mixtures as mobile phases. Spots were detected by staining with $KMnO_4$ solution (5.0 g $KMnO_4$, 33 g K_2CO_3, 10 mL 5% aqueous NaOH in 500 mL H_2O) and subsequent heat treatment.

NMR spectra were recorded by using a Varian Mercury 400 (400 MHz, ^1H; 100 MHz, ^{13}C) spectrometer and calibrated using residual undeuterated solvent as an internal reference.
High-resolution mass spectra were recorded at LTQ Orbitrap with Accela HPLC-System (column Hypersil Gold, length 50 mm, inside diameter 1 mm, particle size 1.9 µm, ionization method: Electrospray Ionization). Products were characterized by NMR (^1H, ^{13}C) and HRMS.

For mass spectrometric detection the electrospray ionization was carried out in positive ionization mode by using a source voltage of 4 kV. The capillary voltage was set to 18 V, the capillary temperature to 275 °C, and the tube lens voltage to 115 V. Spectra were acquired in full scan centroid mode with a mass-to-charge range from 200 to 2000.

IV.2 Synthesis of compounds 4-8

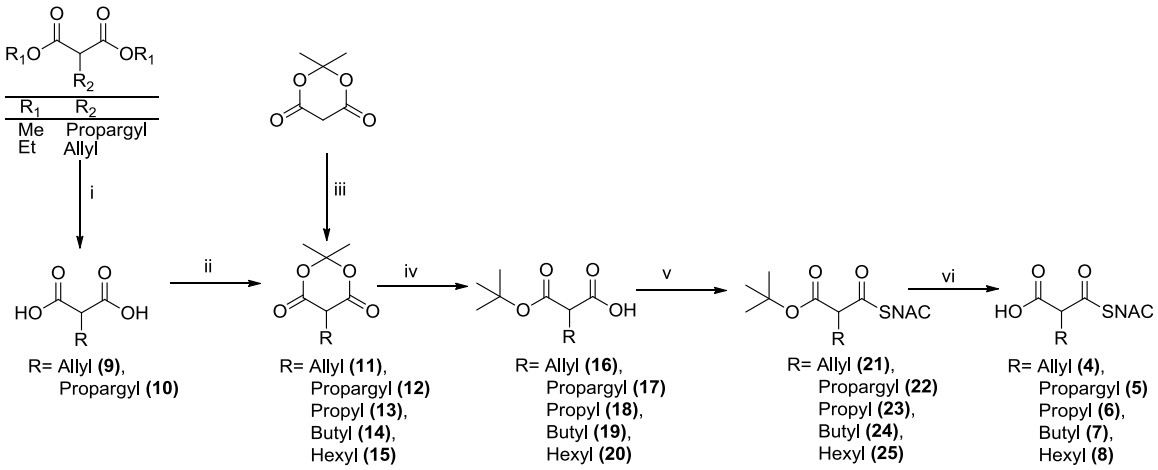

SI Figure14: Synthesis ofcompounds **4-8**; i) 3.0 eqLiOH*H_2O, H_2O, 18h, RT; ii) 1.01 eqisoprenylacetate, 0.06 eq H_2SO_4, neat, 18h, RT; iii) 1.0 eqboranedimethylaminecomplex, 3.0 eqaldehyde, 1h, RT; iv) *t*BuOH, 6h, 90-100°C; v) 1.1 eq CDI, 0.3 eq DMAP, 1.2 eq SNAC, THF, 18h, RT; vi) 2.5 eq $TiCl_4$, DCM, 6h, RT.RT: room temperature, CDI: N,N'-Carbonyldiimidazole, DMAP: 4-Dimethylaminopyridine, SNAC: *N*-acetylcysteamine.

Synthesis of *N*-acetylcysteamine (SNAC)[21]: 20.00 g (259 mmol) cysteamine hydrochloride, 36.97 g (440 mmol) $NaHCO_3$ and 11.62 g (259 mmol) KOH were added to 500 mL of deionized H_2O. After everything was dissolved, 19.77 g (18.31 ml, 259 mmol) acetic anhydride was added dropwise at 0°C. After stirring at room temperature for 18 h, the light rose solution was brought to pH= 1 with conc. HCl and the colorless solution was extracted three times with 150 ml EtOAc. The combined organic layers were dried over Na_2SO_4 to obtain 20.47 g (98%) of the desired product as colorless oil.

^{1}H-NMR (400 MHz, $CDCl_3$-d_1): 1.34–1.38 (t, *J* = 8.4 Hz, 1H), 1.97 (s, 3H), 2.60–2.66 (m, 2H), 3.36–3.40 (m, 2H), 6.33 (bs, 1H); **^{13}C-NMR** (101 MHz, $CDCl_3$-d_1): 23.1, 24.5, 42.6, 170.5; **HRMS:** calc. for 120.04776 $C_4H_{10}ONS$ $[M+H]^+$; found: 120.04730 $C_4H_{10}ONS$ $[M+H]^+$; R_f**:** 0.42 (DCM/MeOH 9:1, $KMnO_4$).

General procedure for the saponification of malonic acid diesters 9 + 10: The commercially available malonic diester was added to H_2O (10 ml/g) and 3.0 eq LiOH*H_2O were added at once. The solution was stirred for 18h, then washed with 100 ml Et_2O. The aqueous phase was acidified to pH1 using conc. HCl and extracted three times with 150 ml EtOAc. The combined organic layers were dried over Na_2SO_4 to obtain the desired product as withe solid.

2-Allyl-malonic acid (9): **^{1}H-NMR:** (400 MHz, D_2O-d_2) δ =2.49-2.51 (m, 2H), 3.17-3.21 (t, J= 7.8 Hz, 1H), 5.04-5.16 (m, 2H), 5.83-5.93 (m, 1H); **^{13}C-NMR:** (101MHz, MeOD-d_4) δ = 34.1, 52.9, 117.5, 135.8; 172.5; **mp:** 103.3-103.6°C; yield: 18.59 g; 95% (27.0 g scale, 134.8 mmol).

2-(Prop-2-yn-1-yl)malonic acid (10): **^{1}H-NMR:** (400 MHz, MeOD-d_4) δ = 2.31-2.32 (t, J= 2.7 Hz, 1H), 2.68-2.71 (dd, J= 7.6, 2.7 Hz, 2H), 3.49-3.53 (t, J= 7.6 Hz, 1H, 2-H, CH); **^{13}C-NMR:** (101MHz, MeOD-d_4) δ = 19.2, 52.6, 71.2, 81.4, 171.4; **mp:** 141°C-141.6°C ; yield: 10.42 g; 98% (12.6 g scale, 74.13 mmol).

General procedure for the synthesis of Meldrum's acid derivatives 11 + 12[22]:

For the formation of Meldrum's acid derivatives **11**-**12** the general procedure of Singh and Danishefsky was used.[22] 1.01 eq isoprenylacetate was added under argon protection to the corresponding malonic acid derivative. To the resulting white slurry 0.06 eq. sulfuric acid were added dropwise at 0°C. The resulting yellow to brown solution was stirred for 18h to reach room temperature. 100 g ice and 10 ml 1M HCl were added to the brown reaction mixture (at 10 g synthesis scale). The resulting precipitate was filtered and washed twice with 20 ml cold water.

In cases where the reaction mixture became solid after 18h, water was added to form a slurry. To this slurry 100 g ice and 10 ml 1M HCl were added (for 10 g synthesis scale). The resulting precipitate was filtered and washed twice with 20 ml of ice cold water. The resulting white to brown product usually was directly submitted to the next synthesis step.

If material of higher purity was needed the white to brown solids obtained from the first precipitation were dissolved in a small volume MeOH at RT. After adding ice and a few drops of conc.HCl the white precipitate was filtered and washed twice with 20 ml of ice cold water.

5-Allyl-2,2-dimethyl-1,3-dioxane-4,6-dione (11): **^{1}H-NMR:** (400 MHz, $CDCl_3$-d_1) δ = 1.76 (s, 3H), 1.79 (s, 3H), 2.86-2.90 (m, 2H), 3.57-3.60 (t, J= 5.3 Hz, 1H), 5.14-5.26 (m, 2H), 5.81-5.92 (m, 1H); **^{13}C-NMR:** (101MHz, $CDCl_3$-d_1) δ = 27.2, 28.6, 30.5, 46.4, 105.1, 132.8, 165.1; **HRMS:** calc.: 185.08084 $C_9H_{13}O_4$ $[M+H]^+$;found: 185.08071 $C_9H_{13}O_4$ $[M+H]^+$; **mp:** 71°C; ***R$_f$*:** 0.56 (EtOAc/Cyclohexane 1:1, $KMnO_4$); yield: 23.05 g; 65% (27.95 g scale, 193.96 mmol).

2,2-Dimethyl-5-(prop-2-yn-1-yl)-1,3-dioxane-4,6-dione (12): **^{1}H-NMR:** (400 MHz, $CDCl_3$-d_1) δ = 1.80 (s, 3H), 1.81 (s, 3H), 2.05-2.06 (t, J= 2.6 Hz, 1H), 3.02-3.04 (dd, J= 4.9, 2.6 Hz, 2H), 3.67-3.96 (t, J= 4.9 Hz, 1H); **^{13}C-NMR:** (101MHz, $CDCl_3$-d_1) δ = 16.7, 27.2, 28.7, 46.1, 70.9, 79.4, 105.5, 164.1; **HRMS:** calc.: 183.06519 $C_9H_{11}O_4$ $[M+H]^+$; found: 183.06512 $C_9H_{11}O_4$

$[M+H]^+$; **mp:** 140.0°C-140.4°C; **R_f:** 0.66 (EtOAc/Cyclohexane 1:1, $KMnO_4$); yield: 29.67 g; 73% (31.9 g scale, 224.47 mmol).

General procedure for the reductive alkylation of Meldrum's acid 13-15[23]: The alkylation was carried out as described by Hurubowchak and Smith.[23] Meldrum's acid was dissolved in abs. MeOH. Subsequently, 1.01 eq boranedimethylaminecomplex were added. After the borane was dissolved completely 3.0 eq of the corresponding aldehyde were added in 3 min at RT under a stream of N_2. After 1 h the yellow reaction mixture was quenched by 100 g ice and 10 ml of 1M HCl. The resulting suspension was filtered and washed twice with 25 ml cold water. The resulting white solid was dried *in vacuo* and can directly be submitted to the next reaction step.

If material of higher purity is needed the white to brown solids obtained from the first precipitation were dissolved in a minimum of MeOH at RT. After adding ice and a view drops of conc. HCl the white precipitate was filtered and washed twice with 20 ml of ice cold water.

2,2-Dimethyl-5-propyl-1,3-dioxane-4,6-dione (13): ^{1}H-NMR: (400 MHz, $CDCl_3$-d_1) δ = 0.93-0.98 (t, J= 7.3 Hz, 3H), 1.44-1.54 (m, 2H), 1.75 (s, 3H), 1.78 (s, 3H), 2.05-2.11 (m, 2H), 3.47-3.50 (t, J= 5.1 Hz, 1H); **^{13}C-NMR:** (101MHz, $CDCl_3$-d_1) δ = 14.1, 20.1, 27.13, 28.6, 28.9, 46.1, 104.9, 165.8; **HRMS:** calc.: 187.09649 $C_9H_{15}O_4$ $[M+H]^+$; found: 187.09637 $C_9H_{15}O_4$ $[M+H]^+$; **mp:** 74°C-74.5°C; **R_f:** 0.71 (EtOAc/cyclohexane 1:1, $KMnO_4$); yield : 7.52 g ; 72% (8.0 g scale, 55.5 mmol).

5-Butyl-2,2-dimethyl-1,3-dioxane-4,6-dione (14): ^{1}H-NMR: (400 MHz, $CDCl_3$-d_1) δ = 0.90-0.93 (t, J= 7.1 Hz), 1.32-1.47 (m, 4H), 1.73 (s, 3H), 1.78 (s, 3H), 2.07-2.13 (m, 2H), 3.47-3.50 (t, J= 5.1 Hz, 1H); **^{13}C-NMR:** (101MHz, $CDCl_3$-d_1) δ = 13.9, 22.8, 26.6, 27.1, 28.6, 28.8, 46.3, 104.9, 165.80; **HRMS:** calc.: 201.11214 $C_{10}H_{17}O_4$ $[M+H]^+$; found: 201.11206 $C_{10}H_{17}O_4$ $[M+H]^+$; **mp:** 55.6-56.1°C; **R_f:** 0.73 (EtOAc/cyclohexane 1:1, $KMnO_4$); yield : 19.31 g; 86% (18.0 g scale, 123.17 mmol).

5-Hexyl-2,2-dimethyl-1,3-dioxane-4,6-dione (15): ^{1}H-NMR: (400 MHz, $CDCl_3$-d_1) δ = 0.85-0.89 (t, J= 6.5 Hz), 1.28-1.35 (6H), 1.40-1.47 (2H), 1.75 (3H), 1.77 (3H), 2.06-2.12 (2H), 3.47-3.50 (t, J= 5.0 Hz, 1H);**^{13}C-NMR:** (101MHz, $CDCl_3$-d_1) δ = 14.1, 22.6, 26.6, 26.9, 27.1, 28.6, 29.3, 31.56, 46.3, 104.9, 165.8; **HRMS:** calc.: 229.14344 $C_{12}H_{21}O_4$ $[M+H]^+$; found: 229.14332 $C_{12}H_{21}O_4$ $[M+H]^+$; **R_f:** 0.50 (DCM/MeOH, $KMnO_4$); yield: 13.12 g ; 83% (10.0 g scale ; 69.38 mmol).

General procedure for the synthesis *t*Butylmalonic acids 16-20: *t*BuOH (125 ml/10 g) was added to Meldrum's acid and heated up to 95-100°C for 6h (DC-control). Then *t*BuOH was evaporated *in vacuo* and the resulting oil was purified by column chromatography (PE/EtOAc 1:0→ 85:15, gradient in 5%-steps) to obtain the desired products as clear oil.

2-(tert-butoxycarbonyl)pent-4-enoic acid (16): ^{1}H-NMR: (400 MHz, $CDCl_3$-d_1) δ = 1.47 (s, 9H), 2.58-2.68 (m, 2H), 3.36-3.40 (t, J= 7.3 Hz, 1H), 5.07-5.16 (m, 2H), 5.73-5.83 (m, 1H) **;** **^{13}C-NMR:** (101MHz, $CDCl_3$-d_1) δ = 28.0, 33.2, 52.1, 82.8, 117.9, 133.8, 168.5, 174.4; **HRMS:** calc.: 201.11214 $C_{10}H_{17}O_4$ $[M+H]^+$, 223.09408 $C_{10}H_{16}O_4Na$ $[M+Na]^+$,218.13868 $C_{10}H_{20}O_4N$ $[M+NH_4]^+$; found: 201.11217 $C_{10}H_{17}O_4$ $[M+H]^+$, 223.09421 $C_{10}H_{16}O_4Na$ $[M+Na]^+$,218.13878 $C_{10}H_{20}O_4N$ $[M+NH_4]^+$; **Rf:** 0.55 (EtOAc/cyclohexane, $KMnO_4$); yield: 3.01 g; 91% (3.0 g scale, 35.34 mmol).

2-(*tert*-butoxycarbonyl)-pent-4-yl acid (17): ^{1}H-NMR: (400 MHz, $CDCl_3$-d_1) δ = 1.46 (s, 9H), 2.04 (t, J= 2.6 Hz, 1H), 2.17-2.18 (s, 1H), 2.94-2.95 (d, J= 2.6 Hz, 2H); **^{13}C-NMR:** (101MHz, $CDCl_3$-d_1) δ = 23.1, 28.1, 57.2, 72.2, 78.8, 83.8, 167.7, 174.4; **HRMS:** calc.: 199.09649 $C_{10}H_{15}O_4$ $[M+H]^+$, 221.07843 $C_{10}H_{15}O_4Na$ $[M+Na]^+$; found: 221.07845 $C_{10}H_{15}O_4$, $[M+Na]^+$; **mp:** 95.6-96.7°C; **R_f:** 0.54 (MeOH/$CHCl_3$ 1:9, $KMnO_4$); yield: 30.35 g ; 94% (29.67 g scale, 162.8 mmol).

2-(tert-butoxycarbonyl)pentanoicacid (19): ^{1}H-NMR: (400 MHz, $CDCl_3$-d_1) δ = 0.92-0.96 (t, J= 7.3 Hz, 3H), 1.36-1.41 (m, 2H), 1.47 (s, 9H), 1.83-1.90 (m, 2H), 3.27-3.31 (t, J= 7.4 Hz, 1H); **^{13}C-NMR:** (101MHz, $CDCl_3$-d_1) δ = 13.8, 20.6, 28.0, 31.3, 52.4, 82.6, 169.2, 175.4; **HRMS:** calc.: 201.11323 $C_{10}H_{17}O_4$ [M-H]; found: 201.11383 $C_{10}H_{17}O_4$ [M-H]; **R_f:** 0-0.61 (EtOAc/cyclohexane 1:1, $KMnO_4$); yield: 4.77 g; 62% (7.02 g scale; 37.7 mmol).

2-(tert-butoxycarbonyl)hexanoicacid (19): ^{1}H-NMR: (400 MHz, $CDCl_3$-d_1) δ = 0.88-0.92 (t, J=7.0 Hz, 3H), 1.32-1.35 (m, 4H), 1.47 (s, 9H), 1.85-1.91 (m, 2H), 3.25-3.29 (t, J= 7.4 Hz, 1H); **^{13}C-NMR:** (101MHz, $CDCl_3$-d_1) δ = 13.9, 22.5, 28.0, 28.9, 29.5, 52.5, 82.6, 164.3, 174.9; **HRMS:** calc.: 215.12888 $C_{11}H_{19}O_4$ [M-H]; found: 215.12939 $C_{11}H_{19}O_4$ [M-H]; **R_f:** 0-0.51 (EtOAc/cyclohexane 1:1, $KMnO_4$); yield : 2.73 g; 80% (2.8 g scale, 14.0 mmol).

2-(tert-butoxycarbonyl)octanoicacid (20): ^{1}H-NMR:(400 MHz, $CDCl_3$-d_1) δ = 0.86-0.89 (t, J= 6.9 Hz, 3H), 1.28-1.32 (m, 8H), 1.47 (s, 9H), 1.84-1.91 (m, 2H), 3.26-3.29 (t, J= 7.3 Hz, 3H); **^{13}C-NMR:** (101MHz, $CDCl_3$-d_1) δ = 14.2, 22.6, 27.3, 28.0, 28.9, 29.4, 31.6, 52.5, 82.7,

169.4, 175.1**; HRMS:** calc.: 243.16018 $C_{13}H_{23}O_4$ [M-H]; found: 243.16086 $C_{13}H_{23}O_4$ [M-H]; **R_f:** 0-0.47 (EtOAc/cyclohexane 1:1, $KMnO_4$); yield : 8.02 g; 56% (13.2 g scale , 57.8 mmol).

General procedure for the thioesterfication of compounds 21-25: *tert*-butylcarboxylic acid was dissolved in abs. THF (10 ml/g) under argon. Subsequently, 1.2 eq CDI was added at 0°C, and the mixture was stirred for 30 min at 0°C followed by 3h at RT before 0.3 eq. DMAP and 1.3 eq. SNAC were added. After 18 h at RT the solvent was removed *in vacuo* and the residue was suspended 300 ml EtOAc and washed three times with 100 ml 1M $K_2CO_3$and twice with 100 ml 1M HCl. The organic layer was dried over Na_2SO_4, and purified by column chromatography (DCM/MeOH 99:1) to obtain the desired thioesters as slightly yellow oils.

tert-butyl 2-(((2-acetamidoethyl)thio)carbonyl)pent-4-enoate (21): ^{1}H-NMR: (400 MHz, $CDCl_3$-d_1) δ = 1.43 (s, 9H), 1.94 (s, 3H), 2.58-2.62 (m, 2H), 2.99-3.11 (m, 2H), 3.34-3.48 (m, 2H), 3.55-3.59 (t, J= 7.5Hz, 1H), 5.03-5.12 (m, 2H), 5.66-5.77 (m, 1H), 6.00 (bs, 1H); **^{13}C-NMR:** (101MHz, $CDCl_3$-d_1) δ = 23.3, 28.1, 28.9, 33.5, 39.6, 60.6, 82.7, 117.9, 133.9, 167.4, 170.6, 195.5; **HRMS:** calc: 302.14206 $C_{14}H_{24}O_4NS[M+H]^+$, 324.12400 $C_{14}H_{23}O_4NNaS$ $[M+Na]^+$, 319.16860 $C_{14}H_{27}O_4N_2S$ $[M+NH_4]^+$; found: 302.14231 $C_{14}H_{24}O_4NS[M+H]^+$, 324.12418 $C_{14}H_{23}O_4NNaS$ $[M+Na]^+$, 319.16919 $C_{14}H_{27}O_4N_2S$ $[M+NH_4]^+$; **R_f:** 0.68 (DCM/MeOH 9:1, $KMnO_4$); yield : 3.73 g ; 82% (3.02 g scale, 15.06 mmol).

***tert*-butyl 2-(((2-acetamidoethyl)thio)-carbonyl)pent-4-ynoate (22): ^{1}H-NMR:** (400 MHz, $CDCl_3$-d_1) δ = 1.47 (s, 9H),1.96 (s, 3H),2.01-3.03 (t, J= 2.7 Hz, 1H),2.74-2.76(dd, J= 7.6, 2.7,0.6 Hz,2H),3.09-3.12 (m, 2H),3.43-3.47 (m, 2H,),3.69-3.73 (t, J= 7.6 Hz, 1H),5.87 (bs, 1H); **^{13}C-NMR:** (101MHz, $CDCl_3$-d_1) δ = 18.8, 23.3, 27.9, 29.1, 39.5, 59.6, 70.7, 79.9, 83.3, 166.3, 170.5, 194.4; **HRMS:** calc.: 300.12641 $C_{14}H_{22}O_4NS$ $[M+H]^+$, 322.10835 $C_{14}H_{22}O_4NSNa$ $[M+Na]^+$, 317.15295 $C_{14}H_{25}O_4N_2S$ $[M+NH_4]^+$; found: 300.12664 $C_{14}H_{22}O_4NS$ $[M+H]^+$, 322.10861 $C_{14}H_{22}O_4NSNa$ $[M+Na]^+$, 317.15325 $C_{14}H_{25}O_4N_2S$,$[M+NH_4]^+$; **R_f:**0.69 (DCM/MeOH 9:1, $KMnO_4$); yield:83% (10.8 g scale, 54.49 mmol).

***tert*-butyl 2-(((2-acetamidoethyl)thio)carbonyl)pentanoate (23): ^{1}H-NMR:** (400 MHz, $CDCl_3$-d_1) δ = 0.89-0.92 (t, J= 7.3 Hz, 3H), 1.23-138 (m, 2H), 1.43 (s, 9H), 1.77-1.88 (m, 2H), 1.94 (s, 3H), 2.98-3.11 (m, 2H), 3.34-3.47 (m, 3H), 6.02 (bs, 1H); **^{13}C-NMR:** (101MHz, $CDCl_3$-d_1) δ = 13.8, 20.6, 23.2, 27.9, 28.8, 31.5, 39.6, 60.9, 82.3, 167.9, 170.5, 196.2;**HRMS:**

calc.:304.15771 $C_{14}H_{26}O_4NS$ $[M+H]^+$, 326.13965 $C_{14}H_{25}O_4NNaS$ $[M+Na]^+$, 321.18425 $C_{14}H_{29}O_4N_2S$ $[M+NH_4]^+$; found: 304.15800 $C_{14}H_{26}O_4NS$ $[M+H]^+$, 326.13987 $C_{14}H_{25}O_4NNaS$ $[M+Na]^+$, 321.18487 $C_{14}H_{29}O_4N_2S$ $[M+NH_4]^+$; **R_f:** 0.67 (DCM/MeOH 9:1, $KMnO_4$) ; yield : 1.34 g ; 74% (1.211 g scale, 5.99 mmol).

tert-butyl 2-(((2-acetamidoethyl)thio)carbonyl)hexanoate (24): ^{1}H-NMR:(400 MHz, $CDCl_3$-d_1) δ = 0.84-0.88 (t, J=7.0 Hz, 3H), 1.26-1.28 (m, 4H), 1.42 (s, 9H), 1.80-1.87 (m, 2H), 1.96 (s, 3H), 2.99-3.08 (m, 2H), 3.33-3.47 (m, 3H), 6.09 (bs, 1H); **^{13}C-NMR:** (101MHz, $CDCl_3$-d_1) δ = 13.8, 22.4, 23.2, 27.9, 28.7, 29.2, 29.4, 39.6, 61.2, 82.3, 167.9, 170.5, 196.1; **HRMS:** calc.: 318.17336 $C_{15}H_{28}O_4NS$ $[M+H]^+$, 340.15530 $C_{15}H_{27}O_4NNaS$ $[M+Na]^+$, 335.19990 $C_{15}H_{31}O_4N_2S$ $[M+NH_4]^+$; found: 318.17390 $C_{15}H_{28}O_4NS$ $[M+H]^+$, 340.15569 $C_{15}H_{27}O_4NNaS$ $[M+Na]^+$, 335.20083 $C_{15}H_{31}O_4N_2S$ $[M+NH_4]^+$; **R_f:**0.69 (DCM/MeOH 9:1, $KMnO_4$); yield : 23.00 g ; 78% (20.0 g scale, 92.48 mmol).

tert-butyl 2-(((2-acetamidoethyl)thio)carbonyl)octanoate (25): ^{1}HNMR: (400 MHz, $CDCl_3$-d_1) δ = 0.86-0.89 (t, J= 6.9Hz, 3H), 1.27-1.29 (m, 8H), 1.46 (s, 9H), 1.85-1.88 (m, 2H), 1.96 (s, 3H), 3.00-3.13 (m, 2H), 3.37-3.51 (m, 3H), 5.85 (bs, 1H); **^{13}C-NMR:** (101MHz, $CDCl_3$-d_1) δ = 14.2, 22.7, 23.3, 27.3, 28.03, 28.06, 28.8, 29.03, 29.6, 31.6, 39.7, 61.3, 82.4, 168.0, 170.6, 196.3; **HRMS:** calc: 346.20466 $C_{17}H_{32}O_4NS$ $[M+H]^+$, 368.18660 $C_{17}H_{31}O_4NNaS$ $[M+Na]^+$, 363.23120 $C_{17}H_{35}O_4N_2S$ $[M+NH_4]^+$; found: 346.20494 $C_{17}H_{32}O_4NS$ $[M+H]^+$, 368.18686 $C_{17}H_{31}O_4NNaS$ $[M+Na]^+$, 363.23182 $C_{17}H_{35}O_4N_2S$ $[M+NH_4]^+$; **R_f:**0.79 (DCM/MeOH 9:1, $KMnO_4$); yield : 9.61 g ; 53% (12.77 g scale ; 52.27 mmol).

General procedure for the deprotection of compounds 4-8: The thioester was dissolved in abs. DCM (10 ml/100 mg) under argon. At 0°C 2.5 eq. $TiCl_4$ was dropwise added. The dark brown reaction mixture was stirred for 5 min at 0°C, then for another 6h at room temperature. After 6h (DC-control) the reaction mixture was quenched with aq. Na_2CO_3-solution (10.0 eq. Na_2CO_3) in an ice bath to reach a final concentration of 0.1M of product. The white suspension was filtered and washed twice with 10 ml MeOH. The combined solvents were evaporated at 30°C under reduced pressure. The resulting brown solution or white slurry was transferred to polypropylene tubes and cooled for 2 h at -20°C; after warming to 4°C, Na_2CO_3 precipitated. The precipitate was removed by centrifugation at 4°C/4000 rpm for 10 min. Subsequently, the supernatant was freeze dried. The resulting white/yellow solid was transferred into polypropylene tubes and dissolved in SM16 medium to yield a 100 mM

solution. The resulting slightly brown solution was centrifuged at 4°C/4000 rpm for 10 min and the supernatant was sterile filtered and used directly for feeding experiments.
For analysis of the reaction product by NMR, the product was dissolved in D_2O instead of SM16 medium.

2-(((2-acetamidoethyl)thio)carbonyl)pent-4-enoic acid (4): ^{1}**H-NMR:** (400 MHz, D_2O-d_2) δ = 2.26 (s, 3H), 2.83-2.87 (m, 2H), 3.30-3.43 (m, 2H), 3.59-3.69 (m, 2H), 3.96-3.99 (t, J= 7.6 Hz, 1H), 5.35-5.39 (m, 2H), 6.05-6.13 (m, 1H,); ^{13}**C-NMR:** (101MHz, D_2O-d_2) δ = 22.8, 28.7, 34.2, 39.1,117.6, 135.6, 174.8, 175.7, 201.2; **HRMS:** calc.: 246.07946 $C_{10}H_{16}O_4NS[M+H]^+$, 268.06140 $C_{10}H_{15}O_4NNaS$ $[M+Na]^+$; found: 246.07949 $C_{10}H_{16}O_4NS$ $[M+H]^+$, 268.06048 $C_{10}H_{15}O_4NNaS$ $[M+Na]^+$; **R_f**: 0.12 (DCM/MeOH 9:1, $KMnO_4$).

2-(((2-acetamidoethyl)thio)carbonyl)pent-4-ynacid (5): ^{1}**H-NMR:** (400 MHz, D_2O-d_2) δ = 1.88 (s, 3H); 2.30-2.32 (t, J= 2.6 Hz, 1H), 2.61-2.63 (m, 2H); 2.99-3.04 (m,2H); 3.26-3.32 (m, 2H), 3.68-3.72 (t, J= 7.6 Hz, 1H); ^{13}**C-NMR:** (101MHz, D_2O-d_2) δ = 19.1, 22.5, 28.6, 38.9, 174.2, 174.7, 199.6; **HRMS:**cal.: 244.06381 $C_{10}H_{14}O_4NS$ $[M+H]^+$; found: 244.06402 $C_{10}H_{14}O_4NS$ $[M+H]^+$; **R_f**: 0.18 (DCM/MeOH 1:9, $KMnO_4$).

2-(((2-acetamidoethyl)thio)carbonyl)pentanoicacid (6): ^{1}**H-NMR:** (400 MHz, D_2O-d_2) δ = 1.08-1.12 (t, J= 7.4 Hz, 3H), 1.44-153 (m, 2H), 1.96-2.09 (ddd, J= 15.1, 7.6, 1.5, 2H), 2.17 (s, 3H), 3.21-3.35 (m, 2H), 3.56-3.59 (m, 2H), 3.77-3.81 (t, J= 7.6Hz, 1H); ^{13}**C-NMR:** (101MHz, D_2O-d_2) δ = 13.7, 20.7, 22.6, 28.6, 32.4, 39.0, 64.2, 174.7, 176.6, 201.8; **HRMS:** cal.: 248.09511 $C_{10}H_{18}O_4NS$ $[M+H]^+$, 270.07705 $C_{10}H_{17}O_4NSNa$ $[M+Na]^+$; found: 248.09514 $C_{10}H_{18}O_4NS$ $[M+H]^+$, 270.07632 $C_{10}H_{17}O_4NSNa$ $[M+Na]^+$; **R_f:** 0.24 (DCM/MeOH 9:1, $KMnO_4$).

2-(((2-acetamidoethyl)thio)carbonyl)hexanoicacid (7): ^{1}**H-NMR:** (400 MHz, $CDCl_3$-d_1) δ = 1.12-1.16 (t, J= 7.1 Hz, 3H), 1.53-1.57 (m, 4H), 2.05-2.11 (m, 2H), 2.25 (s, 3H) 3.28-3.43 (m, 2H), 3.63-3.67 (m, 2H), 3.82-3.85 (t, J= 7.6 Hz, 1H); ^{13}**C-NMR:** (101MHz, $CDCl_3$-d_1) δ =16.5, 24.9, 25.4, 31.3, 32.1, 32.7, 41.7, 67.1, 177.2, 179.1, 204.6; **HRMS:** cal.: 262.11076 $C_{11}H_{20}O_4NS$ $[M+H]^+$, 284.09270 $C_{11}H_{19}O_4NNaS$ $[M+Na]^+$; found: 262.11083 $C_{11}H_{20}O_4NS$ $[M+H]^+$, 284.09226 $C_{11}H_{19}O_4NNaS$ $[M+Na]^+$; **R_f**:0.13 (DCM/MeOH 9:1, $KMnO_4$).

2-(((2-acetamidoethyl)thio)carbonyl)octanoicacid (8): ^{1}**H-NMR:** (400 MHz, D_2O-d_2/MeOD-d_4) δ = 0.83-0.86 (m, 3H), 1.25-1.27 (m, 8H), 1.78-1.84 (m, 2H), 1.88 (s, 3H,), 2.94-2.98 (m, 2H), 3.26-3.27 (m, 2H), 3.41-3.44 (t, J=7.4 Hz, 1H); ^{13}**C-NMR:** (101MHz, MeOD-d_4) δ = 14.4, 22.6, 23.6, 28.8, 29.2, 30.2, 31.7, 32.8, 40.1, 65.9, 173.4, 175.6, 199.8; **HRMS:** calc.:

290.14206 $C_{13}H_{24}O_4NS$ $[M+H]^+$, 312.12400 $C_{13}H_{23}O_4NaS$ $[M+Na]^+$; found: 290.14226 $C_{13}H_{24}O_4NS$ $[M+H]^+$, 312.12417 $C_{13}H_{23}O_4NaS$ $[M+Na]^+$; ***R_f*:** 0.23 (DCM/MeOH 9:1, $KMnO_4$).

V NMR-Spectra of synthetic compounds

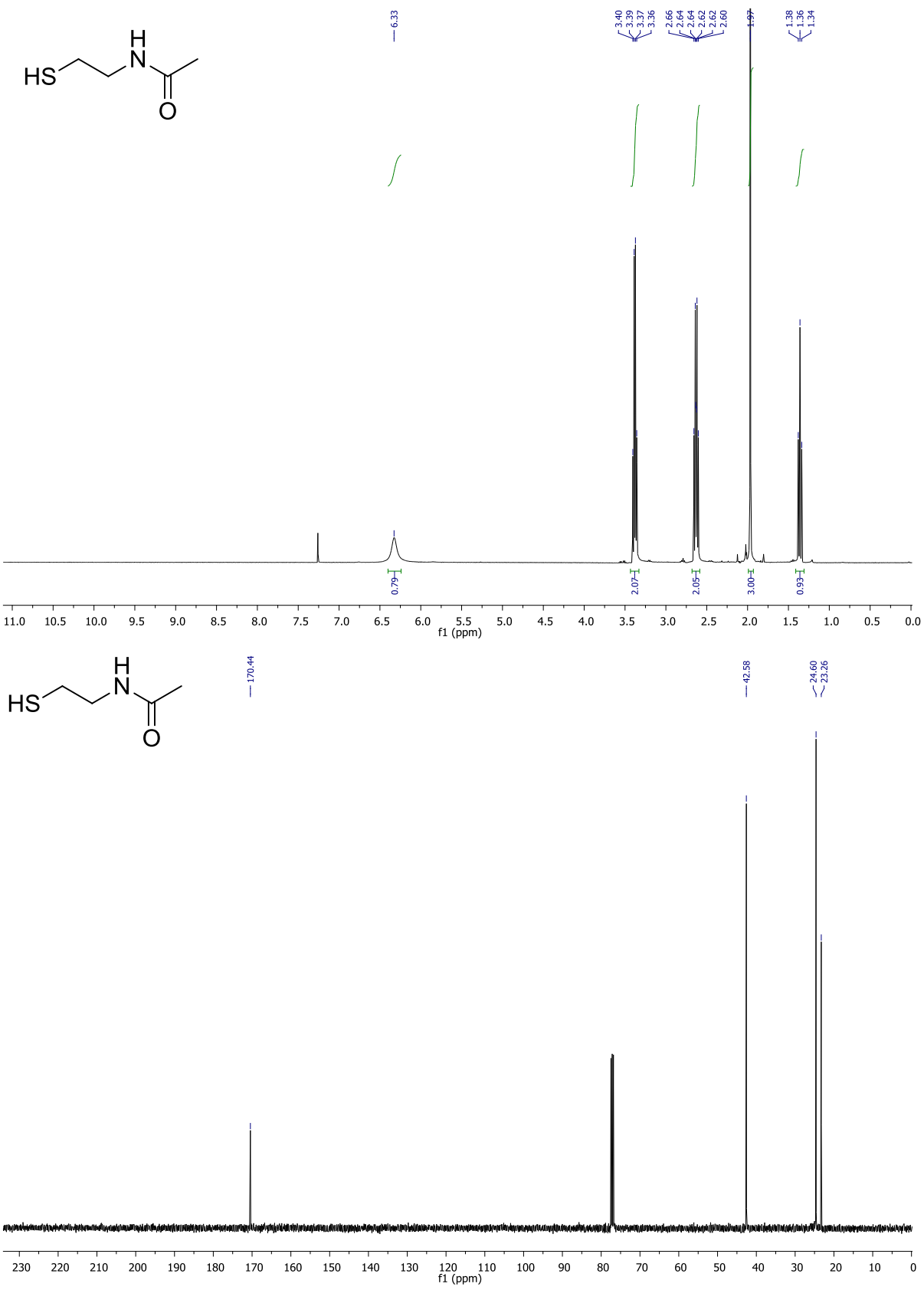

SI Figure 15: ^{1}HNMR- and ^{13}C-Spectra of SNAC in $CDCl_3$-d_1.

NMR-spectra of the Malonic acids

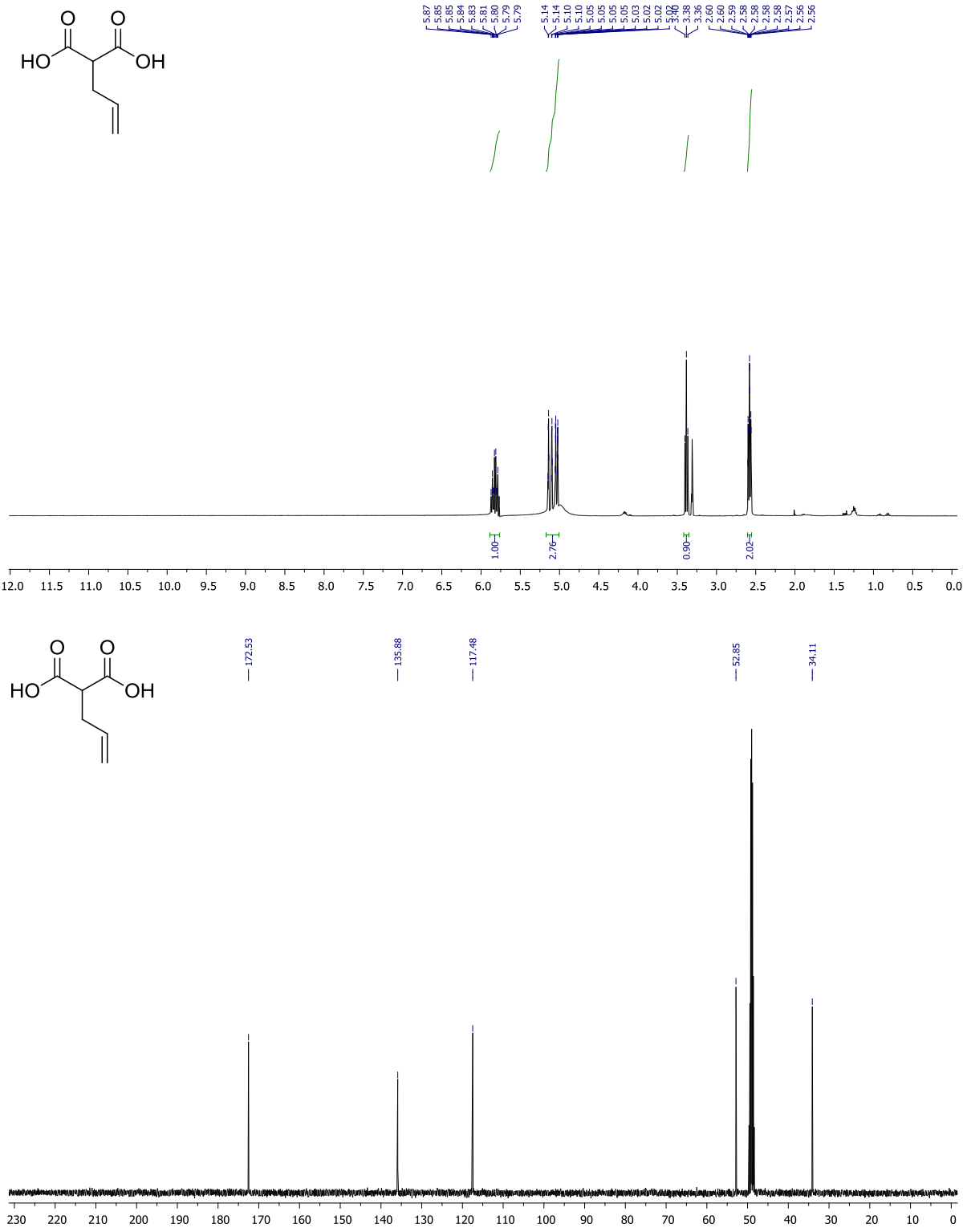

SI Figure 16: ^{1}HNMR- and ^{13}C-Spectra of 2-Allyl-malonic acid (**9**) in MeOD-d_4.

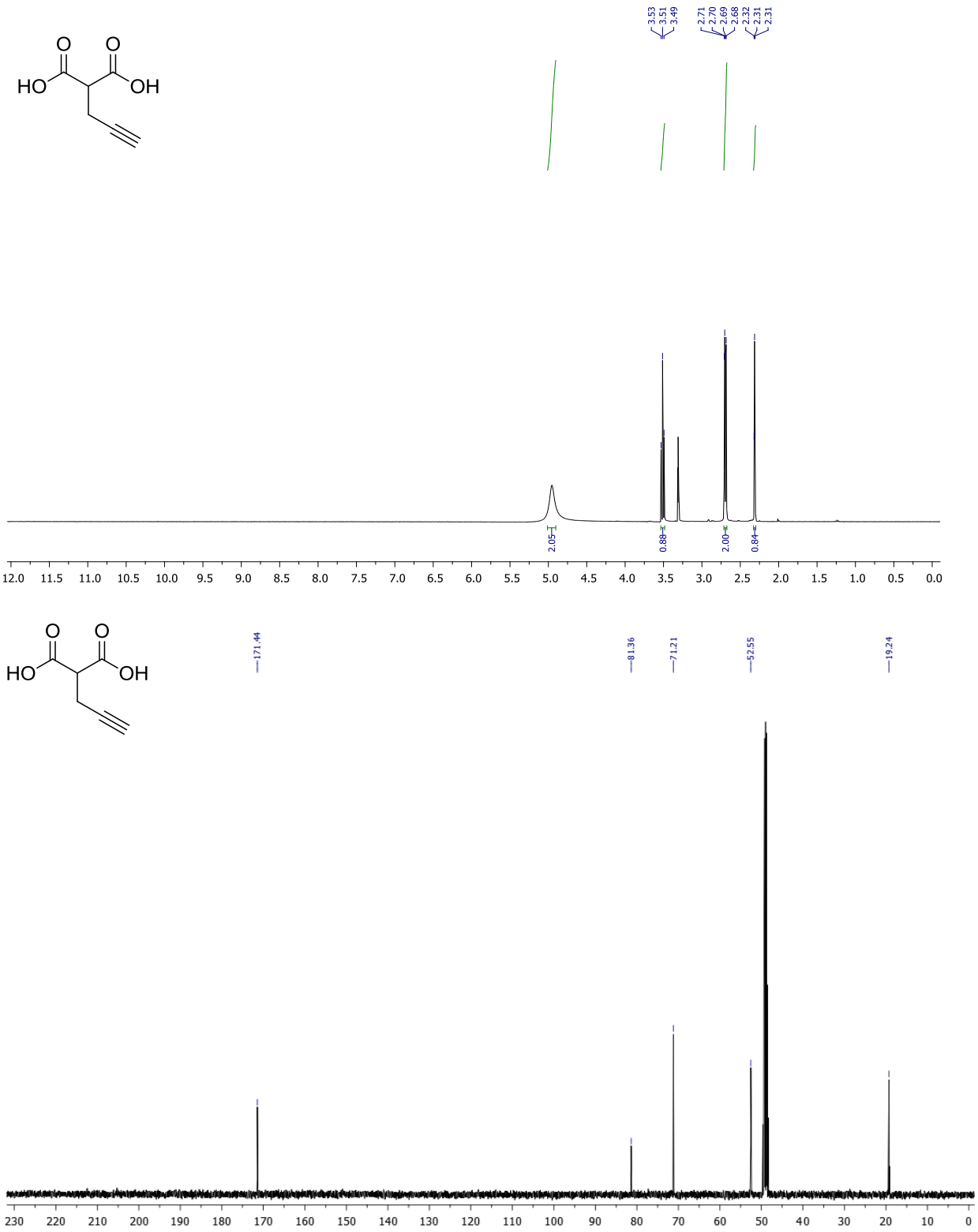

SI Figure 17: ^{1}HNMR- and ^{13}C-Spectra of 2-(Prop-2-yn-1-yl)malonicacid (**10**) in MeOD-d_4.

NMR-spectra of Meldrum's acid derivatives

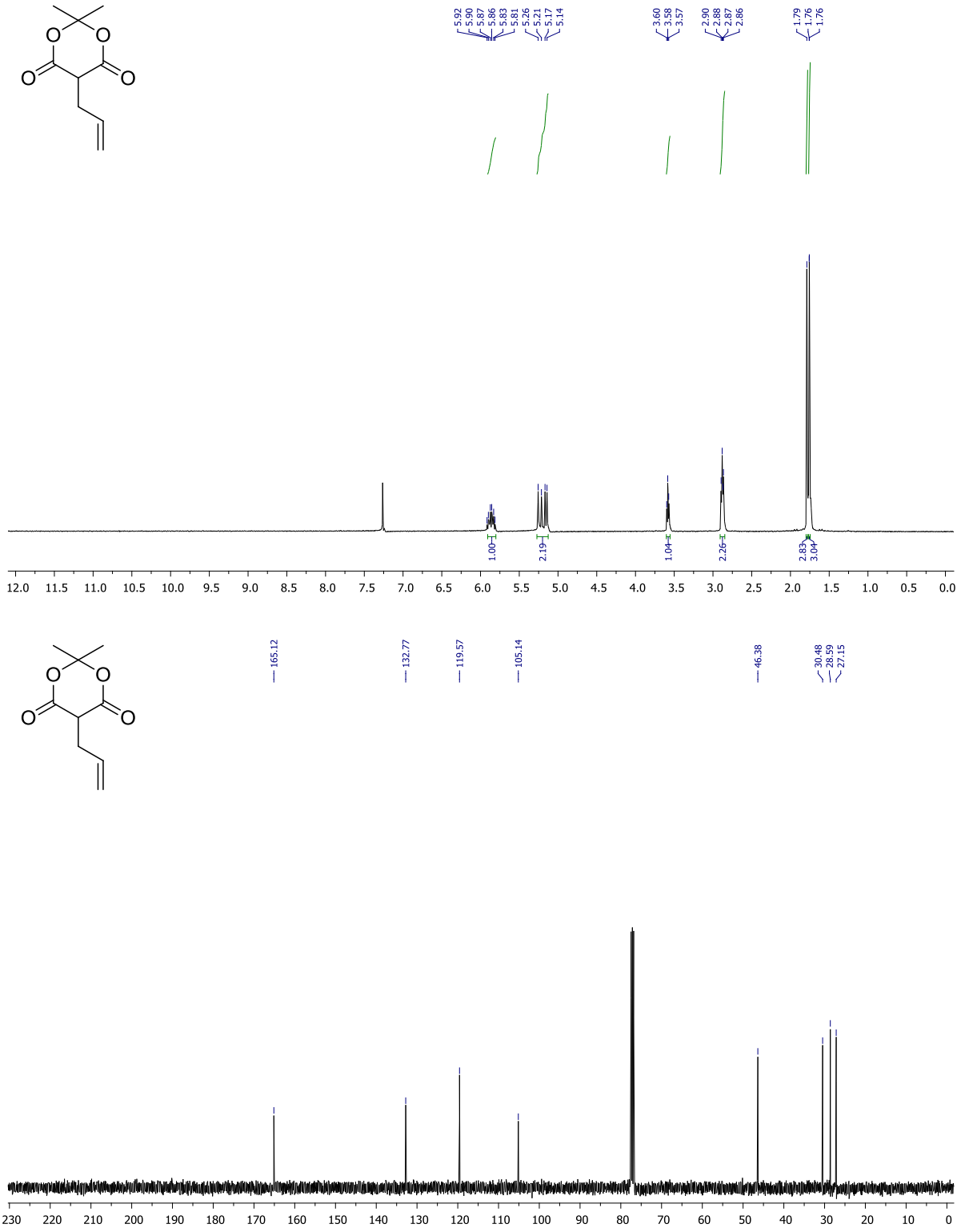

SI Figure 18: ^{1}HNMR- and ^{13}C-Spectra of 5-Allyl-2,2-dimethyl-1,3-dioxane-4,6-dione (**11**) in $CDCl_3$-d_1.

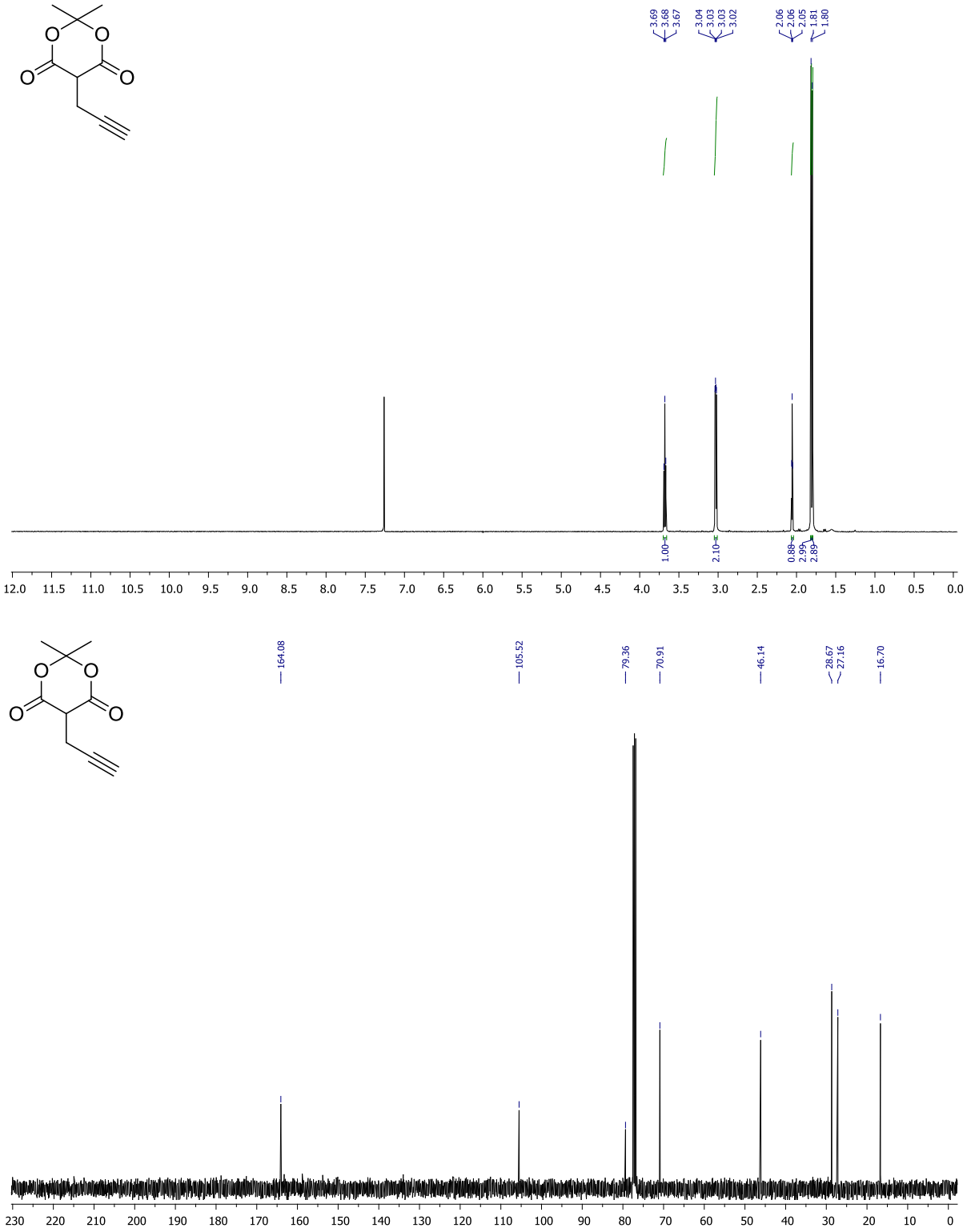

SI Figure 19: ^{1}HNMR- and ^{13}C-Spectra of 2,2-Dimethyl-5-(prop-2-yn-1-yl)-1,3-dioxane-4,6-dione (**12**) in $CDCl_3$-d_1.

NMR-spectra for the reductive alkylation of Meldrum's acid

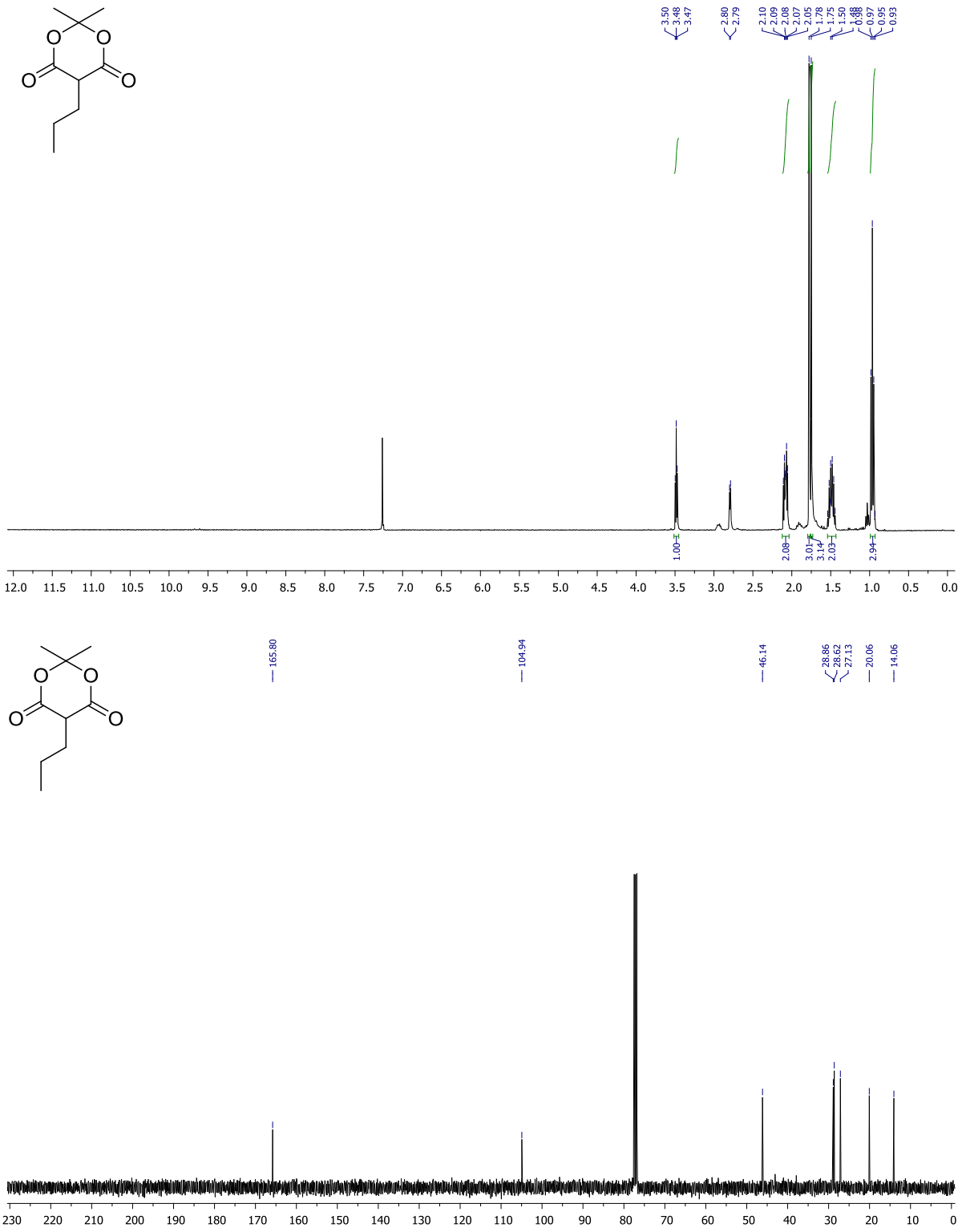

SI Figure 20: ^{1}HNMR- and ^{13}C-Spectra of 2,2-Dimethyl-5-propyl-1,3-dioxane-4,6-dione (**13**) in $CDCl_3$-d_1.

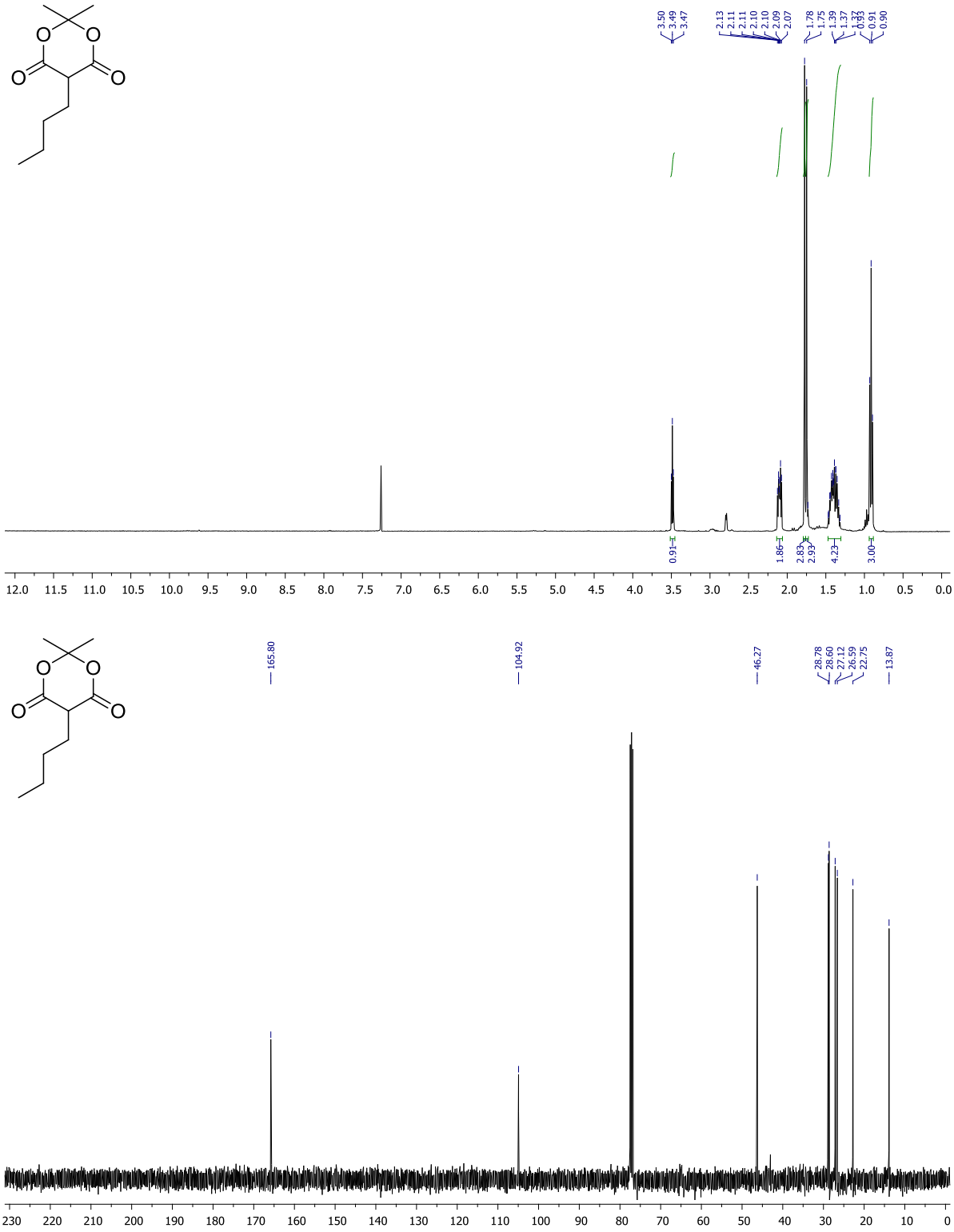

SI Figure 21: ^{1}HNMR- and ^{13}C-Spectra of 5-Butyl-2,2-dimethyl-1,3-dioxane-4,6-dione (**14**) in $CDCl_3$-d_1.

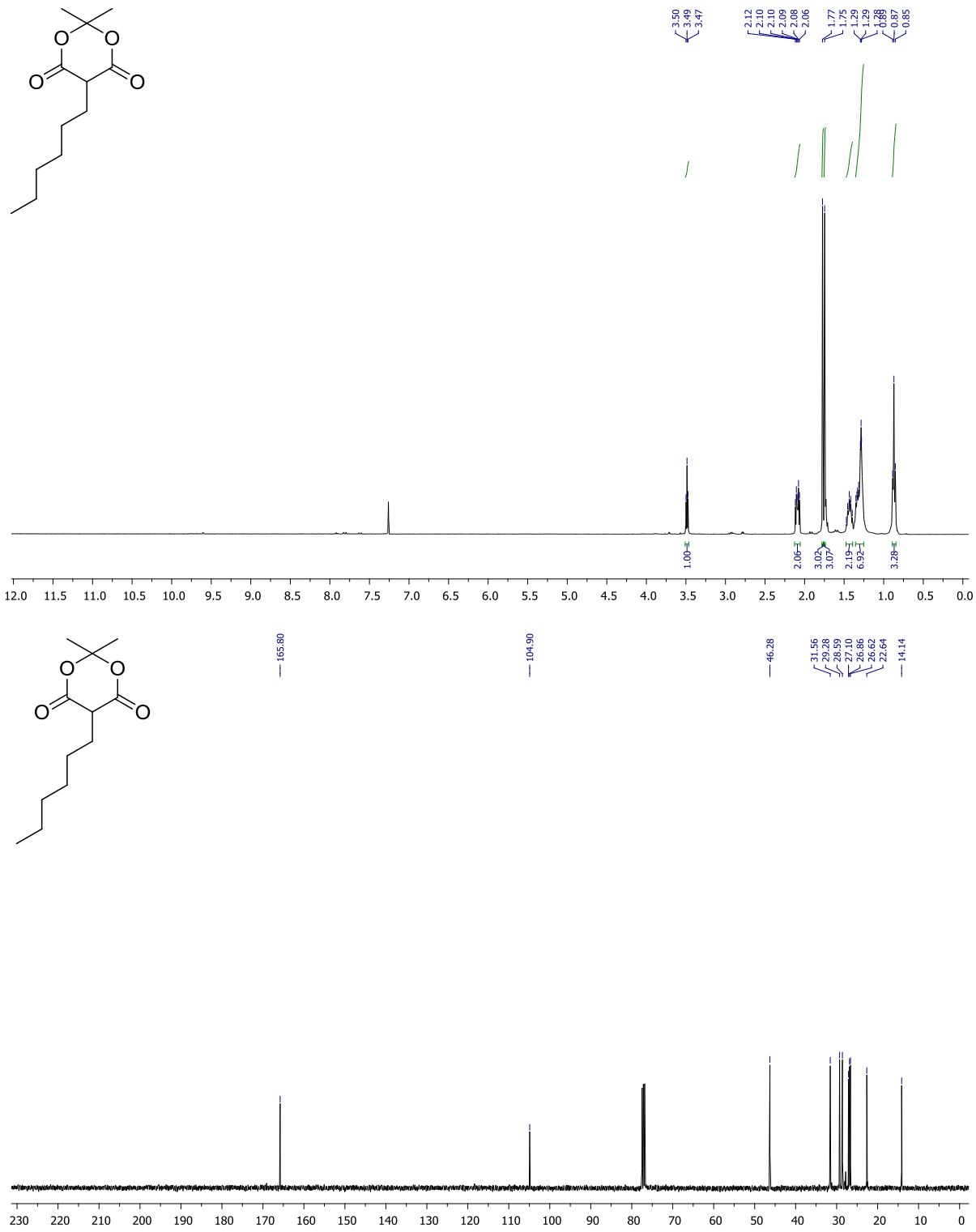

SI Figure 22: ^{1}HNMR- and ^{13}C-Spectra of 5-Hexyl-2,2-dimethyl-1,3-dioxane-4,6-dione (**15**) in $CDCl_3$-d_1.

NMR-spectra of *t*Butylmalonic acid

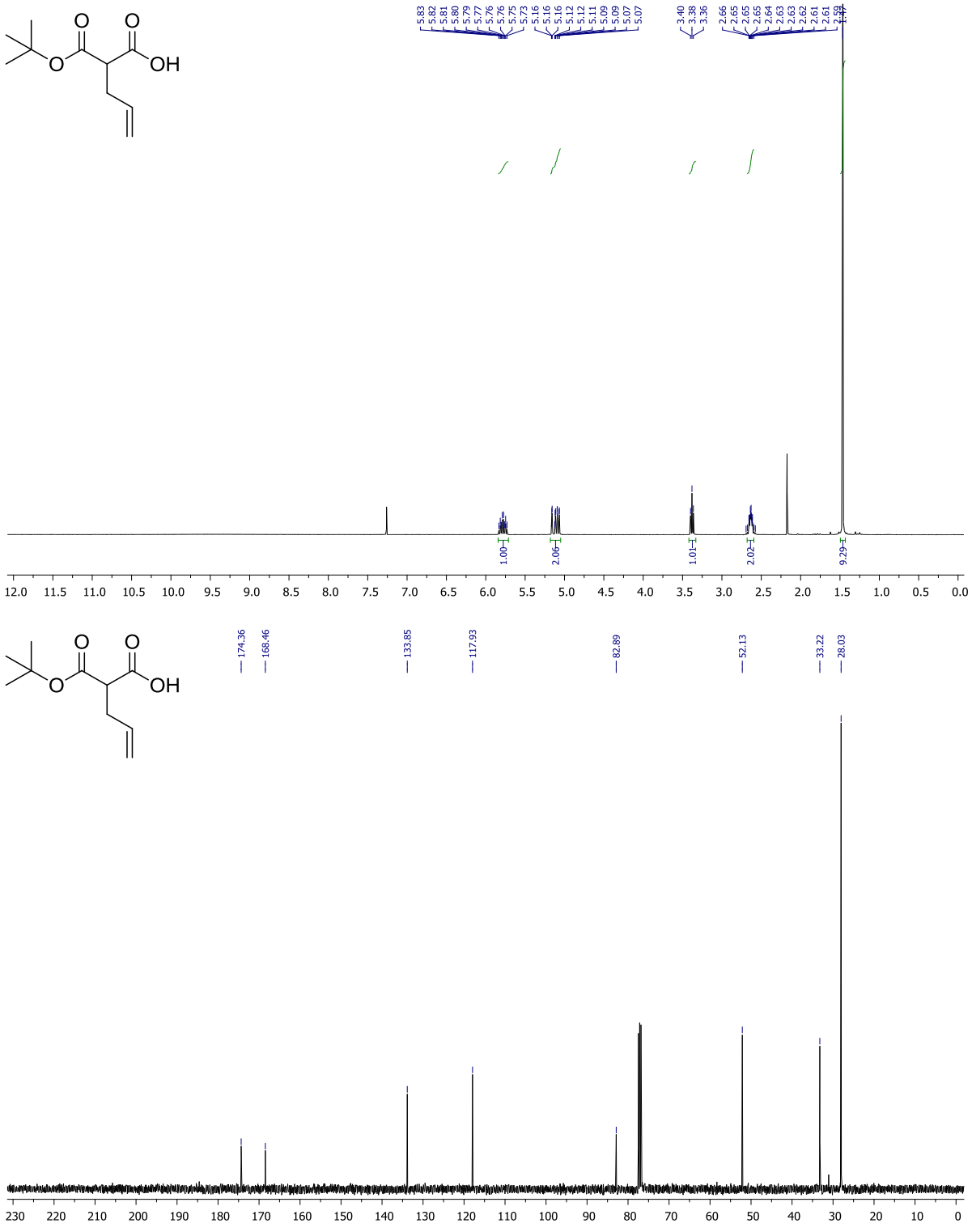

SI Figure 23: ^{1}HNMR- and ^{13}C-Spectra of 2-(*tert*-butoxycarbonyl)pent-4-enoic acid (**16**) in $CDCl_3$-d_1.

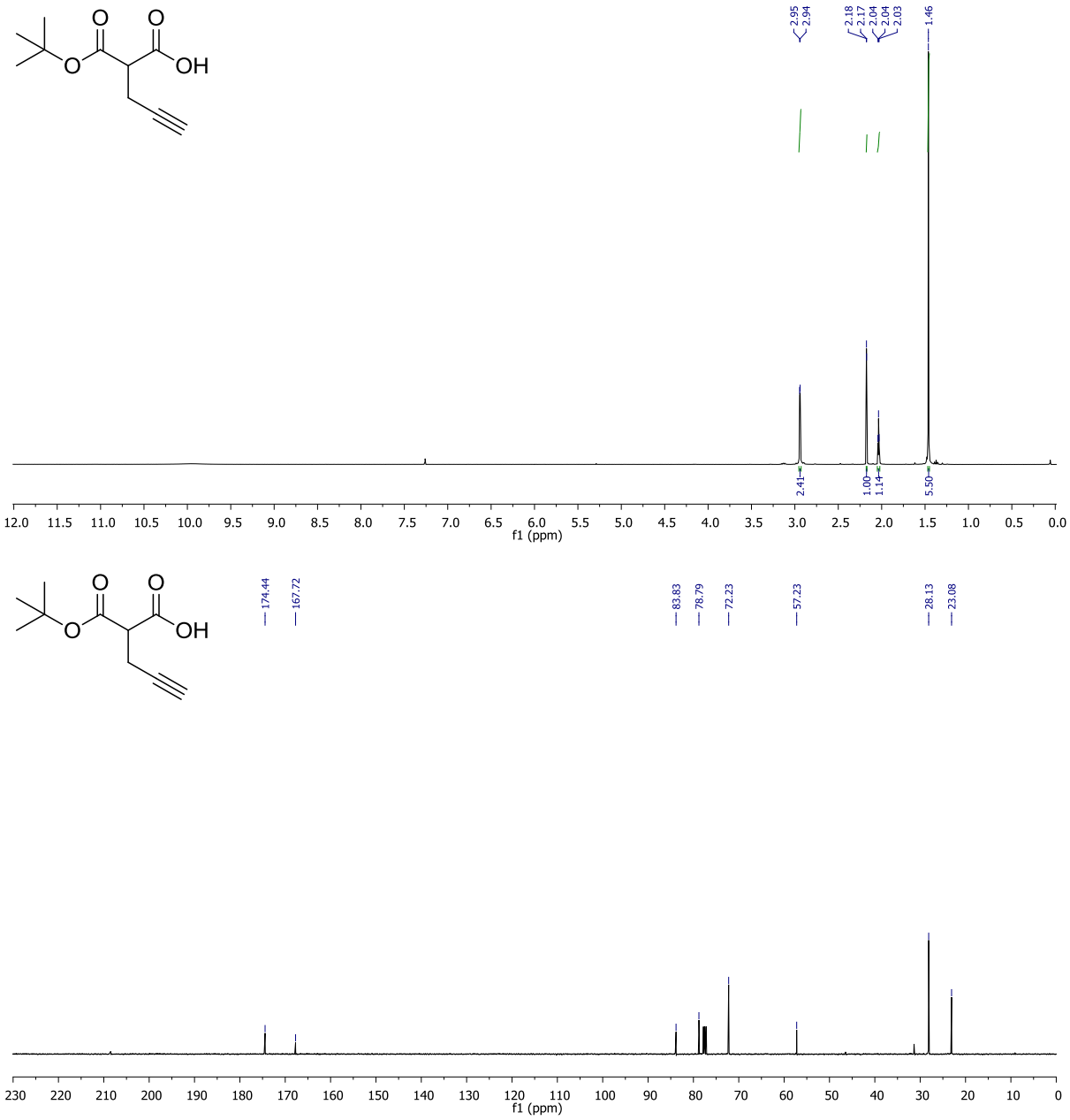

SI Figure 24: ^{1}HNMR- and ^{13}C-Spectra of 2-(*tert*-butoxycarbonyl)pent-4-ynoic acid (**17**) in $CDCl_3$-d_1.

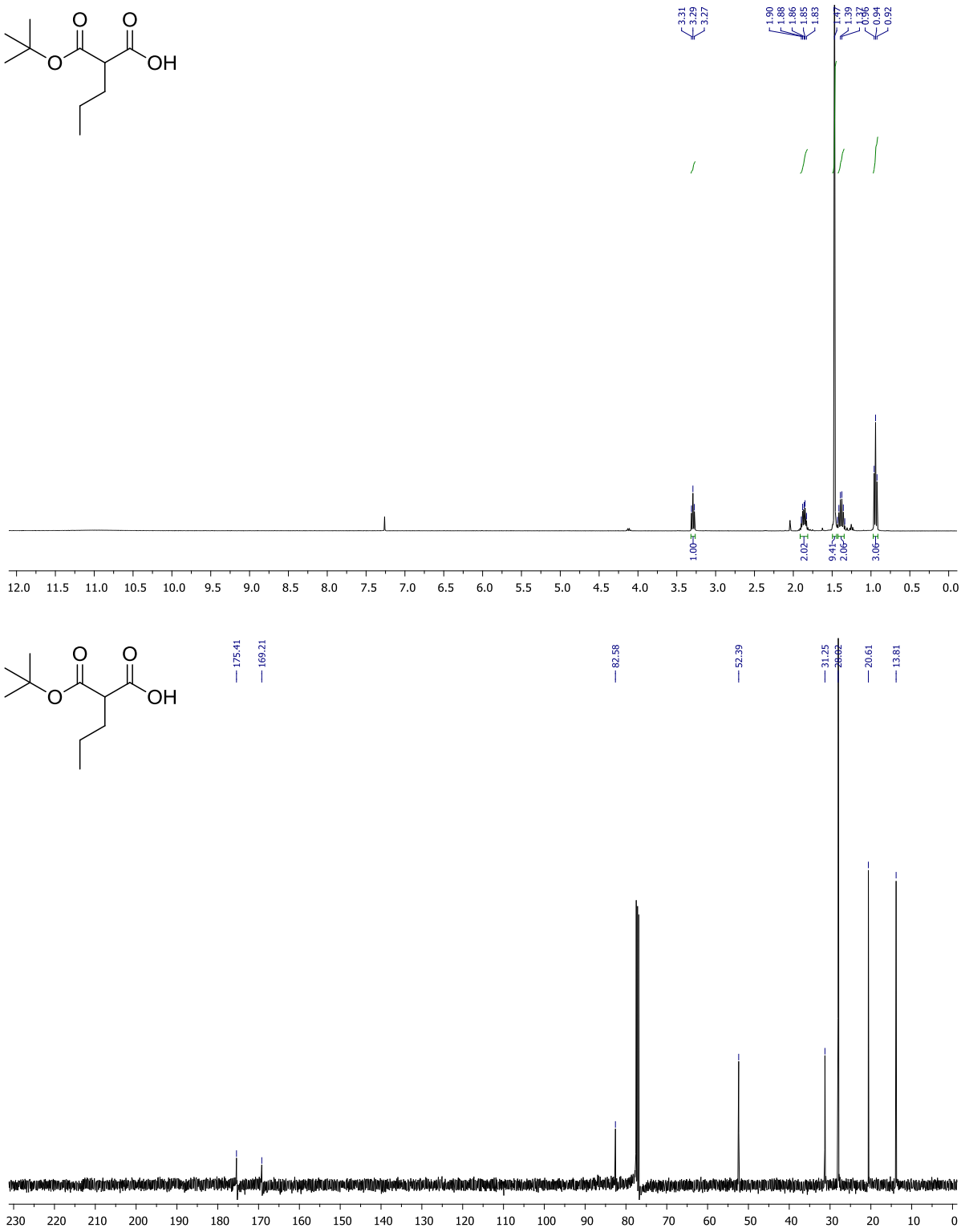

SI Figure 25: ^{1}HNMR- and ^{13}C-Spectra of 2-(*tert*-butoxycarbonyl)pentanoicacid (**18**) in $CDCl_3$-d_1.

SI Figure 26: ^{1}HNMR- and ^{13}C-Spectra of 2-(*tert*-butoxycarbonyl)hexanoicacid (**19**) in $CDCl_3$-d_1.

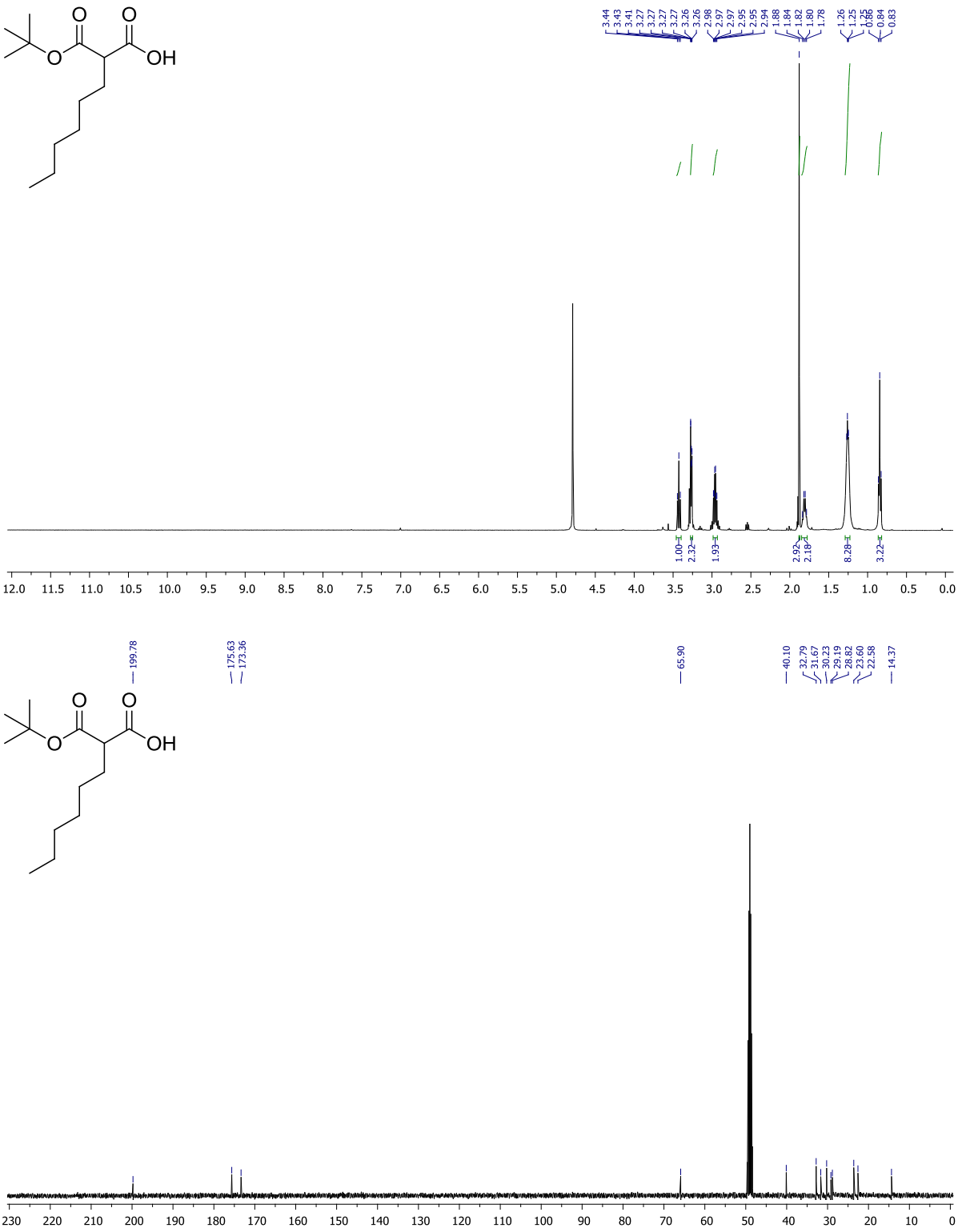

SI Figure 27: ^{1}HNMR- and ^{13}C-Spectra of 2-(*tert*-butoxycarbonyl)octanoicacid (**20**) in $CDCl_3$-d_1.

NMR-spectra of thioester

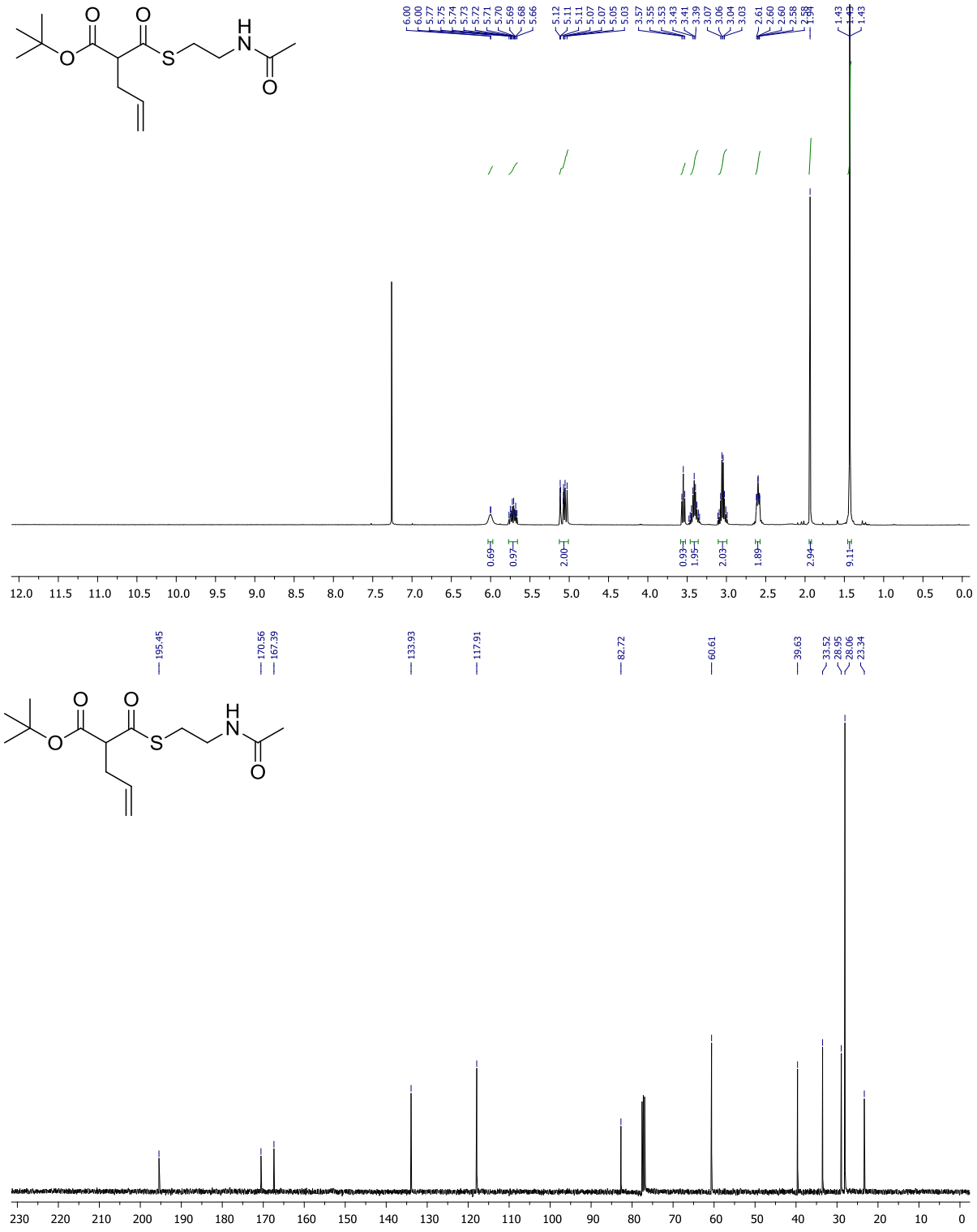

SI Figure 28: ^{1}HNMR- and ^{13}C-Spectra of *tert*-butyl 2-(((2-acetamidoethyl)thio)carbonyl)pent-4-enoate (**21**) in $CDCl_3$-d_1.

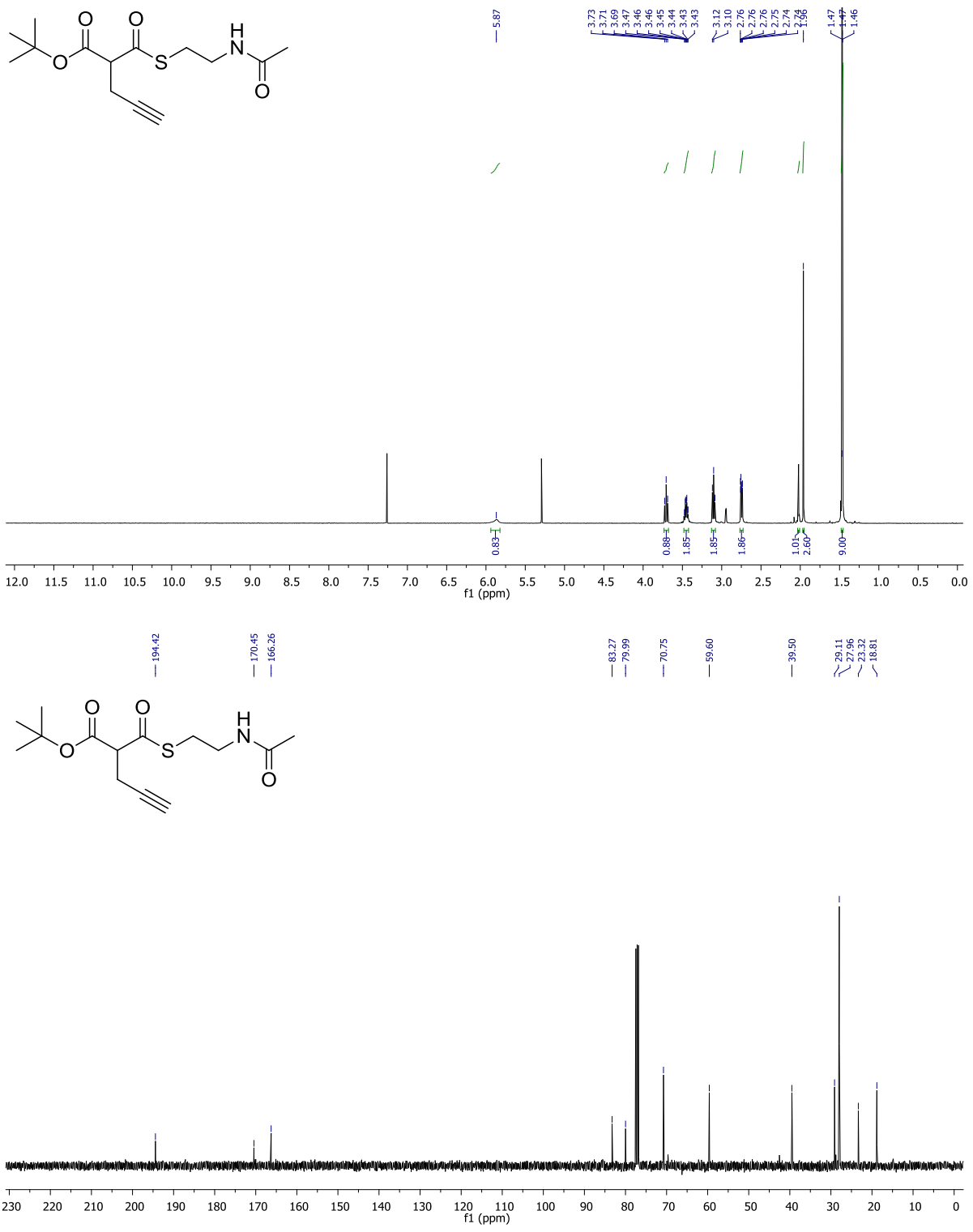

SI Figure 29: ^{1}HNMR- and ^{13}C-Spectra of *tert*-butyl 2-(((2-acetamidoethyl)thio)-carbonyl)pent-4-ynoate (**22**) in $CDCl_3$-d_1.

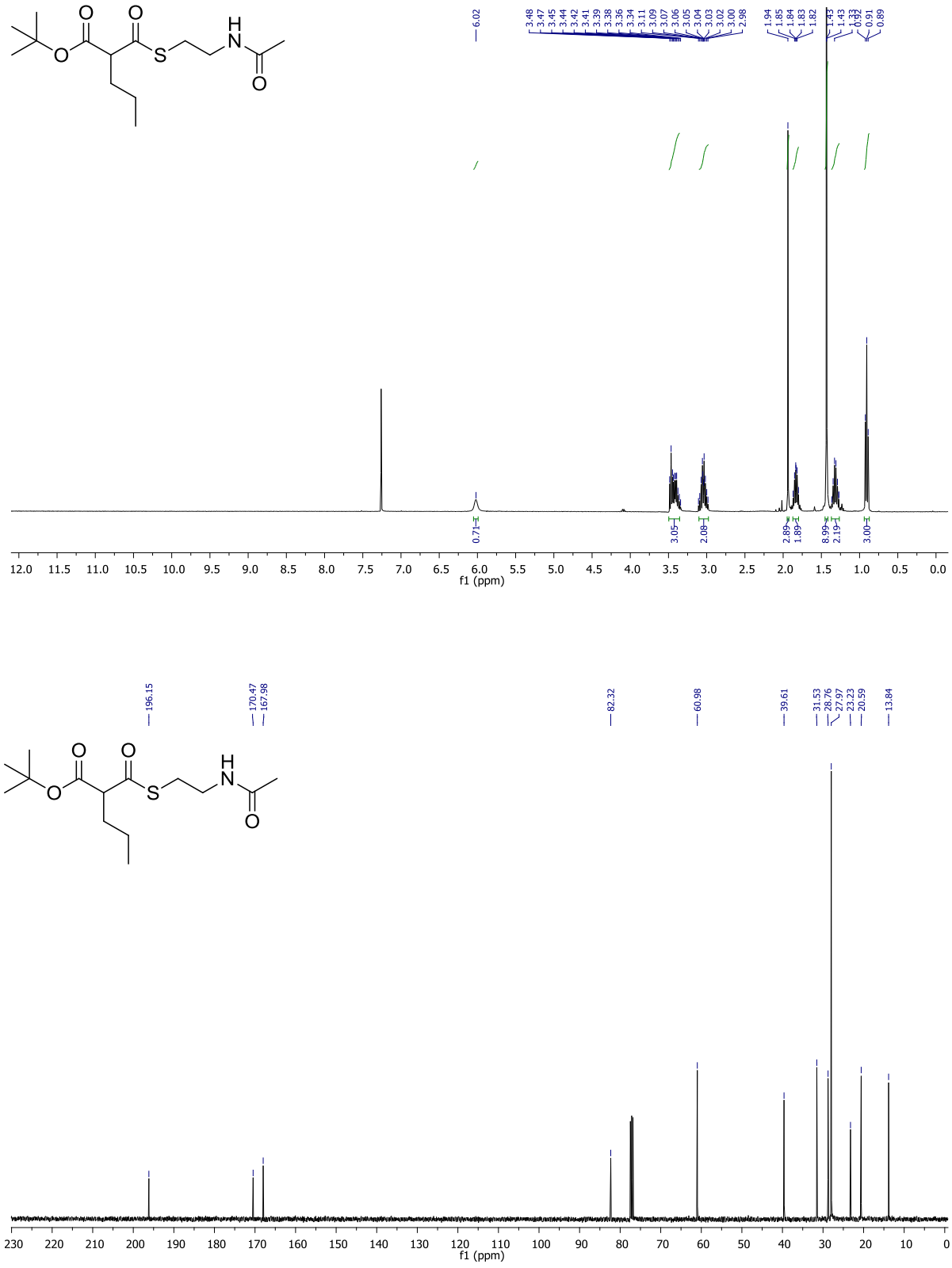

SI Figure 30: ^{1}HNMR- and ^{13}C-Spectra of *tert*-butyl 2-(((2-acetamidoethyl)thio)carbonyl)pentanoate (**23**) in $CDCl_3$-d_1.

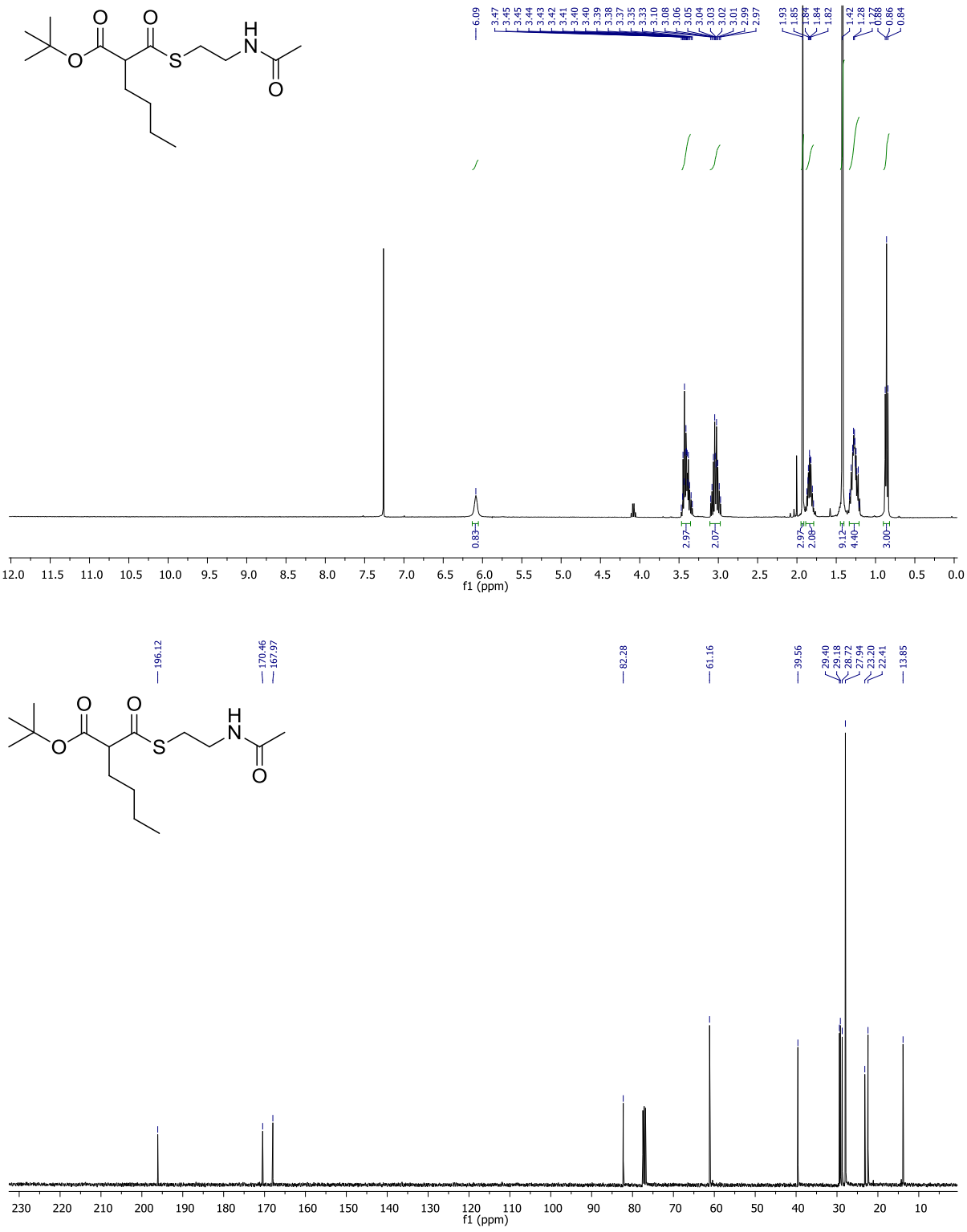

SI Figure 31: ^{1}HNMR- and ^{13}C-Spectra of *tert*-butyl 2-(((2-acetamidoethyl)thio)carbonyl)hexanoate (**24**) in $CDCl_3$-d_1.

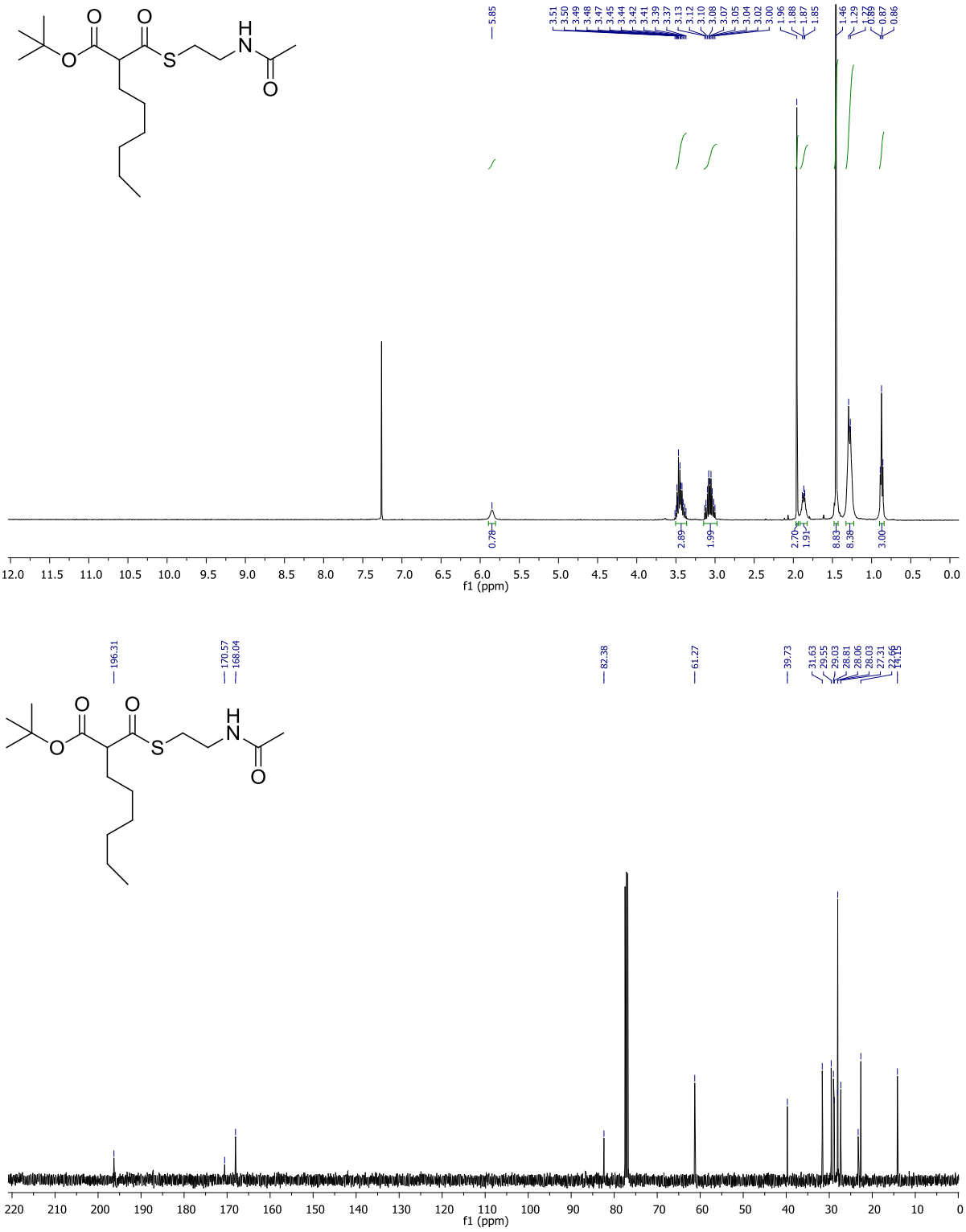

SI Figure 32: ^{1}HNMR- and ^{13}C-Spectra of *tert*-butyl 2-(((2-acetamidoethyl)thio)carbonyl)octanoate (**25**) in $CDCl_3$-d_1.

NMR-spectra of the SNAC-malonic acid

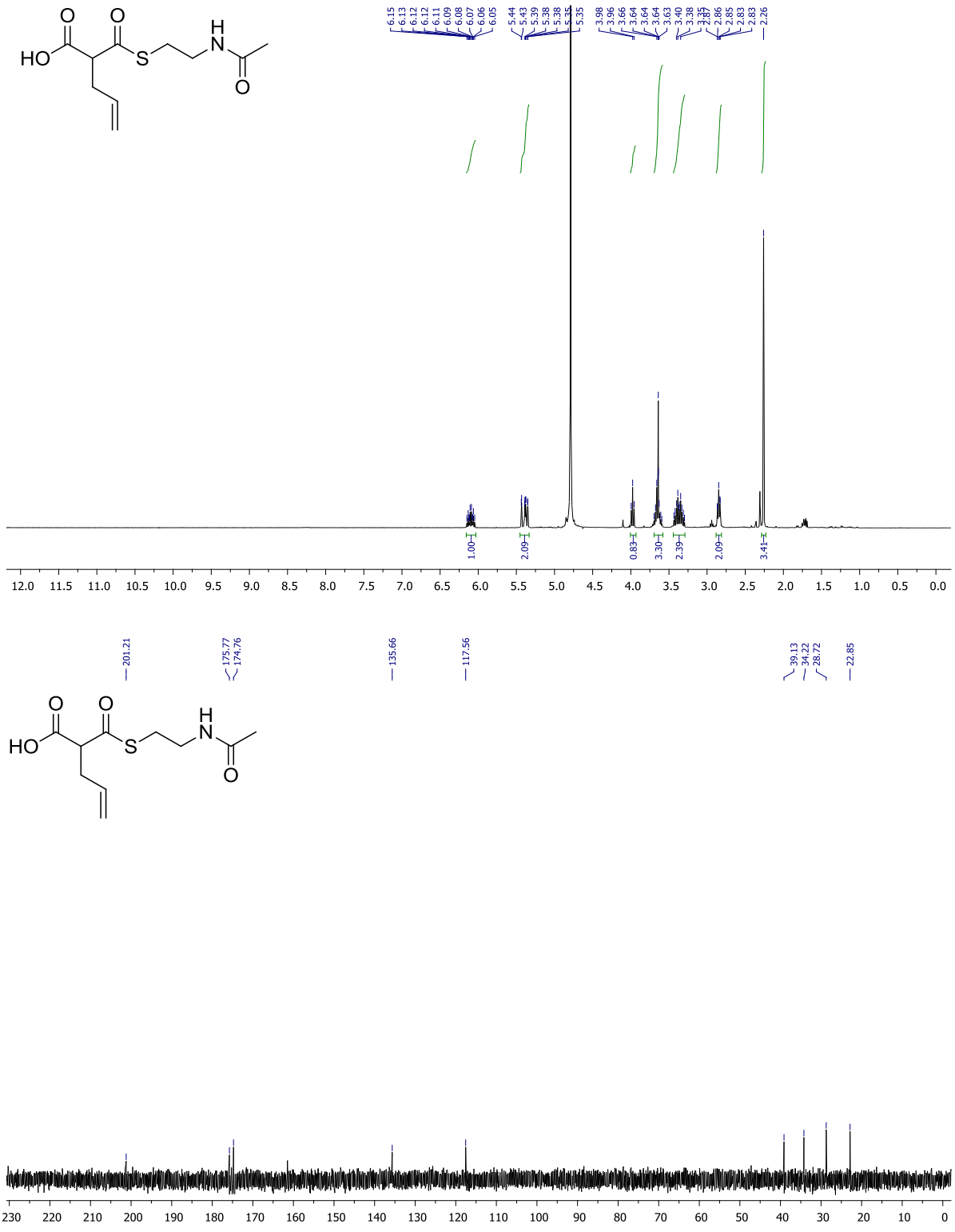

SI Figure 33: ^{1}HNMR- and ^{13}C-Spectra of 2-(((2-acetamidoethyl)thio)carbonyl)pent-4-enoic acid (**4**) in D_2O-d_2

SI Figure 34: ^{1}HNMR- and ^{13}C-Spectra of 2-(((2-acetamidoethyl)thio)carbonyl)pent-4-enoic acid (**5**) in D_2O-d_2.

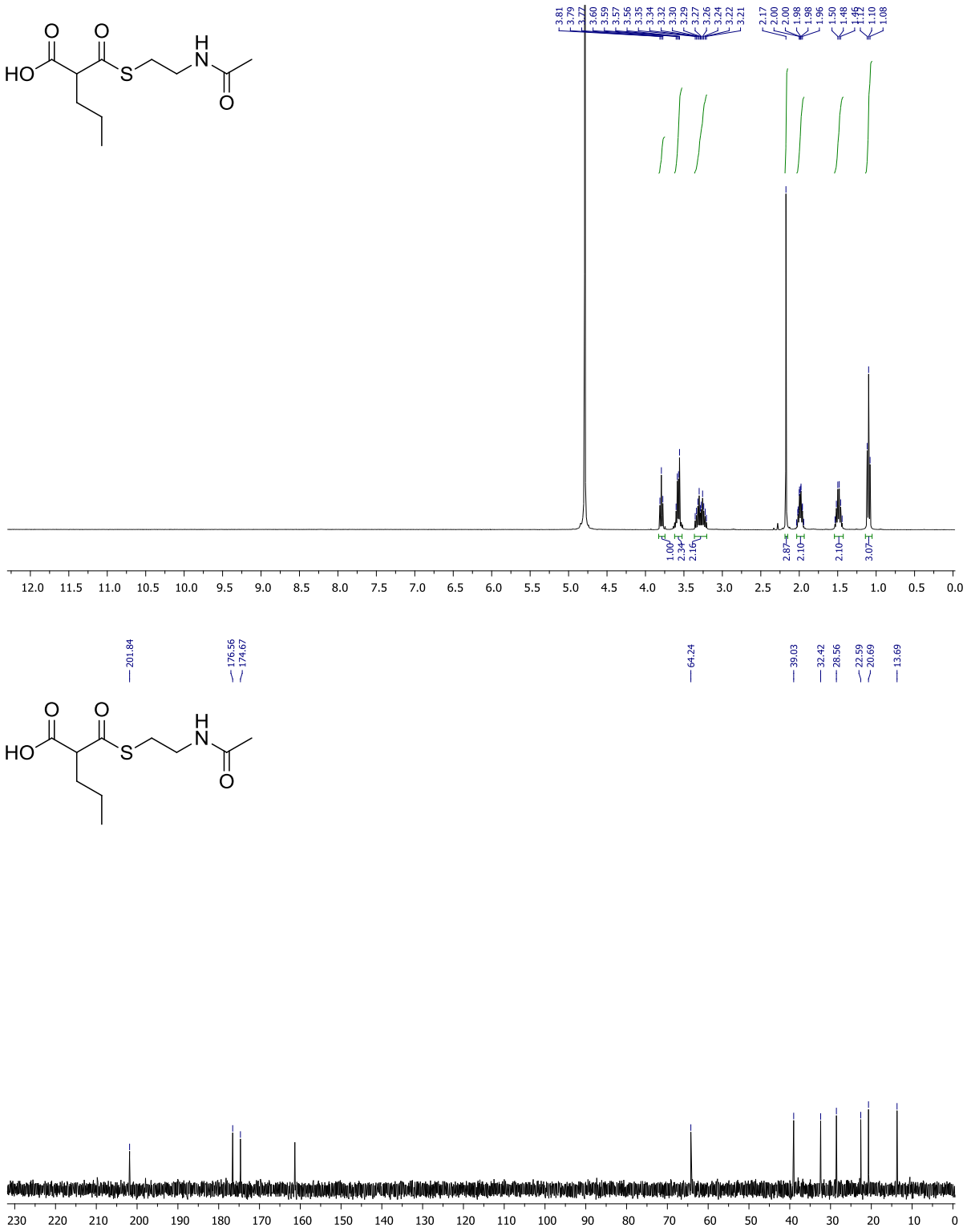

SI Figure 35: ^{1}HNMR- and ^{13}C-Spectra of 2-(((2-acetamidoethyl)thio)carbonyl)pentanoicacid (**6**) in D_2O-d_2.

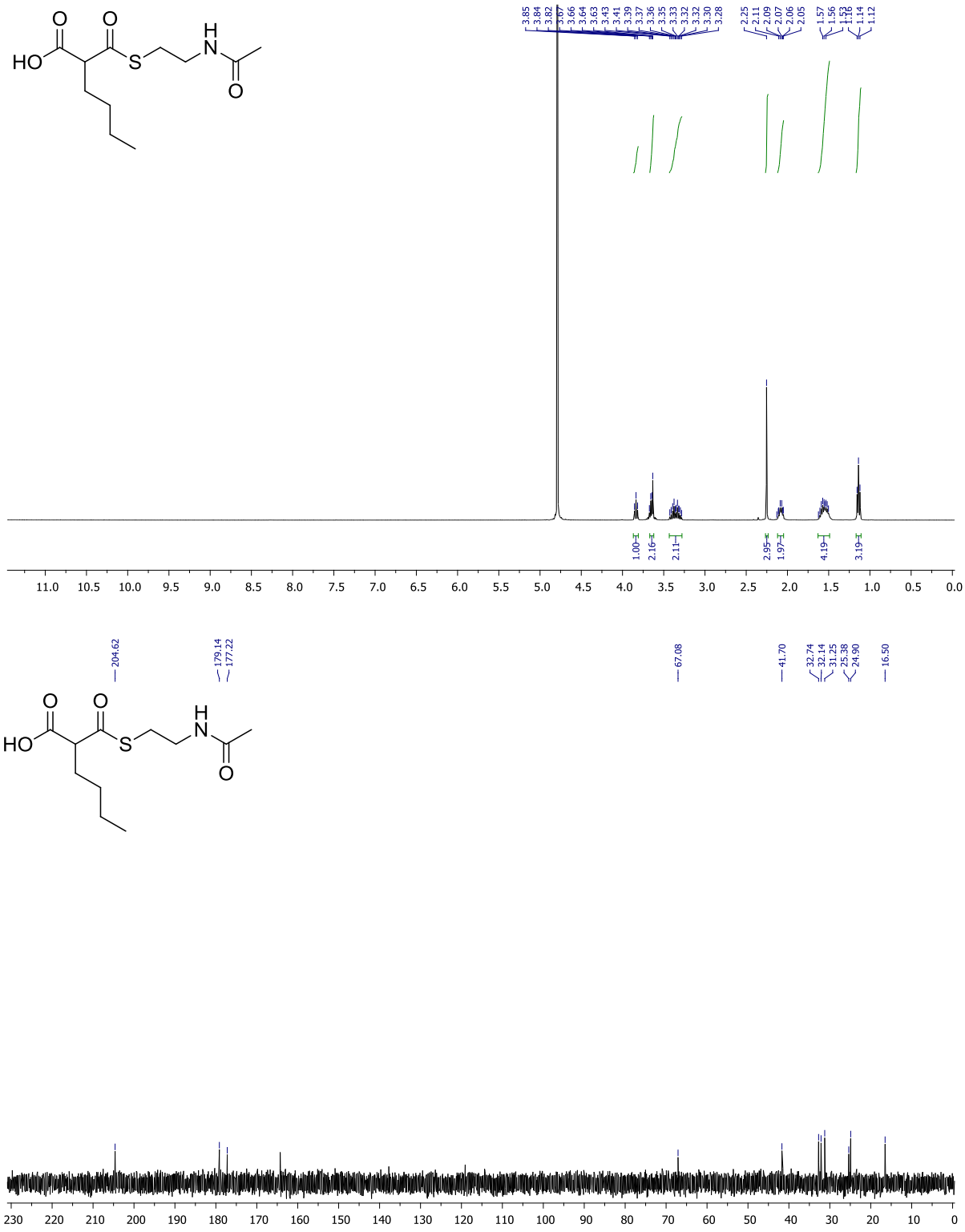

SI Figure 36: ^{1}HNMR- and ^{13}C-Spectra of 2-(((2-acetamidoethyl)thio)carbonyl)hexanoicacid (**7**) in D_2O-d_2.

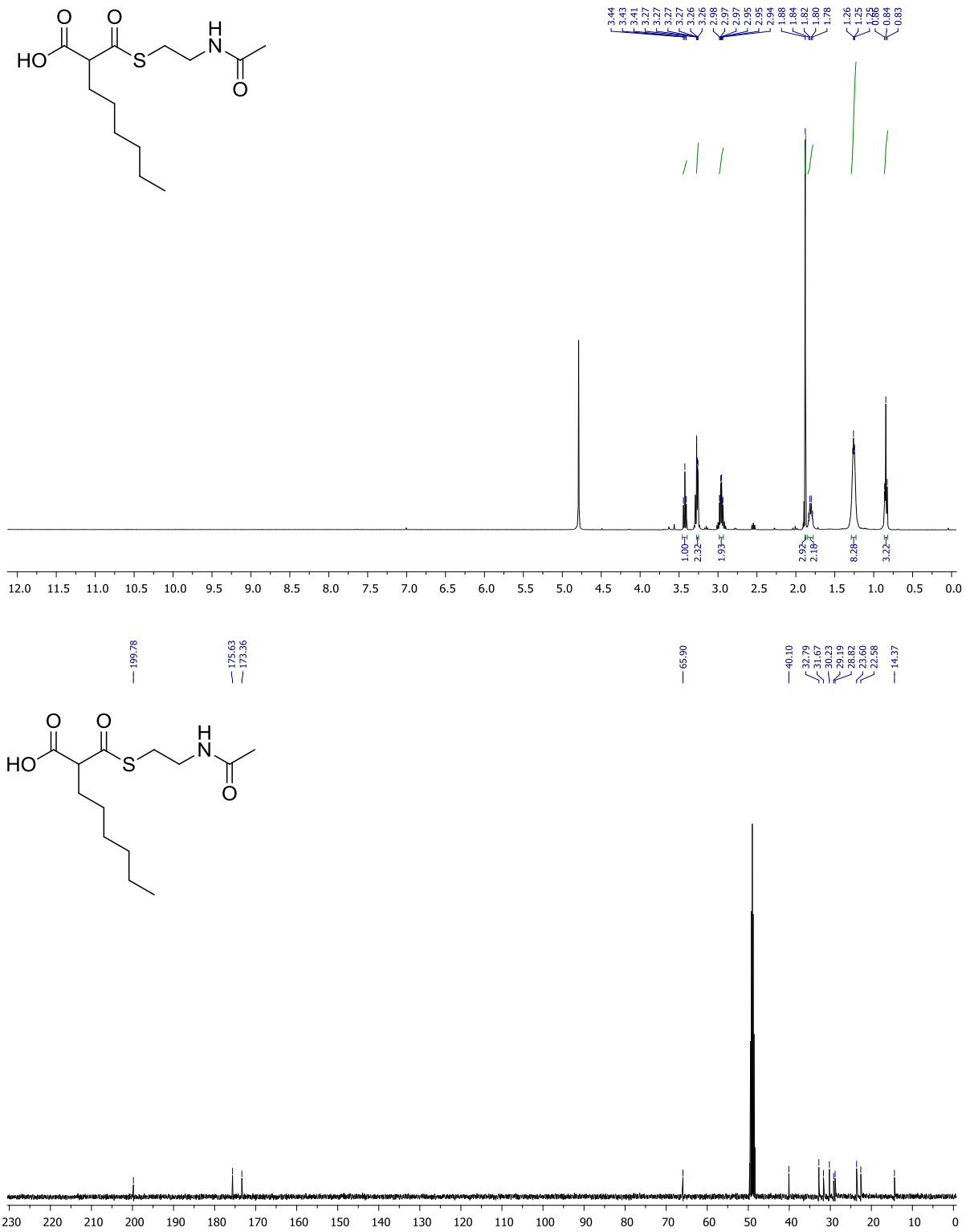

SI Figure 37: ^{1}HNMR- and ^{13}C-Spectra of 2-(((2-acetamidoethyl)thio)carbonyl)octanoicacid(**8**) in D_2O-d_2 (^{1}H-NMR), MeOD-d_4 (^{13}C-NMR).

VI References

[1] Y. Tang, A. Y. Chen, C.-Y. Kim, D. E. Cane, C. Khosla, *Chemistry & Biology* **2007**, *14*, 931-943.

[2] Y. Tang, C.-Y. Kim, I. I. Mathews, D. E. Cane, C. Khosla, *Proc. Natl. Acad. Sci. USA* **2006**, *103*, 11124-11129.

[3] M. A. Martí-Renom, A. C. Stuart, A. Fiser, R. Sánchez, F. Melo, A. Šali, *Annu. Rev. Biophys. Biomol. Struct.***2000**, *29*, 291-325.

[4] U. Sundermann, K. Bravo-Rodriguez, S. Klopries, S. Kushnir, H. Gomez, E. Sanchez-Garcia, F. Schulz, *ACS Chem. Biol.***2013**, *8*, 443-450.

[5] H. Li, A. D. Robertson, J. H. Jensen, *Proteins: Struct., Funct., Bioinf.***2005**, *61*, 704-721.

[6] J. C. Phillips, R. Braun, W. Wang, J. Gumbart, E. Tajkhorshid, E. Villa, C. Chipot, R. D. Skeel, L. Kalé, K. Schulten, *J. Comput. Chem.***2005**, *26*, 1781-1802.

[7] A. D. Mackerell, M. Feig, C. L. Brooks, *J. Comput. Chem.***2004**, *25*, 1400-1415.

[8] W. L. Jorgensen, J. Chandrasekhar, J. D. Madura, R. W. Impey, M. L. Klein, *J. Chem. Phys.***1983**, *79*, 926-935.

[9] V. Zoete, M. A. Cuendet, A. Grosdidier, O. Michielin, *J. Comput. Chem.* **2011**, *32*, 2359-2368.

[10] U. Essmann, L. Perera, M. L. Berkowitz, T. Darden, H. Lee, L. G. Pedersen, *J. Chem. Phys.***1995**, *103*, 8577-8593.

[11] W. Humphrey, A. Dalke, K. Schulten, *J. Mol. Graphics***1996**, *14*, 33-38, 27-38.

[12] a) P. Kollman, *Chem. Rev.***1993**, *93*, 2395-2417;b)R. W. Zwanzig, *J. Chem. Phys.* **1954**, *22,* 1420-1426.

[13] P. Liu, F. Dehez, W. Cai, C. Chipot, *J.Chem.Theory Comput.***2012**, *8*, 2606-2616.

[14] C. H. Bennett, *J. Comput. Phys.***1976**, *22*, 245-268.

[15] a) A. D. Becke, *J. Chem. Phys.***1992**, *97*;b) S. Grimme, *J. Comput. Chem.***2006**, *27*, 1787-1799.

[16] S. R. Billeter, A. J. Turner, W. Thiel, *Phys. Chem. Chem. Phys.* **2000**, *2*, 2177-2186.

[17] a) R. Ahlrichs, M. Bär, M. Häser, H. Horn, C. Kölmel, *Chem. Phys. Lett.***1989**, *162*, 165-169;b) W. Smith, T. R. Forester, *J. Mol. Graphics***1996**, *14*, 136-141.

[18] a) ChemShell, a Computational Chemistry Shell, see www.chemshell.org,b)P. Sherwood, A. H. de Vries, M. F. Guest, G. Schreckenbach, C. R. A. Catlow, S. A. French, A. A. Sokol, S. T. Bromley, W. Thiel, A. J. Turner, S. Billeter, F. Terstegen, S. Thiel, J. Kendrick, S. C. Rogers, J. Casci, M. Watson, F. King, E. Karlsen, M. Sjøvoll, A. Fahmi, A. Schäfer, C. Lennartz, *J. Mol.Struc.-THEOCHEM***2003**, *632*, 1-28.

[19] S. Kushnir, U. Sundermann, S. Yahiaoui, A. Brockmeyer, P. Janning, F. Schulz, *Angew. Chem. Int. Ed.***2012**, *51*, 10664-10669.

[20] D. Wätzlich, I. Vetter, K. Gotthardt, M. Miertzschke, Y. X. Chen, A. Wittinghofer, S. Ismail, *EMBO Rep.***2013**, *14*, 465-472.

[21] I. Koryakina, G. J. Williams, *ChemBioChem* **2011**, *12*, 2289-2293.

[22] R. K. Singh, S. Danishefsky, *J. Org. Chem.***1975**, *40*, 2969-2970.

[23] D. M. Hrubowchak, F. X. Smith, *Tetrahedron Lett.***1983**, *24*, 4951-4954.